DISSERTATIONES
TECHNOLOGIAE
UNIVERSITATIS
TARTUENSIS
63

LIVIA MATT

Novel isosorbide-based polymers

DISSERTATIONES TECHNOLOGIAE UNIVERSITATIS TARTUENSIS
63

DISSERTATIONES TECHNOLOGIAE UNIVERSITATIS TARTUENSIS
63

LIVIA MATT

Novel isosorbide-based polymers

UNIVERSITY OF TARTU
Press

Institute of Technology, Faculty of Science and Technology, University of Tartu, Estonia

Dissertation is accepted for the commencement of the degree of *Doctor Philosophiae* in Engineering of Bioactive Compounds on November 11th, 2021 by the Council of the Institute of Technology, Faculty of Science and Technology, University of Tartu.

Supervisors:	Lauri Vares, PhD Associate Professor of Organic Chemistry, Institute of Technology, Faculty of Science and Technology, University of Tartu, Estonia
	Patric Jannasch, PhD Visiting Professor, Institute of Technology, Faculty of Science and Technology, University of Tartu, Estonia; Professor of Polymer Technology, Department of Chemistry, Faculty of Science, Lund University, Sweden
Reviewer:	Erki Enkvist, PhD Associate Professor of Bioorganic Chemistry, Institute of Chemistry, Faculty of Science and Technology, University of Tartu, Estonia
Opponent:	René Saint-Loup, PhD Polymer Chemistry R&D Manager, Roquette Frères, Lestrem Research Center, France
Commencement:	Auditorium 121, Nooruse 1, Tartu, Estonia, at 13.00 on December 15th, 2021

Publication of this thesis is granted by the Institute of Technology, University of Tartu.

ISSN 2228-0855
ISBN 978-9949-03-765-0 (print)
ISBN 978-9949-03-766-7 (pdf)

University of Tartu Press
www.tyk.ee

ABSTRACT

The vision of a more sustainable economy needs an environmentally friendly alternative for the utilization of non-renewable fossil resources in the production of materials. Particularly plastics, that are predominantly composed of oil-based polymers, are problematic in essence. Biobased polymers could be the appropriate substitute for materials originating from fossil feedstock. For that reason, isosorbide, a rigid diol derived from bioresources, was used as a starting material in this study.

Linear polymethacrylates and polyethers bearing isosorbide units as pendant groups were prepared and characterized. The influence of various substituents and the regiochemistry of the monomers to the properties of the obtained polymers were also studied. These biobased polymers proved to exhibit competitive properties to conventional polymeric materials.

Furthermore, the synthesis of isosorbide derivatives with elongated carbon chain was demonstrated with the aid of hydroformylation method. By the implementation of this strategy, the derivatization of isosorbide through its secondary hydroxyl groups can be avoided, and new building blocks with a carbon-carbon bond elongated isosorbide structure can be utilized for polymer synthesis.

In brief, this thesis presents novel isosorbide-based compounds and polymers that can contribute to the field of biobased materials aimed to replace plastics from non-renewable fossil resources.

TABLE OF CONTENTS

LIST OF ORIGINAL PUBLICATIONS

This thesis is based on the following publications. The articles are referred in the text by Roman numerals I–III.

I **Matt, L.**; Parve, J.; Parve, O.; Pehk, T.; Pham, T. H.; Liblikas, I.; Vares, L.; Jannasch, P. Enzymatic Synthesis and Polymerization of Isosorbide-Based Monomethacrylates for High-T_g Plastics. *ACS Sustainable Chem. Eng.* **2018**, *6*, 17382–17390. https://doi.org/10.1021/acssuschemeng.8b05074

II **Matt, L.**; Liblikas, I.; Bonjour, O.; Jannasch, P.; Vares, L. Synthesis and anionic polymerization of isosorbide mono-epoxides for linear biobased polyethers. *Polym. Chem.* **2021**, *12* (41), 5937–5941. https://doi.org/10.1039/d1py00687h

III Villo, P.*; **Matt, L.***; Toom, L.; Liblikas, I.; Pehk, T.; Vares, L. Hydroformylation of Olefinic Derivatives of Isosorbide and Isomannide. *J. Org. Chem.* **2016**, *81*, 7510–7517. https://doi.org/10.1021/acs.joc.6b01179

* Designates shared first authorship.

Related publication (referred in the text by Roman numeral IV):

IV Laanesoo, S.; Bonjour, O.; Parve, J.; Parve, O.; **Matt, L.**; Vares, L.; Jannasch, P. Poly(alkanoyl isosorbide methacrylate)s: From Amorphous to Semicrystalline and Liquid Crystalline Biobased Materials. *Biomacromolecules* **2021**, *22*, 640–648. https://doi.org/10.1021/acs.biomac.0c01474

Author contributions:

Paper I: Performed all the polymerizations and contributed to the synthesis of monomers. Responsible for the preparation of the first draft of the manuscript.

Paper II: Performed the polymerization experiments and contributed to the monomer's synthesis. Responsible for the preparation of the manuscript.

Paper III: Performed half of the experimental work. Participated in the writing of the manuscript.

ABBREVIATIONS

Ac	acetate
acac	acetylacetonate anion
ACN	acetonitrile
AIBN	azobis(isobutyronitrile)
AROP	anionic ring-opening polymerization
BD	1,4-butanediol
BPA	bisphenol A
Bu	butyl
Cbz	benzyloxycarbonyl
cod	1,5-cyclooctadiene
CROP	cationic ring-opening polymerization
$Đ$	polydispersity index ($Đ = M_w/M_n$)
DMSO	dimethyl sulfoxide
DSC	differential scanning calorimetry
DTG	derivative thermogravimetry
ECH	epichlorohydrin
Et	ethyl
HRMS (ESI)	high resolution mass spectroscopy analysis in which electrospray ionization technique is used to produce ions
IR (ATR)	infrared spectroscopy analysis carried out by Fourier-transform infrared spectrophotometer with attenuated total reflectance sampling technique
i-Bu_3	triisobutyl
Im	imidazole
Me	methyl
2-MeTHF	2-methyltetrahydrofuran
M_n	number average molecular mass
mol%	mole percent
M_w	weight average molecular mass
NMR	nuclear magnetic resonance spectroscopy
Oct	octyl
OTf	triflate
PB	phosphazene base
PEG	poly(ethylene glycol) (PEO with $M_n < 20$ kg mol^{-1})
PEO	poly(ethylene oxide) ($M_n > 20$ kg mol^{-1})
PET	poly(ethylene terephthalate)
p.ether	petroleum ether
Ph	phenyl

$P(ODBP)_3$	tris(2,4-di-*tert*-butylphenyl) phosphite
(*R*,*R*)-Ph-BPE	(–)-1,2-bis((2*R*,5*R*)-2,5-diphenylphospholano)ethane
r.t.	room temperature
SEC	size-exclusion chromatography
(*S*,*S*)-Ph-BPE	(+)-1,2-bis((2*S*,5*S*)-2,5-diphenylphospholano)ethane
(*S*,*S*,*S*)-DiazaPhos-PPE	2,2′-[(1*S*,3*S*)-2,3,5,10-tetrahydro-5,10-dioxo-2-phenyl-1*H*-[1,2,4]diazaphospholo[1,2-*b*]phthalazine-1,3-diyl]bis[*N*-(1*S*)-1-phenylethyl]benzamide
TBDMS	*tert*-butyldimethylsilyl
TBDPS	*tert*-butyldiphenylsilyl
t-Bu	*tert*-butyl
T_g	glass transition temperature
TGA	thermogravimetric analysis
THF	tetrahydrofuran
T_m	crystalline melting temperature
TMEDA	*N*,*N*,*N*′,*N*′-tetramethylethylenediamine
T_p	peak temperature at highest mass-loss rate on DTG curve
δ	solubility parameter (unit: $MPa^{½}$)
$[\eta]$	intrinsic viscosity (unit: dL g^{-1})

INTRODUCTION

Mankind dependence on polymer industry has increased to the extent that is hard to comprehend, but it can be appropriately illustrated by the increase of annual plastic production quantities in the world from 1950 to 2015 (Figure 1). Polymers, that are generally known as plastics to people from a wider audience, can be found almost everywhere, e.g., in transportation industry, food packaging, furniture, medical devices, building constructions etc. For clarification, plastics represent a large group of materials with a wide range of mechanical properties that are mostly composed of polymers, but that can also include other components (e.g., fillers, plasticizer) in their final structure in order to improve performance and/or reduce the cost.[1,2] Concurrently, polymers are macromolecules comprised of many smaller molecules with relatively low molecular mass that have been joined together into large repetitive sequences.[1,3]

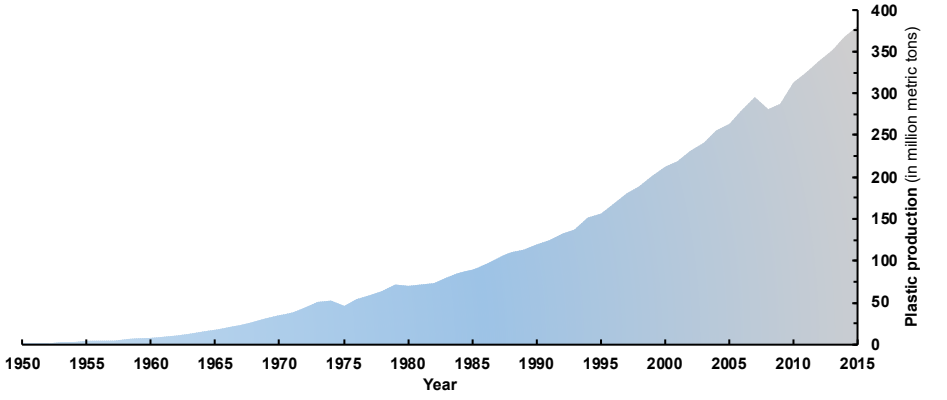

Figure 1. Global plastic production from 1950 to 2015.[4]

Plastics have proven to be very advantageous in numerous applications, but today, due to the increasing demand for these polymeric materials, complex environmental challenges have come forth. Not only are we struggling with vast plastic pollution, but also the utilization of oil as raw material and, at the same time, the depletion of fossil resources have great impact on our economy, which thereby also increases the overall inequality in the world. To lessen the influence of polymer industry to our environment and society, it is necessary to find some applicable and preferably sustainable solutions to these expanding issues.

From a chemist's perspective, there are three main strategies that could be implemented. The first is to produce polymers, and plastic materials thereof, from biobased resources with the attempt to decrease the utilization of petrochemicals. This approach has no influence on the reduction of plastic pollution nor the recycling of plastics but would decrease the dependence on fossil feedstock, which we know is not an infinite source for raw substances.

The second strategy is to prepare easily biodegradable polymers. But the drawback with this strategy is the small scope of possible applications, e.g., a car with biodegradable parts would have a short lifespan and not meaningful to produce. However, in packaging sector this approach is favourable, as packages are generally thrown away after a one-time use, and if not properly recycled, can escalate the plastic pollution in our environment.

The third strategy is to use the plastics we already have in hand, but then develop a competitive recycling system in order to reuse these products repetitively. Notably, monomaterials containing primarily only one type of material should be preferred to make this approach effective. The third approach would decrease the amount of fossil feedstock used, but it must be kept in mind that plastics cannot be recycled infinite times, and also addition of virgin polymer is generally needed during recycling to not diminish the mechanical properties of the material.

It is evident that potential solutions to the problems relating to polymeric materials do exist, but much more effort needs to be made to establish easily applicable processes, and to spread these ideas among majority of people in the world.

In this thesis the first strategy of making polymers from renewable feedstock was set as the ambition. Isosorbide[5] (Scheme 1), a well-known rigid biobased compound, was chosen as the main building block for novel biobased polymers. Isosorbide has already proven to be an interesting component in many polycondensation polymers,[6] but usually energy extensive processes are implemented and thus, severely coloured products can form.[7] Additionally, most isosorbide-based polymers prepared so far incorporate the whole isosorbide unit into the polymer backbone. Hence, it was decided to synthesize biobased polymers with isosorbide as a pendant group. Isosorbide-based linear polymethacrylates and polyethers were set as the main goal. Furthermore, olefinic derivatives of isosorbide were also synthesized and thereafter converted to aldehydes by hydroformylation reaction. This derivatization strategy affords novel isosorbide-based compounds with a carbon-carbon bond elongation that overcomes the low reactivity problem of the secondary hydroxyl groups in isosorbide structure. Moreover, this approach can also find usage in the formation of other novel building blocks for biobased polymers.

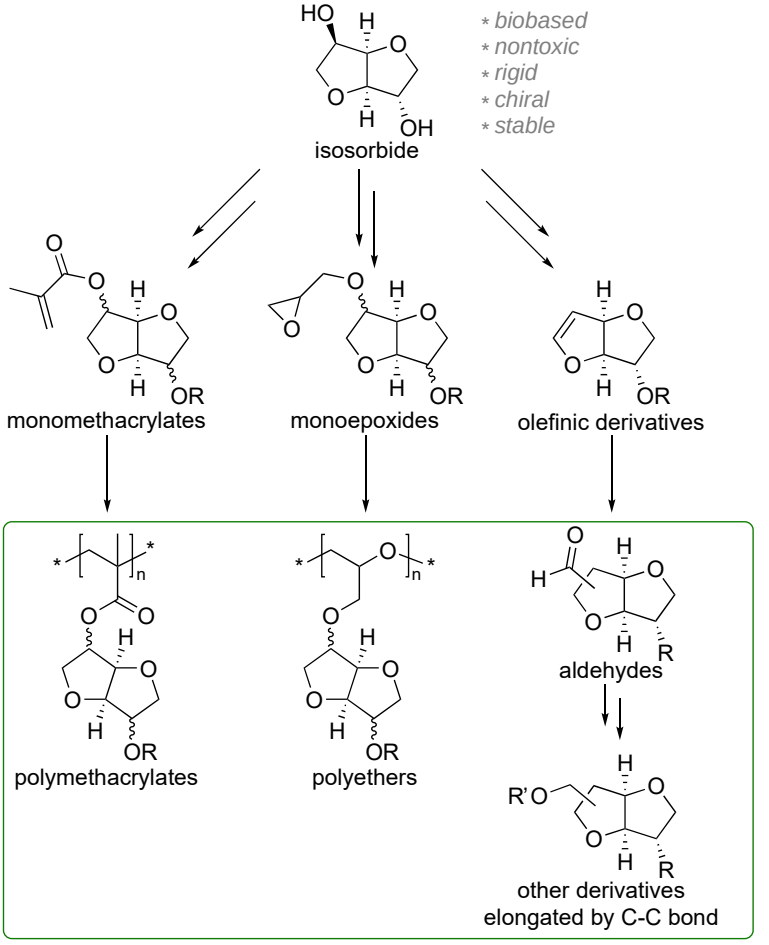

Scheme 1. Outline of the current thesis. The main aims are highlighted in the rectangular box.

1. LITERATURE OVERVIEW

In this section of the thesis, brief synopsis of the main topics included in this study is presented. Therefore, biobased polymers, isosorbide and its derivatives, different polymerization methods used in this research, and also, hydroformylation reaction are introduced under the following subheadings.

1.1. Biobased polymers

From the beginning of the last century to this day, polymer chemistry has developed from a lab-scale experiments into a huge plastic industry, providing us with many beneficial materials, starting from lightweight packages to durable construction materials.

But synthetic polymers prepared from fossil feedstock is not a sustainable approach. As an alternative to fossil carbon source, lignocellulosic biomass could be used for polymer production, because it is the most abundant raw material available at this time.[8,9] Lignocellulosic biomass consists primarily of three components, cellulose (40–50%), hemicellulose (25–35%), and lignin (15–20%) that all can provide valuable building blocks for polymers.[8,10] Cellulose is a semi-crystalline polysaccharide composed of glucose units, whereas hemicellulose is a carbohydrate polymer with amorphous structure mostly formed by xylose, and lignin is an amorphous hetero-polymer with varying structure containing many aromatic sections (Figure 2).[11] The exact composition of lignocellulosic biomass depends on the specific feedstock.[10]

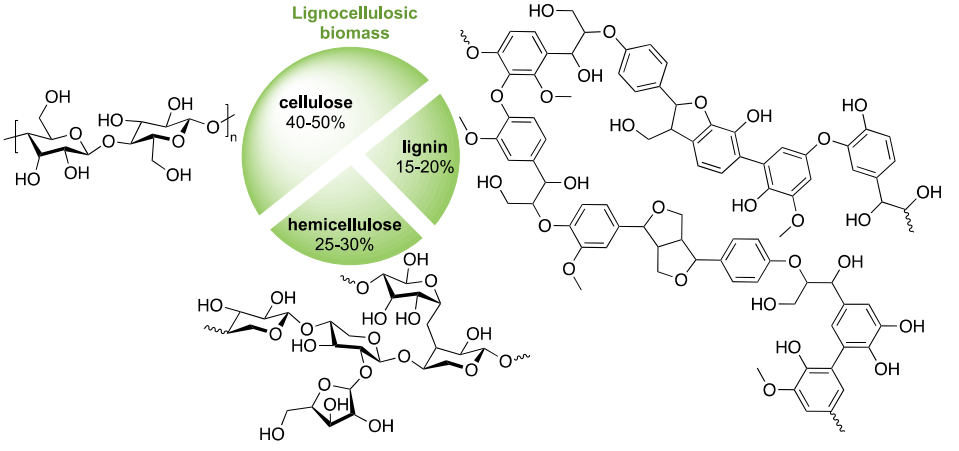

Figure 2. Composition of lignocellulosic biomass and representative chemical structures of cellulose, hemicellulose, and lignin.

Chemical substances derived from biomass are considered *biobased* compounds and the polymers made thereof *biobased polymers*.[2,12] With the latter, quite a lot of confusion in terminology occurs (Figure 3), sometimes also in scientific literature.

Biobased polymers is a term that subsumes all man-made polymers synthesized from biomass-originated monomers.[13] For instance, polyethylene that is a well-known petrochemical polymer can also be a *biobased polymer*, if the ethylene monomers are obtained from bioresources.[14] In other words, this Bio-PE is structurally identical to fossil-based polyethylene, but it is considered a *biobased* due to the origin of its monomers. Additionally, it should be elucidated that *biobased polymers* is not equal to *biopolymers*, since the latter is defined as biomacromolecules produced by living organisms like plants, animals, algae, microorganisms.[2,15] Examples of *biopolymers* are polypeptides, polysaccharides, and polynucleotides.

Another term that is often interchangeably used with *biobased* is *biodegradable*. To be clear, *biodegradability* refers to the quality of a material to degrade in the natural environment, and a *biodegradable polymer* is therefore a polymer that is prone to a breakdown into smaller fractions by biological activity usually in conjunction with other environmental factors.[2,16] If a polymer is *biobased*, it does not instantly denote that it is also *biodegradable*. The origin of the material does not predetermine its ability to degrade in the environment.[15] In practice, *biodegradability* depends more on the susceptibility of the polymers molecular structure to be broken down by microorganisms.[16] Furthermore, *biodegradability* of a plastic material is actually a very complicated subject and this quality cannot be assigned to a material very easily, because it not only determined by the properties of the polymer, but also by all the ingredients (like fillers, plasticizers etc) in the final plastic product, and by the conditions under which the degradation of the material is conducted.[17] Therefore, *biobased polymers* can be *biodegradable* if their structure meets the requirements for biodegradation. In the same way, polymers from petrochemical feedstock can also be *biodegradable*. For instance, polycaprolactone of fossil-origin is a biodegradable polymer.[16]

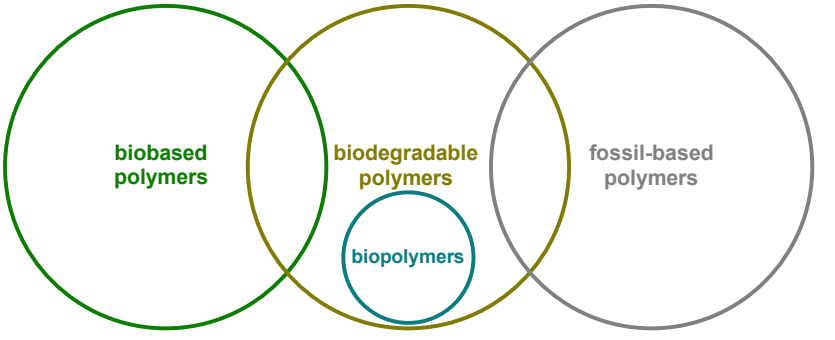

Figure 3. Figurative image for explaining the confusing terms *biopolymers*, *biobased polymers,* and *biodegradable polymers*.

Besides, more confusion comes forth in case of plastic materials. *Bioplastics* is used as a general term for plastics that can be either *biobased* or *biodegradable*,[15,16,18] even though according to the definition,[2] the term *bioplastic* does not specify the materials' ability to biodegrade, but rather refers to the biomass-origin of the material. Attention should also be drawn to the expression *compostable plastics* because people tend to equate this term with *biodegradable plastics*, but in reality, not all *biodegradable plastics* are compostable under the conditions accessible in a regular home composter.[19]

Probably the final joint opinion on this shortly introduced disconcerting terminology is yet to be more clarified by the scientific community. In this thesis, *biobased polymers* is used for the polymers prepared of monomers originating from biomass.

Due to the increasing demand for polymeric materials and the depletion of fossil feedstock, the research on biobased polymers has increased rapidly during the last decade.[20] Nowadays some of them can be found in everyday applications, e.g., poly(lactic acid).[12] But still, most biobased polymers prepared in laboratory seldom find their way to commercial use. The obstacle is not only the price, but also the poorer quality of the materials and the consequential low competitiveness to fossil-based plastics.[10,21] Additionally, biobased polymers suitable for not only packages, but rather for higher value engineering and speciality applications are hard to achieve. The problem lies in the structure of the monomers. More precisely, there are not many rigid compounds derived from biomass that can pass along their stiffness to the corresponding polymeric materials. The polymers containing rigid monomer units usually also exhibit improved thermal and mechanical properties suitable for high engineering plastics.[22] One such rigid compound from biomass is isosorbide[23] that was chosen as a starting material for this research too.

1.2. Isosorbide

Isosorbide (**1**, Figure 4, left), also known as 1,4:3,6-dianhydro-D-sorbitol and 1,4:3,6-dianhydro-D-glucitol, is a rigid platform chemical produced from sorbitol.[5,24] It is a white hygroscopic crystalline compound with a chemical formula $C_6H_{10}O_4$ and a molecular weight of 146.14 g mol^{-1}.[25] The reported boiling point for isosorbide is 160 °C (10 mmHg) and regarding its stability, it is decomposition occurs at around 270 °C.[25] Additionally, isosorbide is a nontoxic chemical compound.[26] It is soluble in water, alcohols, dioxane, chloroform, and ketones, but almost insoluble in most hydrocarbons, esters, and ethers.[5]

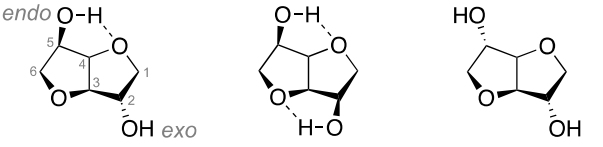

Isosorbide (**1**) Isomannide (**2**) Isoidide (**3**)

Figure 4. Structures of isosorbide, isomannide, and isoidide. Dashed line (- -) between H and O indicates intramolecular hydrogen bonding.

According to molecular structure, isosorbide is a V-shaped chiral diol composed of two *cis*-fused tetrahydrofuran rings with a 120° angle between the rings.[25] Because of the two connected furan units, the overall structure is rigid. Isosorbide is bearing two non-equivalent secondary hydroxyl groups with either *exo* or *endo* configurations at C2 and C5 positions, respectively.[27,28] *Exo* designates the configuration of a group situated outside the V-shaped wedge, and *endo* on the contrary, inside the V-shaped wedge, as can be seen in Figure 4.[27] It should me mentioned that the traditional atom numbering based on carbohydrates is used in this study, as it is also widely implemented in the scientific literature about dianhydrohexitols.

Next to isosorbide, there are also two stereoisomers, isomannide (1,4:3,6-dianhydro-D-mannitol)[29,30] and isoidide (1,4:3,6-dianhydro-L-iditol),[31,32] in which the two hydroxyl groups are in only *endo* or *exo* configuration, respectively (**2** and **3**, Figure 4, middle and right).[27,33] All three isomers are subsumed under a single designation of isohexides (1,4:3,6-dianhydrohexitols).[34] The different configuration of the hydroxyl groups is the reason for the dissimilar physical and chemical properties of the isomers. For example, the melting point of isosorbide is 61.9–64 °C,[5] but for isomannide and isoidide the reported values are 87–88 °C[29] and 43–45.5 °C[27], respectively.

Contrary to its stereoisomers that have only *exo* or only *endo* hydroxyl groups, isosorbide has one *endo*-OH and one *exo*-OH group in the same molecule. This means, the properties of isosorbide are determined by both hydroxyl groups that can exhibit different chemical reactivity depending on the reagents and medium used, but also on steric factors.[25] The *endo* OH-group at C5 forms intramolecular hydrogen bond and has therefore a higher nucleophilicity compared to the *exo* hydroxyl group at C2.[35] On the other hand, the *exo*-OH is sterically less hindered and slightly more reactive in contrast with *endo*-OH.[27]

Typically, the *exo* and *endo* hydroxyl groups in isosorbide have not been differentiated, and therefore, diderivatives have been obtained. But the non-equality of the two hydroxyl-groups also allows to regioselectively functionalize either the C2 or the C5 position in isosorbide structure. Regioselectivity designates the predominant formation of one positional isomer over all other possible positional isomers.[36]

For instance, tosylation of isosorbide with tosyl chloride in pyridine gives preference towards the C5 derivative, despite the higher steric hindrance of the

endo-OH group.[37] On the contrary, acetylation of isosorbide with acetic anhydride in pyridine preferentially affords the C2-substituted product.[38] Additionally, acetylation with acetic anhydride can also give preference towards C5 product, but with PbO at ambient temperature.[39] Likewise, benzylation and allylation of isosorbide have also been investigated thoroughly and can afford either the two derivatives as the major product under selected reaction conditions.[40,41] Consequently, the modification of reaction conditions can favourably give one of the two regioisomers and/or the diderivative of isosorbide.

1.2.1. Synthesis of isosorbide

The synthesis route for isosorbide is very well established and nowadays it is also produced on an industrial scale. The latter makes it an attractive building block for polymer chemists with the ambition to produce polymeric materials of isosorbide on a larger scale.

Isosorbide can be obtained from different carbohydrates of biomass-origin, concisely from D-glucose by hydrogenation and double dehydration sequence (Scheme 2).[23,42,43] Firstly, D-glucose is obtained by depolymerization of polysaccharides (cellulose or starch).[44] Next, catalytic hydrogenation of glucose affords D-sorbitol (D-glucitol), that is also considered among the ten most important biobased platform chemicals.[45] Further, double dehydration of sorbitol yields the desired isosorbide.[46] The last step of cyclodehydration of sorbitol into isosorbide actually involves a two-step mechanism, in which primarily 1,4-sorbitan (77%) and a negligible amount of 3,6-sorbitan (<1%) are formed.[42,47]

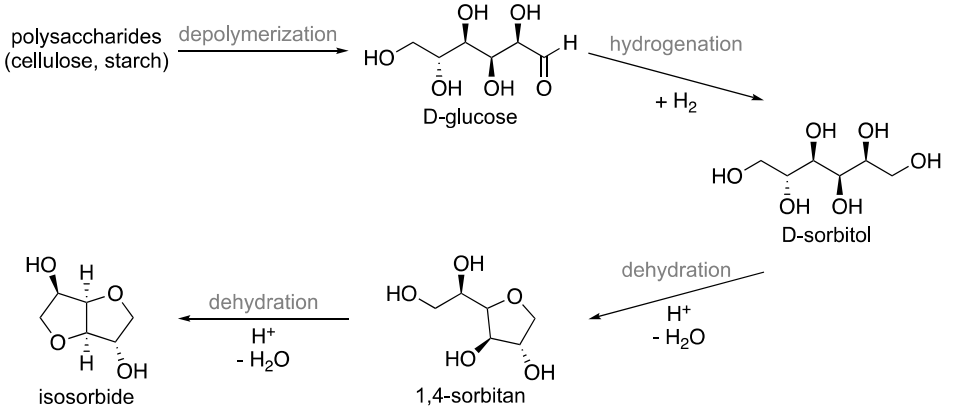

Scheme 2. Synthetic pathway for isosorbide preparation form polysaccharides via D-sorbitol.

The stereoisomeric isomannide can be obtained similarly to isosorbide from fructose by hydrogenation and subsequent cyclodehydration of D-mannitol, but the production process is more expensive as the starting materials are less readily

available.[23,29] The third isomer, isoidide, can be produced from L-idose that rarely exists in nature and that also cannot be extracted from vegetal biomass.[6,31] Even though lately more efficient catalysts have been reported for the epimerization of isosorbide to isoidide,[48,49] both stereoisomer, isomannide and isoidide still remain to be quite expensive substances for manufacturing. Therefore, among the three isomers, isosorbide is the only one produced on an industrial scale. This is well illustrated by the fact that in 2015 a French company called Roquette launched a new unit for the production of isosorbide (POLYSORB®) in Lestrem with a capacity of 20 000 tonnes per year.[50]

Despite the well-known route for isosorbide production, the synthesis can still be enhanced in many aspects. For example, a more sustainable approach could be implemented. One-pot procedure could be the solution, but in this case, a heterogeneous catalyst that is stable in water and tolerates the presence of lignin should be designed.[51] Additionally, a continuous-flow production[52,53] would be a reasonable to implement with the intention to make isosorbide more competitive with the substances derived from fossil feedstock.

1.2.2. Applications of isosorbide and its derivatives

Due to the interesting structural characteristics and availability, isosorbide has been studied and gained importance in a wide variety of applications. In most of these, the sugar derivative has been functionalized through its secondary hydroxyl groups. Less attention has been paid to the preparation of analogues in which the C−O bonds have been substituted with C−C bonds.

Pure isosorbide has been used as diuretic.[26] Additionally, due to its hygroscopic nature, isosorbide has also been applied as humectant in coatings,[54] and in personal care products.[55]

But still, in majority of applications the derivatives of isosorbide are utilized. Probably the most widely known are mono- and dinitrate of isosorbide (Figure 5, left and middle) that are medicines used to cure cardiovascular diseases like angina pectoris and myocardial infarct.[56,57] Another important compound is isosorbide dimethyl ether (Figure 5, right) which can be found in the composition of commercial goods, for example, in dental hygiene[58] and skincare products.[59] But lately it has attracted more attention as a high-boiling green solvent in chemical and pharmaceutical applications.[60, 61]

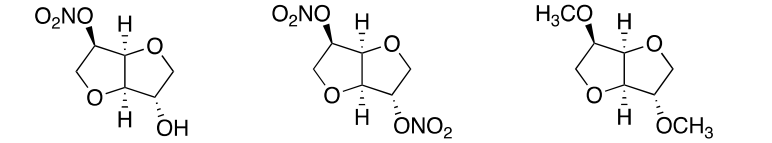

Figure 5. Commonly known isosorbide derivatives.

Furthermore, various derivatives of isosorbide have been used as a ligand in asymmetric synthesis.[62] For instance, isosorbide diphosphite ligand was prepared for Pd-catalyzed asymmetric allylic substitution reactions.[63] In addition, chiral ionic liquids have been synthesized of isosorbide.[64–66]

In the aforementioned examples, isosorbide has been derivatized through its OH-groups. Additonally, there are also compounds containing the subunit of isosorbide with a C–C chain extension through carbons C1 and C6. For example, *kumausallene* (Figure 6)[67] is a natural compound including isosorbide structure, and by a multi-step synthesis the resembling compounds were also afforded as potential antitumour drug candidates,[68] even though this route did not utilize isosorbide as starting material.

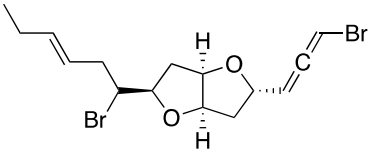

kumausallene

Figure 6. Natural compound that contains the structural unit of isosorbide.

As demonstrated, isosorbide has found use in many fields of research and also in industrial sector. Next to these small compounds derived from isosorbide, another expanding area is polymers containing isosorbide in their structure, which is shortly introduced in the following chapter.

1.2.3. Isosorbide-based polymers to this day

In recent years, isosorbide has gained considerable interest as a building block in polymer chemistry.[6,69] It is assumed that the rigid V-shaped structure of isosorbide is the reason for the enhanced features, like high glass transition temperature (T_g) and improved mechanical properties, of these polymers. T_g denotes the temperature below which an amorphous polymer has the characteristic properties of a glassy state (brittleness, stiffness, rigidity) and above which it is in a viscous liquid form.[1] Hence, T_g is an essential characteristic of a polymer that, according to the desired properties of the material, determines the temperature range in which the polymer can be employed.

Isosorbide has been utilized as a diol in high-performance condensation polymers such as polyesters, polyurethanes, and polycarbonates. The most remarkable examples of isosorbide-based polyesters are probably poly(isosorbide terephthalate)[70], poly(ethylene-*co*-isosorbide)terephthalate[71], and poly(butylene-*co*-isosorbide)terephthalate[72] that all exhibits high T_g-s up to 205, 178, and 92 °C, respectively (Figure 7). These materials enable the preparation of plastic containers with hot-fill opportunity, which is not possible with traditional plastic bottles made of only poly(ethylene terephthalate) (PET, T_g = 72 °C).[73]

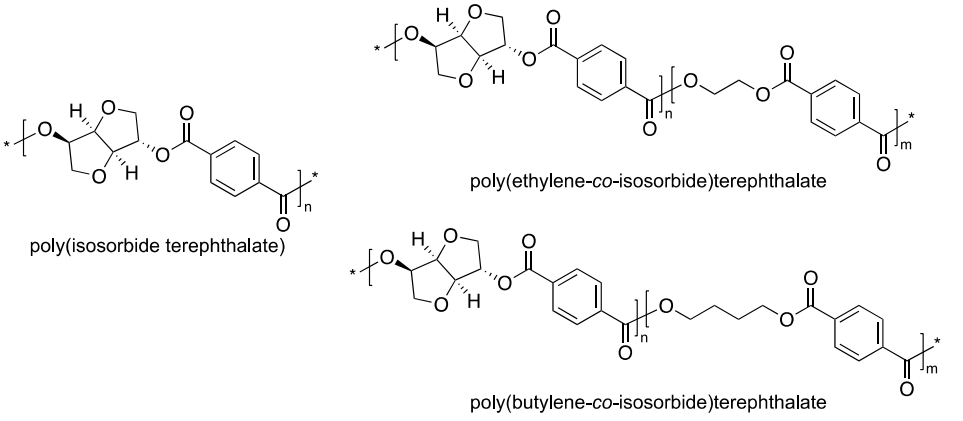

Figure 7. Isosorbide-based polyethers.

Diols are also component used for the synthesis of polyurethanes. Therefore, isosorbide has been reacted with various diisocyanates to corresponding polyurethanes exhibiting T_g-s up to 187 °C and T_m-s up to 235 °C.[74,75] Additionally, isosorbide-based amines[76], isosorbide diisocyanate derivatives,[77–79] and other more complex derivatives[80] have also been used in polyurethanes' structures of which some are possible candidates for biomedical applications (Figure 8, left).

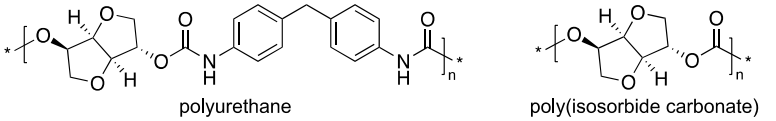

Figure 8. An example of isosorbide-based polyurethane, and structure of isosorbide polycarbonate.

The structural similarity to bisphenol A (BPA, Figure 9, left), a commonly used diol in plastics, has made isosorbide an appealing ingredient in polycarbonates and epoxy resins. The residual BPA in final plastic products may induce chronic toxicity to humans, as it has proven to exhibit endocrine disruptive effect.[81] Therefore, isosorbide is considered to be an innocuous substitute to it. Poly(isosorbide carbonate) prepared under various conditions have shown similar properties to BPA-based polycarbonates (Figure 8, right).[6] Furthermore, copolycarbonates including isosorbide in their structure have been prepared as potential coating materials.[82,83] In addition, a commercial engineering polymer DURABIO™, which is now used in the production of automobile parts, has isosorbide-based polycarbonate in its composition.[84]

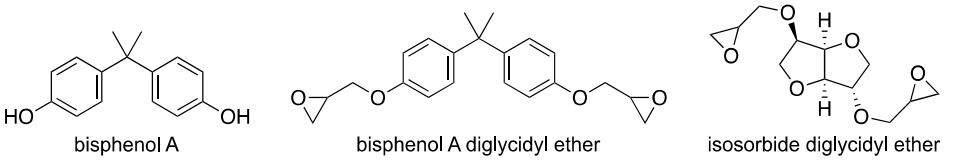

Figure 9. Structures of BPA, diglycidyl ether of BPA, and isosorbide diglycidyl ether.

Isosorbide diglycidyl ether[85] is another compound considered as potential substitute for polymers containing structural units of BPA, more precisely to replace the diclycidyl ether of BPA (Figure 9). This bisepoxides of isosorbide has been extensively studied in the composition of various epoxy networks,[86,87] also hydrogels[88] and resins with isosorbide-based amines.[89,90] The diglycidyl ether of isosorbide can be prepared by a two-step process of sequential allylation and oxidation, or even more easily by the addition of epichlorohydrin (ECH) in aqueous hydroxide solution.[86] In case of the excess of ECH, oligomers and longer polymers fragments can form (Figure 10, left).[91,92]

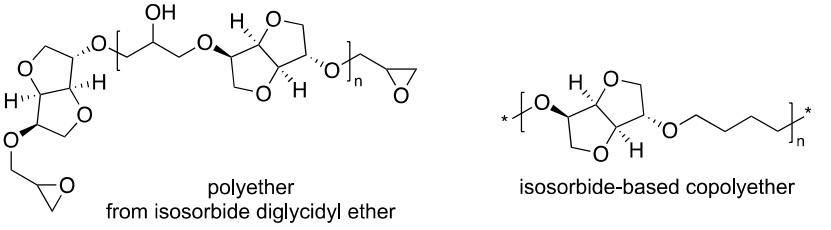

Figure 10. Polyether synthesized from isosorbide diglycidyl ether, and a copolyether of isosorbide.

Copolyethers based on isosorbide and including other chain fractions with a length of 4-12 carbons have also been synthesized (Figure 10, right).[93–95] Lately an interesting study based on annulated isosorbide was conducted by ring-opening polymerization, affording cyclic and linear polyethers (Scheme 3).[96]

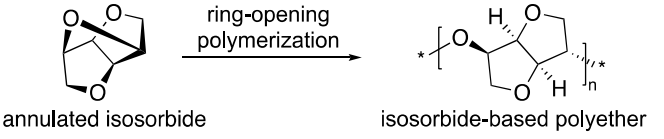

Scheme 3. Polymerization of annulated isosorbide to corresponding polyether.

Due to the possible simultaneous functionalization of its two secondary hydroxyl groups, most isosorbide-based polymers have the entire dianhydrohexitol part incorporated in the backbone of the polymer. On the contrary, polymers having isosorbide unit as pendant groups are not studied so thoroughly yet. This type of polymers can be prepared from the mono-functionalized isosorbide derivatives

that, in turn, are accessible due to the varying chemical reactivity of *endo*- and *exo*-OH group discussed previously in more detail.

Some examples of polymers prepared from isosorbide derivatives with one polymerizable group have been reported. For instance, polymers based on acrylic isosorbide C5-acetates have been demonstrated (Figure 11, left).[97–99] Likewise, isosorbide polymethacrylates have been prepared from methacrylic isosorbide C2-acetates[100] and also, from regioisomeric mixture of corresponding monomers (4:1 = C2-acetate:C5-acetate).[101] In the latter case, for comparison purposes, isomerically pure isosorbide monomethacrylic C5-acetate was separately also polymerized, but it was determined that regiochemistry had no significate impact on the thermal properties of these isosorbide polymers. In comparison, two poly(vinyl-isosorbide-triazole)s from corresponding C2- and C5-triazole isosorbide derivatives (Figure 11, middle) revealed varying solubility and T_g values.[102]

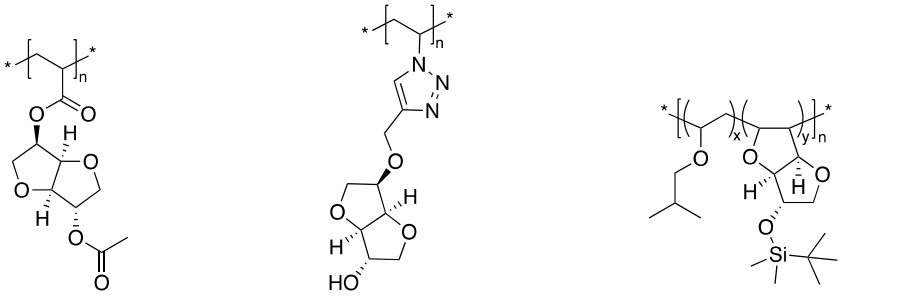

Figure 11. Isosorbide-based polyacrylate and polytriazole, and copolymer from isosorbide-alkene.

Another intriguing polymer containing isosorbide, but in which it is difficult to determine if isosorbide appears as a backbone unit or as a pendant group, is the copolymer of isosorbide- alkene and isobutyl vinyl ether (Figure 11, right).[103] In this case, the polymerization through the functionalized OH-group is avoided and cationic polymerization with unsaturated bonds is achieved.[103]

Based on the presented examples, isosorbide has proven its relevant role as build block in polymer structures, therefore the research on this topic is still of great interest among polymer chemists.

1.3. Polymerization methods

Today we know that polymers are formed by a chemical reaction in which many repeating units called monomers are joined together with covalent bonds. But in the first half of 20th century, when Hermann Staudinger presented the concept of macromolecules, his ideas were not welcomed very well among scientific community.[104] Nevertheless, the principles of polymer science was adopted gradually

and nowadays, it is hard to imagine the world without polymer chemistry nor polymeric materials.

According to reaction mechanism, polymerization methods are divided into two major groups of *chain-growth* and *step-growth* polymerizations.[1] The main differences of the two groups are the species reacting with each other and the molecular weight dependence on the extent of conversion.[1] In case of chain-growth polymerization, initiator is used to start the polymerization reaction and then the growth of the chain occurs by adding one monomer at a time to the active species.[105] So, the molecular weight of the polymer increases rapidly to very high value and at any time, the reaction mixture contains mainly monomers and polymers, but also, small amounts of growing chains.[106]

On the contrary, step-growth polymerization proceeds by the stepwise reaction between the functional groups of the reactants. This means, any two molecular species present (monomer, oligomer, or polymer) can react with each other and the molecular weight of the polymer increases slowly throughout the reaction.[105,106] Besides, large quantities of monomers are already consumed early in the reaction. The difference in reaction kinetics of the two polymerization mechanisms is illustrated in Figure 12 with the average molecular weight dependence on the monomer conversion.[106]

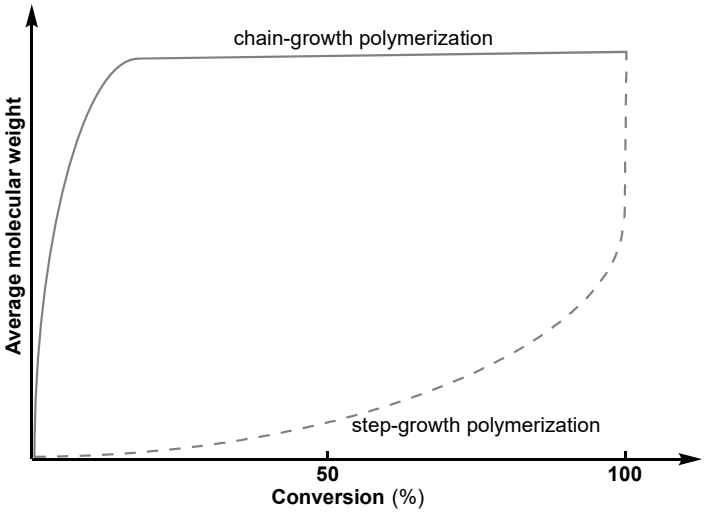

Figure 12. Average molecular weight as a function of monomer conversion for chain-growth and step-growth polymerizations.

Another classification of polymers is based on the polymer structure to *addition* and *condensation* polymers.[1] But, as most *addition* polymers are formed through chain-growth mechanism and most *condensation* polymers by step-growth process, then these terms have not been differentiated in greater detail in this study.[105] However, the two classifications cannot always be used interchangeably. For example, *condensation polymer* is a narrower term compared to *step-growth*

polymer, as the first one includes only these polymers which are formed through polymerization by the elimination of small molecules like water.[1]

After Staudinger proved the concept of polymerization reaction, many different chain-growth methods have been introduced with the aim to prepare various polymeric materials. Since it is hard to include all these numerous methods in one short section, then in the following chapters only the methods used during this study are discussed. Therefore, short overview of only chain-growth polymerizations like conventional radical polymerization of methacrylic monomers, and ionic ring-opening polymerization of epoxides are presented.

1.3.1. Radical polymerization of methacrylates

Commonly applied polymerization method for unsaturated monomers, including methacrylic compounds, is radical chain polymerization that consists of a sequence of three steps: initiation, propagation, and termination. The most widely used initiators in both industrial and research area are thermal homolytic dissociation initiators like peroxides and azo compounds.[107] The most important among the latter group is azobis(isobutyronitrile) (AIBN).[108] In this chapter, radical polymerization mechanism[1,109] is briefly explained.

Firstly, initiator **I** is homolytically cleaved into two radicals **R•** by heating or photolysis. Then the formed initiator radical attacks monomer **M** to afford the first chain initiating radical $\mathbf{M_1}$• (Scheme 4).

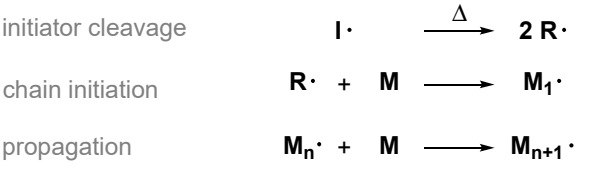

Scheme 4. Initiator cleavage, chain initiation, and propagation in radical polymerization.

Following propagation consists of the growth of polymer chain by the successive additions of many monomer molecules to the initiating species $\mathbf{M_1}$•. Each addition creates a new radical species ($\mathbf{M_{n+1}}$•) that differs from the previous species ($\mathbf{M_n}$•) only by size of one additional monomer unit. Finally, the chain growth stops by termination when two radicals react with each other. It can occur by combination to form one large polymer molecule ($\mathbf{M_{n+m}}$) or disproportionation reactions to form one saturated ($\mathbf{M_n^H}$) and one unsaturated molecule ($\mathbf{M_m^=}$) as shown in Scheme 5.

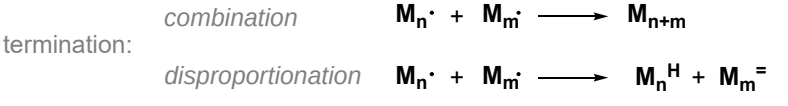

Scheme 5. Termination of radical polymerization by two different ways.

Radical polymerization has proven to be a very facile method for obtaining polymers. It is still widely used on industrial scale as about 45% of synthetic polymers are produced via this method.[107]

Nowadays, next to conventional radical polymerization, more efficient controlled radical polymerization methods, that enable a better definition of the final molecular mass distribution, have been reported. Most commonly known are reversible-deactivation radical polymerization[110] methods like atom-transfer radical polymerization (ATRP),[111] reversible-addition-fragmentation chain-transfer polymerization (RAFT),[112] single-electron transfer living radical polymerization (SET-LRP),[113] etc.

1.3.2. Ionic ring-opening polymerization of epoxides

Ring-opening polymerization is a chain polymerization, including the steps of initiation, propagation, and termination.[1] Anionic and cationic ring-opening polymerizations (AROP and CROP, respectively) are the most commonly used methods for obtaining polyethers from epoxides.[114] In case of anionic mechanism, the chain carriers are anions, and conversely, in case of cationic mechanism, the kinetic chair carriers are cations.[3]

AROP involves initiation of the epoxide by initiator M^+A^- and following propagation step demonstrated in Scheme 6.[1] The reaction is generally initiated by metal hydroxides, alkoxides, oxides, amides, metal alkyls and aryls, or by radical-anion species.[1,115]

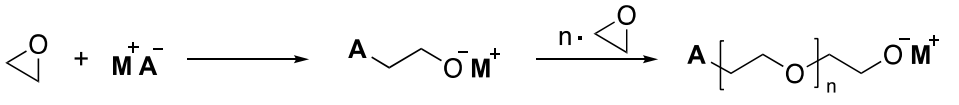

Scheme 6. AROP with ethylene oxide as monomer.

In case of CROP, the principle is similar to AROP, but the chain carriers are cations, and therefore the reaction proceeds via a tertiary oxonium ion (Scheme 7).[1,116] Firstly, initiation with the initiator H^+A^- takes place, and then follows propagation. Generally, strong protic acids like CF_3COOH, HSO_3F, and CF_3SO_3H are used as initiators that form a secondary oxonium ion that react further with a monomer to form tertiary oxonium ion.[1]

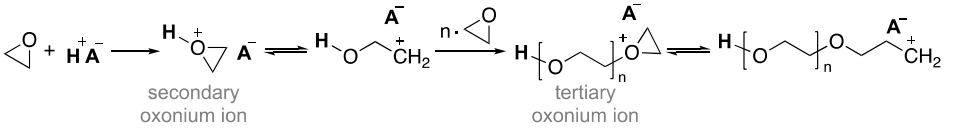

Scheme 7. CROP with ethylene oxide as monomer.

When unsymmetric epoxides are polymerized, then both α and β carbons of the epoxy ring are susceptible to ring-opening and therefore, different polymer chain units can form (Scheme 8).[1,117]

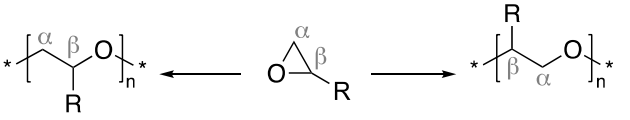

Scheme 8. Formation of different chain units in polymerization of unsymmetrical epoxides.

Ring-opening polymerization of epoxides can also proceed via *activated monomer* mechanism.[1] In case of AROP, epoxide is activated by a Lewis acid catalyst, that reduces the electron density in the epoxide ring and therefore promotes the ring-opening.[118] An "ate complex" composed of the Lewis acid (catalyst) and a weak nucleophile (initiator) is formed in situ and it initiates the polymerization.[115,118] An example of anionic ring-opening polymerization with triisobutylaluminium (*i*-Bu_3Al) as catalyst and tetraoctylammonium bromide ($NOct_4Br$) as initiator is shown in Scheme 9.[119,120] This type of activated monomer mechanism has many advantages, e.g., mild reaction conditions, accessibility to high molecular weight polymers while molecular weight distribution remains narrow.[118]

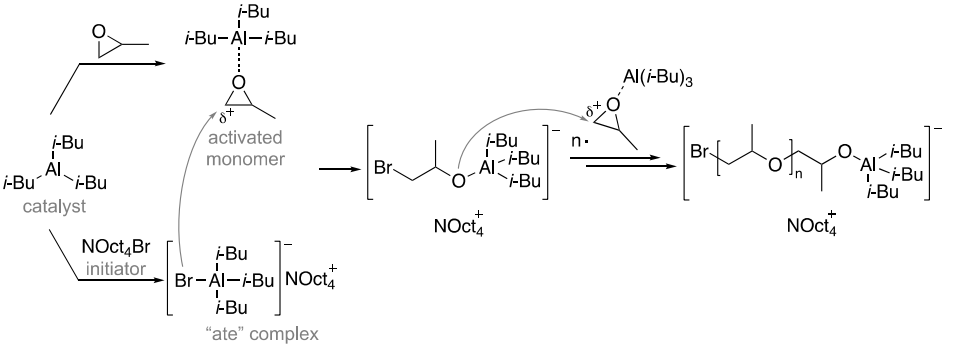

Scheme 9. AROP by *activated monomer* mechanism with propylene oxide as monomer.

When *activated monomer* mechanism is carried out by CROP, then Lewis acids, such as BF_3 etherate, $SnCl_4$, $SbCl_5$, $FeCl_3$, trialkyl oxonium salts, or anhydrides of super acids like CF_3SO_3R, or FSO_3R, are used as initiators.[121] Protic co-initiator, e.g., water, alcohol, or diol, is sometimes needed for interaction with Lewis acids to produce activated monomer that thereafter reacts with a neutral monomer, co-initiator, or chain end.[121] Scheme 10 illustrates the formation of activated monomer with BF_3 etherate as initiator and ROH as co-initiator, and how the activated monomer reacts further with co-initiator to form a macro-monomer, or with a neutral chain end to obtain longer polymer chain, or with a neutral monomer to form an activated chain end.[1,117] Termination occurs by combination of the

propagating ion with either the counterion or an anion derived from the counterion, or by added chain-transfer agent.[1]

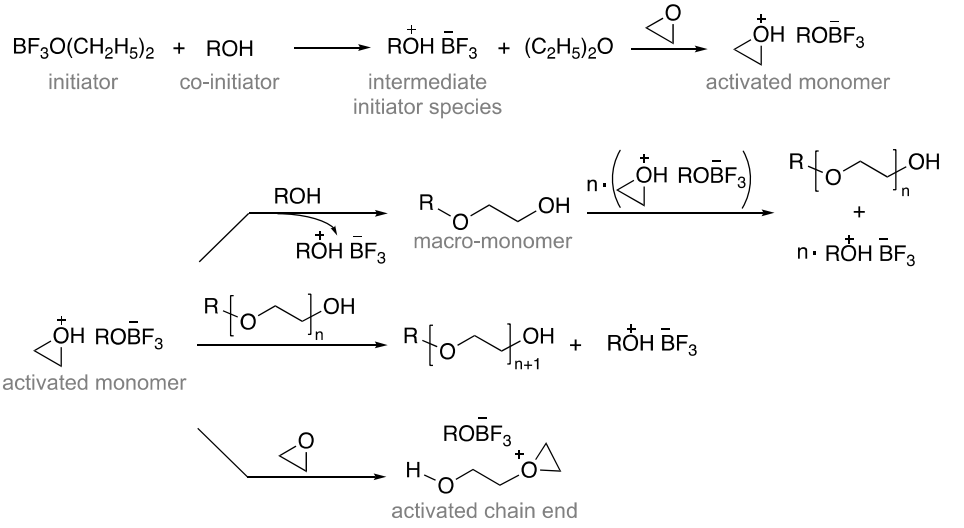

Scheme 10. CROP by *activated monomer* mechanism with ethylene oxide as monomer.

Epoxides, that have a high ring strain, can be polymerized by both, cationic and anionic ring-opening polymerization. Additionally, the activated monomer mechanism has proven to be a very efficient method for obtaining polyethers with high molecular weight.

1.4. Hydroformylation

The reaction between an alkene and synthesis gas (syngas, a 1:1 mixture of CO and H_2) that yields an aldehyde is called hydroformylation (also oxo-reaction or oxonation).[122,123] In case of terminal alkenes, linear and branched aldehydes are formed during this reaction as both sides of the double bond are reactive (Scheme 11).[122] Only ethene yields a single aldehyde as a product. In case of longer terminal alkenes, isomerization of the double bond is possible.[122] A more precise reaction mechanism is represented in the following chapter.

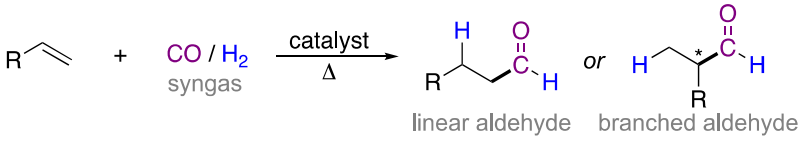

Scheme 11. Hydroformylation of a terminal alkene with syngas. New C–C bond is marked with a bold line.

Hydroformylation was discovered in 1938 by Otto Roelen,[124] when he obtained propanal by the reaction of ethene and syngas in the presence of a cobalt catalyst. From the year 1968, when hydroformylation with rhodium catalysts was developed,[125] the synthesis of aldehydes from aliphatic alkenes became more widely known among industry. Today, hydroformylation is one of the most important transformation carried out in chemical industry with the production reaching nearly 10.4 million metric tons.[126] The conditions required for hydroformylation with syngas are 0.5–30 MPa and 50–130 °C.[123] Additionally, metal catalysts and ligands are needed to determine the selectivity of the products.[126]

Generally, terminal alkenes are the wanted products of industrial hydroformylation process, but in case of organic chemistry, branched aldehydes that can provide stereoisomers might be desired as intermediates for the synthesis of more complex molecular structures.[127] Asymmetric hydroformylation is used in case of a reaction in which a mixture of stereoisomeric aldehydes is obtained, and in this case, additionally to terminal alkenes, alkenes with internal double bond or heterocyclic alkenes are also used.[126,127]

Catalysts employed in hydroformylation reaction are homogeneous transition metal complexes with a general from $[HM(CO)_xL_y]$ in which M is the metal and L is an organic ligand or CO.[123] In industrial applications, the central metal M is usually Rh or Co, but other metals have also been tested on laboratory scale.[128]

Nowadays, precatalysts are frequently used, as they are more stable and also, by the addition of a suitable ligand (or ligands) an active catalyst can be accomplished in a separate vessel before hydroformylation or in situ.[126,127] This type of precatalyst are $HRh(CO)(PPh)_3$, $HRh(PPh)_4$, $Rh(OAc)_3$, $RhCl_3(H_2O)_n$, $Rh_4(CO)_{12}$, Rh(acac)(cod) and $Rh(CO)_2$acac.[126]

Typically, ligands used in hydroformylations are trivalence compounds based on phosphorus, the most common are phosphanes PR_3 and phosphites $P(OR)_3$.[122,123] There are many ligands synthesized to answer the demand for the preparation of various aldehydes, but usually the utilization is still limited by the high price of the ligand.[126]

The traditional hydroformylation process has syngas as the source for CO and H_2, and therefore quite specific apparatus due to high pressure and temperature, but also because of the toxicity of CO, is needed. Nowadays, many alternatives to syngas have been proposed.[129] For example, formaldehyde has been considered as a good alternative because CO and H_2 are formed during its decomposition. Hydroformylation with formalin (formaldehyde 37% solution in H_2O) has been demonstrated as a successful method. Unfortunately, this process is still only used on laboratory scale as the procedure is more complicated and needs expensive catalyst-ligand combinations.[126] For now, the traditional hydroformylation method is still a more straightforward process to be used in the industry.

Aldehydes can be easily converted to other functional groups, for example, to alcohols by hydrogenation, to carboxylic acids via oxidation, and to amines through reductive amination.[122] Therefore, hydroformylation is an important and highly atom-economic method for incorporating new C–C bond into a molecule structure.

1.4.1. Hydroformylation reaction mechanism

The generally accepted hydroformylation reaction mechanism with Rh as a catalyst is illustrated in Scheme 12.[122,130]

The reaction starts with the addition of alkene to the metal catalyst to form π-complex, and after rearrangement, corresponding σ-complex is formed.[122] These two steps determine whether the product will be a linear or a branched aldehyde.[125] Here the catalyst and ligands play an important role.[126]

Next, carbon monooxide enters the cycle and coordinates with the metal atom.[122] Then an acyl species with CO-group situated between metal and alkyl chain is formed.[122,125] In this step new C–C bond is introduced into the molecule. Thereafter, by the addition of gaseous H_2, the aldehyde is separated from the catalyst by reductive elimination, and the catalyst is regenerated.[122] Thus, the reaction cycle can start again from the beginning.

Alongside rhodium, other metal catalysts and also, various ligands are used to perform hydroformylation reaction.[126,128] The mechanism can vary depending on the components, but the overall reaction path is analogous to the one presented here.

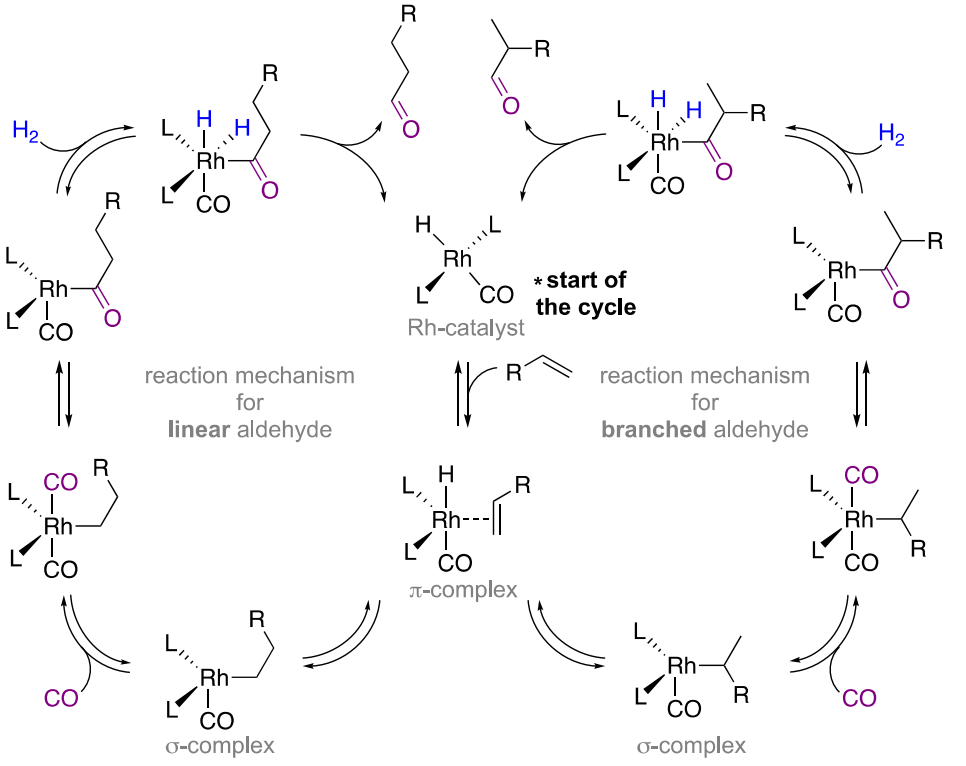

Scheme 12. Hydroformylation reaction mechanism. L is an organic ligand or CO.

2. AIMS OF THE STUDY

The main objective of the current thesis was to prepare novel isosorbide-based compounds and polymers. To reach that aim, the work was divided into three parts:

1) synthesis of different isosorbide polymethacrylates and the investigation of the effect of different side chains on the properties of polymers,

2) polymerization of isosorbide monoepoxides and examination of the properties of these novel polyethers,

3) synthesis of isosorbide aldehydes from corresponding olefinic derivatives by hydroformylation method to obtain C–C elongated isosorbide-based monomers for novel polymeric materials.

3. RESULTS AND DISCUSSION

Firstly, radical polymerization of isosorbide monomethacrylates and characterization of the obtained polymers is discussed. Then follows the synthesis of polyethers from isosorbide monoepoxides, including copolymerization reactions with commercially available polymers. Finally, the results of the synthesis of olefinic derivatives of isosorbide and the consecutive hydroformylation of the obtained alkenes is presented.

3.1. Polymerization of isosorbide monomethacrylates

Paper I

Novel enzymatic synthesis method for the 5-methacrylate of isosorbide was developed by our research group. By using this biocatalytic or chemical acylation, a series of 5-*endo*-methacrylates and 2-*exo*-methacrylates of isosorbide were prepared (Figure 13). These included methacrylates with free OH-group (**M1** and **M2**), acetate group (**M3** and **M4**), dodecanoate (**M5** and **M6**) and cyclohexanoate (**M7**) as side chains. Monomers with odd numbers are *endo*-methacrylates and with even number *exo*-methacrylates of isosorbide.

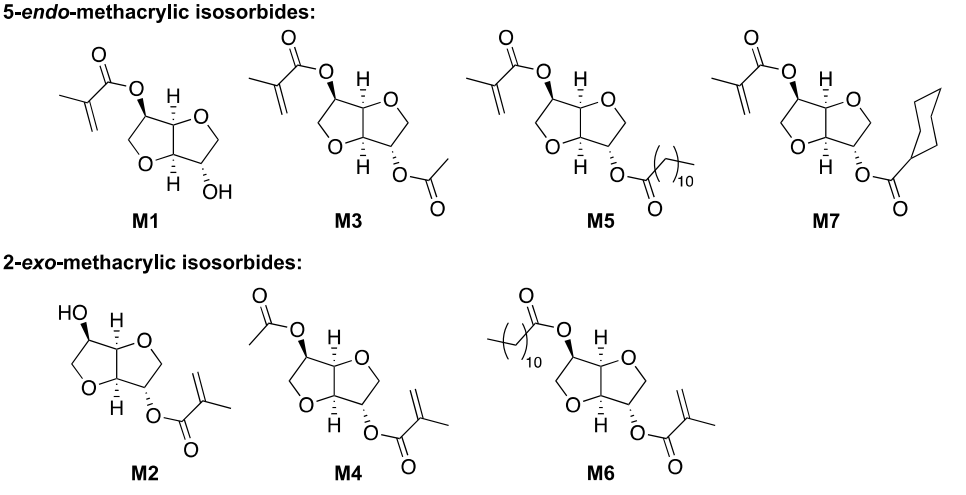

Figure 13. Structures of isosorbide monomethacrylates **M1**–**M7**.

Thereafter, all methacrylic monomers **M1–M7** of isosorbide were polymerized to corresponding polymethacrylates **PM1**–**PM7** by conventional radical polymerization with azobis(isobutyronitrile) (AIBN, 0.5 mol%) as initiator in a solution for 24 h, in an oven at 60 °C. Dimethyl sulfoxide (DMSO) was used as solvent for monomers **M1** and **M2**, ethyl acetate (EtOAc) for methacrylates **M3**–**M7**. Prior to polymerization, the reaction mixture was sparged with argon for

around 45 minutes to remove oxygen from the solution. The polymerization results are presented in Table 1.

Monomer conversions, that were determined by ^{1}H NMR spectroscopy from crude mixture, were very high, up to 96% and 97% for **PM1** and **PM2**, respectively (Table 1, entries 1 and 2). After polymerization reaction, the crude mixture was precipitated into a suitable solvent to remove any residual monomer and filtered from the same solvent, the procedure was repeated three times. Polymers **PM1** and **PM2**, that were precipitated into a mixture (5:1) of diethyl ether (Et_2O) and isopropanol, and filtrated, were obtained as white powders. Polymethacrylates **PM3**, **PM4**, and **PM7** appeared also as white powders after precipitating into and filtrated from Et_2O. Polymers with longer acyl chain, **PM5** and **PM6** were found to precipitate best in MeOH and obtained after final filtration as whitish powder too.

Table 1. Radical polymerization of isosorbide monomethacrylates **M1**–**M7** with AIBN.

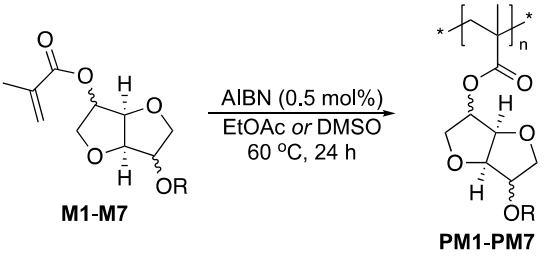

Entry	Monomethacrylate	Polymer	R	Methacrylate conv.[a]	M_n (kg mol^{-1})[b]	$Đ$[b]	$T_{d,95}$ (°C)[c]	$[\eta]$ (dL g^{-1})[d]
1	**M1**	**PM1**	H	96%	n.d.[e]	n.d.[e]	238	0.82
2	**M2**	**PM2**	H	97%	n.d.[e]	n.d.[e]	240	0.46
3	**M3**	**PM3**	$(CO)CH_3$	88%	35	2.6	223	0.30
4	**M4**	**PM4**	$(CO)CH_3$	89%	26	2.8	210	0.28
5	**M5**	**PM5**	$(CO)(CH_2)_{10}CH_3$	87%	43	2.7	226	0.33
6	**M6**	**PM6**	$(CO)(CH_2)_{10}CH_3$	88%	48	2.4	222	0.32
7	**M7**	**PM7**	$(CO)(C_6H_{11})$	89%	42	2.9	208	0.33

[a]Conversion determined from crude polymer ^{1}H NMR spectra. [b]Determined by SEC in THF using poly(ethylene oxide) standards (M_n = 3860, 12 600, 49 640, and 96 100 g mol^{-1}). [c]Determined by TGA under N_2 at 5% weight loss. [d]Intrinsinc viscosity measures at 21 °C in DMSO for **PM1**–**PM4** or in toluene solutions (**PM5**–**PM7**). [e]n.d., not determined (polymer **PM1** and **PM2** were insoluble in THF).

Additionally, the solubility of polymethacrylates was evaluated in a range of solvents categorized according to the hydrogen-bonding capacity and solubility parameter (δ) at 21 °C (for results, please refer to Table S1 in Supplementary Information of Paper I). None of the polymers were found soluble in polar strongly hydrogen-bond-forming solvents (H_2O, MeOH, 1-BuOH), nor in nonpolar moderately hydrogen-bonding Et_2O (δ = 19 $MPa^{½}$). Polymers **PM1** and **PM2** bearing OH-groups were found soluble only in DMSO, a moderately hydrogen-bonding solvent (δ = 25 $MPa^{½}$). Additionally, acetate functional **PM3** and **PM4** were also soluble in DMSO. Chloroform and THF, that have the same solubility parameter value (δ = 19 $MPa^{½}$), but are moderately and poorly hydrogen-bonding, respectively, dissolved very well the polymers with acyl chain **PM3**–**PM7**. Because hydroxyl functional **PM1** and **PM2** did not solubilize in THF nor in $CHCl_3$, the size-exclusion chromatography (SEC) analysis, which helps to determine the molecular mass of the polymers, was not possible to carry out for these two samples. Poorly hydrogen bonding acetonitrile (ACN, δ = 24 $MPa^{½}$), was found to dissolve polymethacrylates **PM3** and **PM4** with acetate groups. Conversely, polymers **PM5**, **PM6**, and **PM7** solubilized in toluene (δ = 18 $MPa^{½}$), that is also a poorly hydrogen-bonding medium. No difference in solubility was determined for polymers of regioisomeric isosorbide monomethacrylates (**PM1** vs **PM2**, **PM3** vs **PM4**, **PM5** vs **PM6**).

Number average molecular weights (M_n) and polydispersity indexes ($Đ$) were determined by SEC for polymers **PM3**–**PM7** that were found to dissolve in THF (Table 1, entries 3–7; Figures S25–S27 in Supplementary Information of Paper I). With 0.5 mol% AIBN, the M_n values varied from 26 kg mol^{-1} for **PM4** to 48 kg mol^{-1} for **PM6**, and $Đ$ values fluctuated between 2.4 to 2.9. In case of monomers **M3** and **M4**, other AIBN concentrations (0.25, 0.13, 0.06 mol%) were also tested. It could be seen that M_n of the polymer increased when AIBN concentration was decreased (for precise values, please refer to Table 1 in Paper I). Regarding M_n and $Đ$ values, also no significant difference was found for polymethacrylates synthesized from regioisomeric monomers.

Next, the thermal properties of isosorbide polymethacrylates were determined. Firstly, thermal stability under N_2 with thermogravimetric analysis (TGA) was investigated. All polymethacrylates exhibited thermal decomposition temperature at 5% weight loss ($T_{d,95}$) over 200 °C (Figure 14). Hydroxyl functional **PM1** and **PM2** showed the highest $T_{d,95}$ of 238 and 240 °C, respectively (Table 1, entries 1 and 2). Somewhat lower were the thermal stability of **PM3** ($T_{d,95}$ = 223 °C) and **PM4** ($T_{d,95}$ = 210 °C) with acetate groups (Table 1, entries 3 and 4). These values are similar to the one reported in the literature for isosorbide polymethacrylate synthesized from 4:1 *endo* and *exo* acetate mixture, $T_{d,95}$ = 251 °C under N_2.[101] Polymers **PM5** and **PM6** with dodecanoate chains exhibited $T_{d,95}$ of 226 and 222 °C, respectively (Table 1, entries 5 and 6). Lastly, polymethacrylate **PM7** showed thermal stability $T_{d,95}$ of 208 °C (Table 1, entry 7). It can be concluded in reference to $T_{d,95}$ values, that polymers of regioisomeric monomers did not exhibit considerably diverse thermal stability.

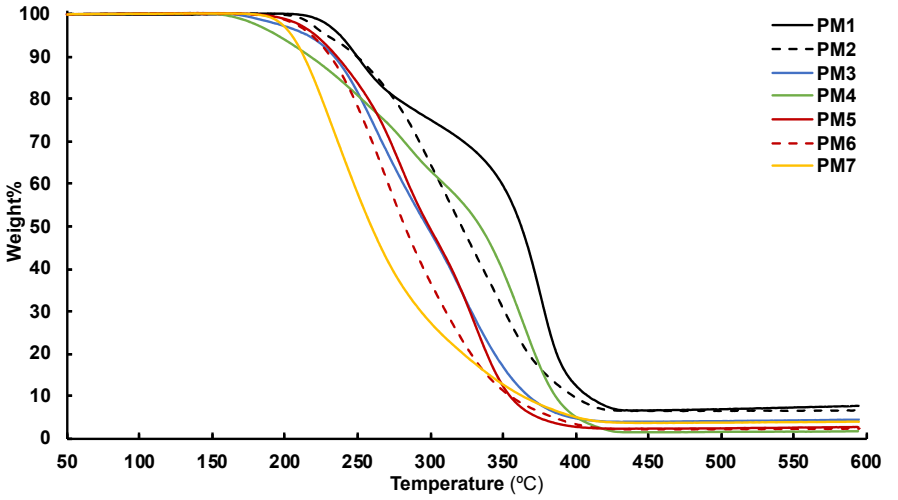

Figure 14. TGA profiles of isosorbide polymethacrylates **PM1**–**PM7**.

Turning to the glass-transition temperatures (T_g) of isosorbide polymethacrylates that were determined by differential scanning calorimetry analysis (DSC) with a scan rate of 10 °C min^{-1}. The polymers **PM3**–**PM7** were first heated to 150 °C, then cooled down to 0 °C, and finally heated to 150 °C. Polymers **PM1** and **PM2** were heated to 195 °C. The T_g values of all the polymers were evaluated from the second heating scans by identifying the inflection points (Figure 15). Polymethacrylates **PM1** and **PM2** both exhibited a very high T_g value of 167 °C. Polymers with acetate group **PM3** and **PM4**, and with cyclohexanoate chain **PM7** showed similar T_g's of 133, 129, and 129 °C, respectively. Again, the T_g's of acetate functional polymethacrylates were consistent with the one reported in literature (130 °C). The T_g values measured for polymers synthesized with other initiator concentrations (AIBN 0.25, 0.13, 0.06 mol%) of monomers **M3** and **M4** did not show large differences and remained around 130 °C as for **PM3** and **PM4** (for precise values, please refer to Figures S22 and S23 in Supplementary Information of Paper I). Usually, T_g increases in accordance with M_n, but in this case the M_n values were not dissimilar enough to have an impact to the T_g's. It can be seen that, the measured T_g values of isosorbide polymethacrytes are higher in comparison to the T_g's of commercially known thermoplastics like poly(methyl methacrylate) (T_g = 105 °C) and polystyrene (T_g = 100 °C).[73]

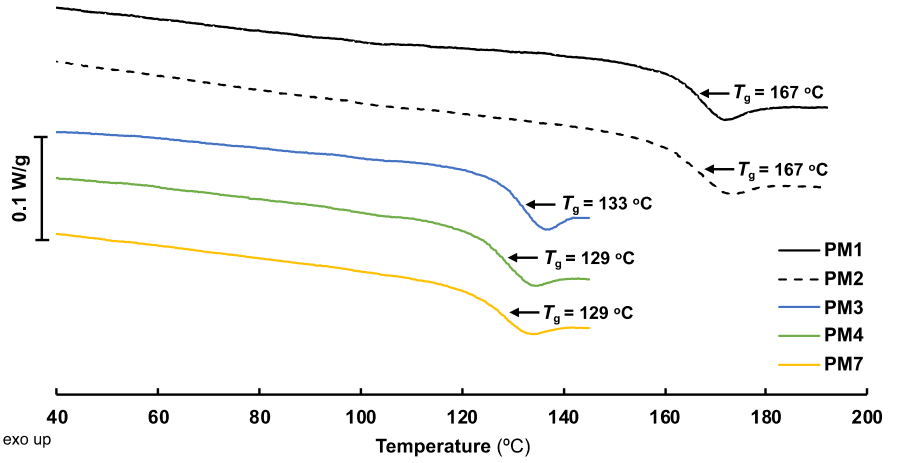

Figure 15. DSC heating curves of polymer **PM1**, **PM2**, **PM3**, **PM4**, and **PM7**.

It is apparent that no significant difference caused by the regioisomeric monomers could be determined with **PM1** vs **PM2**, and **PM3** vs **PM4**. But regarding polymethacrylates **PM5** and **PM6** more than a 10 °C difference in T_g was seen (66 and 54 °C, respectively), but even more significant is the small transition at around 83 °C (ΔH = 3.9 J g^{-1}) that was seen only in the DSC heating curve of **PM5** with *exo*-dodecanoate chain (Figure 16). Conversely, polymer **PM6** with *endo*-dodecanoate chain did not exhibit any transition in this region during heating cycle (Figure 16). It can be hypothesized that the substituents at *endo* position are sterically more shielded that *exo*-groups and therefore, this structural peculiarity of the rigid isosorbide might be the reason for different physical characteristics. Generally, the T_g's of **PM5** and **PM6** were much lower compared to other isosorbide methacrylates (**PM1**–**PM4**, and **PM7**), that is probably because of the additional free volume induced by flexible alkyl chains.

Additionally, a copolymer with 1:1 molar ratio of monomers **M5** and **M6** was prepared. This copolymer **PM(5+6)** with T_g of 65 °C also exhibited a similar transition close to 83 °C (ΔH = 2.7 J g^{-1}, Figure 16) in the heating curve. From the dissimilar thermal properties of **PM5** and **PM6**, it could be deduced that regiochemistry of this type of isosorbide-based monomers has an essential part in the formulation and properties of the corresponding polymers. Therefore, a series of isosorbide-based 5-methacrylates with alkanoyl chains spanning from C2 to C20 were polymerized and characterized in further research by our group (Paper IV). It was discovered that the transition at 83 °C in the DSC curve of **PM5** and **PM(5+6)** was rather an endothermic order-to-disorder transition (not melting temperature T_m as referred in Paper I). This transition is also clarified by an illustrative figure in Paper IV. Additionally, it was observed that polymers with sufficiently long alkanoyl unit exceeding 13 carbons were semicrystalline materials and formed mesophases (presumably nematic liquid crystalline phase)

above their T_m. Besides, it was showed that C18-alkanoyl-isosorbide polymethacrylate from regioisomeric 2-methacrylate with *endo*-alkanoyl chain had no such transitions and therefore, no formation of mesophase. Thus, it was proved that the substitution and orientation of the isosorbide units in the polymethacrylates can be very important in this type of polymers.

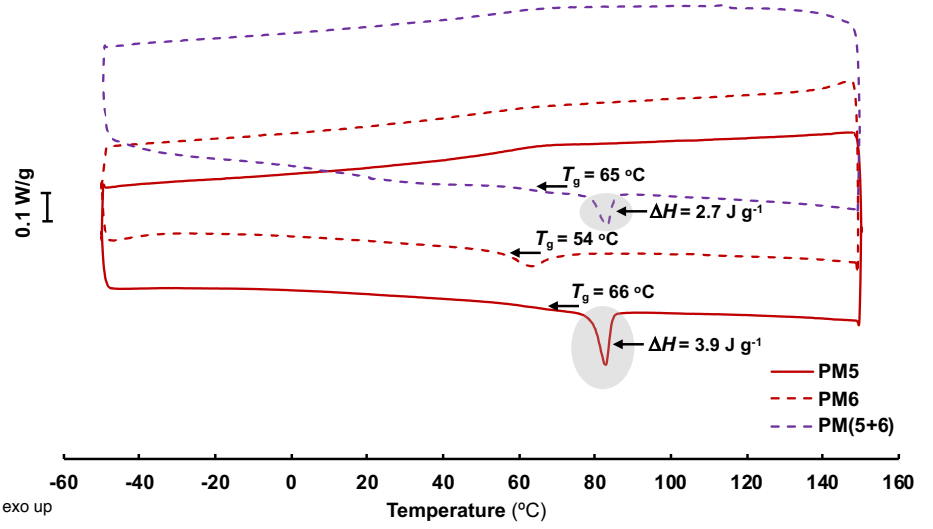

Figure 16. DSC heating and cooling curves of polymers **PM5**, **PM6**, and **PM(5+6)**. Potential order-to-disorder transition marked with a grey circular shape.

The properties of isosorbide polymethacrylates were also compared in DMSO (**PM1**–**PM4**) and toluene (**PM5**–**PM7**) solutions according to intrinsic viscosity [η]. From these results, a clear difference in case of **PM1** and **PM2** prepared from regioisomeric monomers **M1** and **M2**, respectively, could be seen (Table 1, entries 1 and 2). The viscosity of **PM1** was about two times higher than for **PM2** (0.82 and 0.46 dL g^{-1}, correspondingly). It was speculated that the free *exo*-OH in **PM1** can exhibit additional intermolecular hydrogen bonding between polymer chains, as *endo*-OH tends to form intramolecular hydrogen bonds.[35] The latter claim is supported by the acidic nature of the *exo*-OH of **PM1** illustrated by its more downfield shift in ^{1}H NMR spectrum in comparison to **PM2** (for NMR spectra, please refer to Figure 5 in Paper I).

Acetate functional **PM3** and **PM4** exhibited slightly lower [η] of 0.30 and 0.28 dL g^{-1} in DMSO, respectively (Table 1, entries 3 and 4), slightly lower viscosity compared to **PM1** and **PM2** probably because these polymers do not have free OH-groups that can form H-bonds. As polymers **PM5**–**PM7** were not fully soluble in DMSO, then their viscosity was measured in toluene solutions. **PM5** and **PM6** had similar [η] of 0.33 and 0.32 dL g^{-1}, respectively, and polymer **PM7** also exhibited viscosity of 0.33 dL g^{-1} (Table 1, entries 5–7).

In this study, a series of isosorbide 2-*exo*- and 5-*endo*-monomethacrylates were polymerized to corresponding polymers via conventional radical polymerization. The results demonstrate the possibility to optimize the properties of isosorbide-based polymer by the choice of *endo*/*exo*-methacrylic monomer, and also, by the various substituents in monomer structures. Moreover, the high T_g's exhibited by these biobased polymethacrylates make them appealing for higher value engineering plastics and speciality applications.

3.2. Polymerization of isosorbide monoepoxides

3.2.1. Isosorbide polyethers

Paper II

Monoepoxides of isosorbide (**E1** and **E2**) that were used for the synthesis of polyethers are shown in Figure 17. Epoxides **E1** and **E2** were prepared from isosorbide by allylation with allyl bromide and subsequent oxidation with *meta*-chloroperoxybenzoic acid (for more details about the synthesis of epoxides, please refer to Paper II).

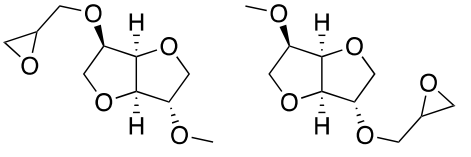

Figure 17. Isosorbide monoepoxides used in this research.

Different cationic and anionic ring-opening polymerization (CROP and AROP) methods were tried to homopolymerize the regioisomeric isosorbide mono-epoxides **E1** and **E2** to corresponding polyethers **PE1** and **PE2** (Scheme 13).

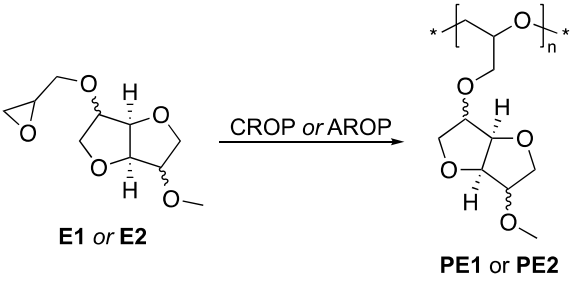

Scheme 13. Polymerization of isosorbide monoepoxides **E1** and **E2** to polyethers **PE1** and **PE2**, correspondingly.

First, homopolymerization attempts were carried out following CROP (for more details, please refer to Table 8 in Chapter 4.1). Both epoxides, **E1** and **E2** were polymerized using 1,4-butanediol (BD) as an initiator and boron trifluoride diethyl etherate (BF_3OEt_2) as a catalyst. In this case, the initiation was performed at 0 °C and then the reaction mixture was let to increase to room temperature. After less than an hour a solid precipitate formation was observed for both epoxides. The obtained solid material was not soluble in any solvent available in common organic chemistry laboratory (DMSO, CH_2Cl_2, ACN, MeOH, 1-BuOH, toluene, $CHCl_3$, Et_2O, hexane). Cationic polymerization are very sensitive

methods. Probably the reaction between BF_3OEt_2 and epoxides happened very fast and therefore, side reactions occurred, as a result a crosslinked polymer structure was formed. It was decided to not look more deeply into this method and try other cationic ring-opening polymerization methods. Therefore, catalysts such as CF_3SO_3H, $SnCl_4$, $AlCl_3$, $Sc(OTf)_3$ were also tested. Unfortunately, no polymers were detected by ^1H NMR spectroscopy. In case of CF_3SO_3H decomposition of the epoxy ring was seen.

As cationic polymerizations were not so successful, it was decided to try *monomer activated* AROP methods. Recently a living ring-opening polymerization of epoxides catalyzed by an organobase and triethylborane (Et_3B) was reported.[131] It was decided to apply this method to isosorbide monoepoxides by using phosphazene bases (PB_1 or PB_2, Figure 18) and Et_3B as the Lewis Pair Catalyst and H_2O as initiator at room temperature (Table 2, entries 1–4). Unfortunately, monomers **E1** and **E2** did not polymerize under these conditions, and even no conversion of epoxides was detected by ^1H NMR spectra. Therefore, this method was not successful in case isosorbide monoepoxides.

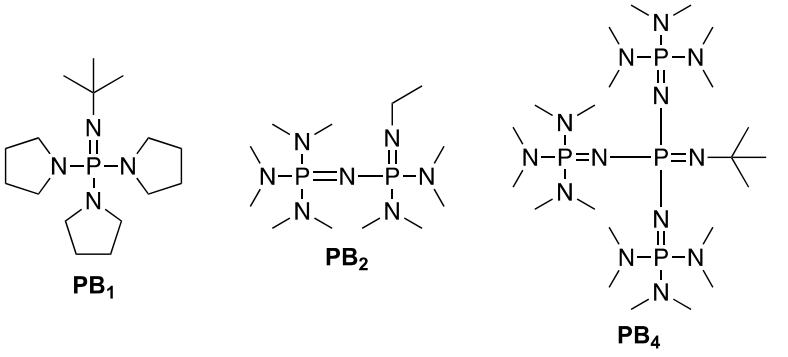

Figure 18. The structure of phosphazene bases PB_1, PB_2, and PB_4 used in this research.

Next, AROP with PB_4 (Figure 18, right) as deprotonating agent, triisobutylaluminium (*i*-Bu_3Al) as an activator, and butane diol (BD) as initiator was applied.[132] Epoxide **E1** conversion by this method was 10%, nonetheless, it was possible to purify the polymer by precipitation into Et_2O (Table 2, entry 5). After filtration and drying, SEC analysis in THF was carried out, but the molecular weight of the obtained polymer turned out to be very low, 2.0 kg mol^{-1} with $Đ$ of 1.1. Results for **E2** were similar, conversion was a bit higher (40%), but M_n still only 2.5 kg mol^{-1} with $Đ$ of 1.4 (Table 5, entry 6).

Grignard reagents have also been used as deprotonating agent in the ring-opening polymerization of epoxides.[133] Methylmagnesium bromide (MeMgBr) was chosen for deprotonation of the initiator (1-BuOH) in the polymerization reaction of **E1** and **E2** with *i*-Bu_3Al as an activator in 2-MeTHF (Table 2, entries 7 and 8). These experiments were not successful either, as no conversion of epoxide was detected.

Table 2. Different AROP experiments with epoxides **E1** and **E2**.[a]

Entry	Epoxide	Initiator	DA[b]	Catalyst	Reaction conditions	[epoxide]/ [initiator]/ [DA]/[catalyst]	Epoxide conv.[c]
1	**E1**	H_2O	PB_1	Et_3B	**(1)**	80/1.0/0.05/0.15	0%
2	**E1**	H_2O	PB_2	Et_3B	**(1)**	80/1.0/0.05/0.15	0%
3	**E2**	H_2O	PB_1	Et_3B	**(1)**[d]	80/0.5/0.05/0.15	0%
4	**E2**	H_2O	PB_2	Et_3B	**(1)**	80/1.0/0.05/0.15	0%
5	**E1**	BD	PB_4	*i*-Bu_3Al	**(2)**	90/1/2/5	10%[e]
6	**E2**	BD	PB_4	*i*-Bu_3Al	**(2)**	90/1/2/5	40%[f]
7	**E1**	1-BuOH	MeMgBr	*i*-Bu_3Al	**(3)**	23/1/1/1.5	0%
8	**E2**	1-BuOH	MeMgBr	*i*-Bu_3Al	**(3)**	46/1/1/2	0%

[a]Reaction conditions **(1):** THF, [epoxide] = 7 mol L^{-1}, 24 h, r.t.; **(2)**: toluene, [epoxide] = 2 mol L^{-1}, 24 h, –30 °C to r.t.; **(3)**: 2-MeTHF, [epoxide] = 3 mol L^{-1}, 24 h, –30 °C to r.t. [b]Deprotonating agent. [c]Conversion determined by ^{1}H NMR spectroscopy. [d][epoxide] = 2 mol L^{-1}. [e]M_n = 2.0 kg mol^{-1}, $Đ$ = 1.1. [f]M_n = 2.5 kg mol^{-1}, $Đ$ = 1.4.

After so many unsuccessful experiments, finally a method that afforded the wanted polymers was found. AROP in toluene with tetraoctylammonium bromide ($NOct_4Br$) as initiator and *i*-Bu_3Al as an activator provided polyethers **PE1** and **PE2** with monomer conversions of 99% and 89%, respectively (Table 3, entries 2 and 3). The combination of $NOct_4Br$ and *i*-Bu_3Al has been widely used for polymerizing other epoxides also.[119, 120, 134-137]

Table 3. Anionic ring-opening polymerization of isosorbide epoxides with $NOct_4Br$ as an initiator and *i*-Bu_3Al as a catalyst.

Entry	Epoxide	Polymer	[epoxide]/ [$NOct_4Br$]/ [*i*-Bu_3Al]	Epoxide conv.[b]	M_n (kg mol^{-1})[c]	$Đ$[c]	T_p (°C)[d]
1	**E1**	–	100/0.4/1.2	0%	–	–	–
2	**E1**	**PE1**	100/0.4/2.3	99%	13.2	1.7	390
3	**E2**	**PE2**	100/0.4/2.3	89%	17.8	2.1	394

[a]Reaction conditions: toluene, [epoxide] = 3 mol L^{-1}, –30 °C to r.t. [b]Conversion determined from crude polymer ^{1}H NMR spectra. [c]Determined by SEC in THF using poly(ethylene oxide) standards (M_n = 3860, 12 600, 49 640, and 96 100 g mol^{-1}). [d]Determined by TGA under N_2 from DTG curve.

Firstly, the solubility of the two polyethers was evaluated using the same method as was applied for isosorbide polymethacrylates. Wide variety of solvents categorized according to their hydrogen-bonding capacity and solubility parameter (δ) were tested at 21 °C (for more details, please refer to Table S1 in Supplementary Information of Paper II). Even though the polyethers **PE1** and **PE2** have many oxygens atoms in their structure, that can act as hydrogen bond acceptors,

both polymers were found insoluble in strongly H-bonding H_2O (δ = 48 $MPa^{½}$) and 1-BuOH (δ = 23 $MPa^{½}$). Conversely, these polyethers did dissolve in MeOH (δ = 30 $MPa^{½}$). Moderately hydrogen-bonding DMSO (δ = 25 $MPa^{½}$) and THF (δ = 19 $MPa^{½}$) were also found suitable for solubilizing polyethers **PE1** and **PE2**. As expected, the nonpolar moderately H-bonding Et_2O did not dissolve isosorbide-based polymers **PE1** and **PE2**. Therefore, this solvent was chosen for the precipitation of these polymers in order to remove monomer residues. Poorly hydrogen-bonding ACN that has the solubility parameter δ similar to DMSO (24 and 25 $MPa^{½}$, respectively) did not dissolve polyethers **PE1** and **PE2** unlike to DMSO. By contrast, $CHCl_3$ (δ = 19 $MPa^{½}$) and toluene (δ = 18 $MPa^{½}$) both were found as suitable solvents for solubilizing polymers **PE1** and **PE2**, even though these two are also poorly H-bonding in essence. It can be concluded that the two polymers of regioisomeric monomers **E1** and **E2** did not exhibit difference in solubility among the tested solvents.

Analysis by SEC in THF revealed number average molecular weight of 13.2 kg mol^{-1} and $Đ$ = 1.7 for polymer **PE1** (Table 3, entry 2), but polymer **PE2** had a bit higher M_n of 17.8 kg mol^{-1} and also, a higher polydispersity index of 2.1 (Table 3, entry 3; Figure S1 in Supplementary Information of Paper II). Generally, molecular weights of these polyethers are lower and $Đ$ values are higher compared to poly(propylene oxide)[119] and poly(epichlorohydrin)[134] prepared using the same method. The cause can be the complexation of *i*-Bu_3Al by oxygen atoms (Figure 19).[118] In isosorbide monoepoxide there are altogether five oxygen atoms, but e.g., in propylene oxide and epichlorohydrin there are only one oxygen atom that can coordinate with *i*-Bu_3Al. Due to the rigid structure of isosorbide monoepoxides, it is hard to assess which oxygen atoms are coordinated at the same time with one *i*-Bu_3Al molecule and which are not. Therefore, an excess of catalyst (*i*-Bu_3Al) with respect to the initiator ($NOct_4Br$) is needed to overcome this strong coordination capability.[118] With isosorbide polyethers this phenomenon was also seen clearly, because with a smaller amount of *i*-Bu_3Al no polymer was detected by ^1H NMR (Table 3, entry 1).

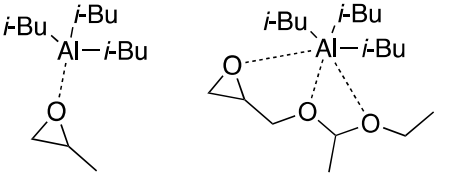

Figure 19. Complexation of *i*-Bu_3Al molecule by one oxygen atom in propylene oxide and by three oxygen atoms in ethoxy ethyl glycidyl ether.

The onset of thermal decomposition measured by TGA under N_2 can be seen at around 300 °C in the DTG curves (Figure S2 in Supplementary Information of Paper II) for both polyethers. The peak temperatures (T_p) at highest mass-loss rates for the polyethers were 390 °C for **PE1** and 394 °C for **PE2**, therefore a

negligible difference between the two polymers from regioisomeric monomers can be seen.

Next, T_g of isosorbide polyethers were determined by DSC with a scan rate of 10 °C min^{-1}. The polymers **PE1** and **PE2** were first heated to 150 °C, then cooled down to –50 °C, and finally heated to 150 °C. The T_g values of the polyethers were evaluated from the second heating scans by identifying the inflection points (Figure 20). Polymer **PE1** exhibited glass transition at 10 °C and **PE2** at 15 °C. These T_g values are quite high compared to T_g's of other polyethers poly(propylene oxide) (–74 °C) and poly(epichlorohydrin) (–22 °C).[73] The reason for this phenomenon is apparently the stiff isosorbide unit in the side chain of the polymer.

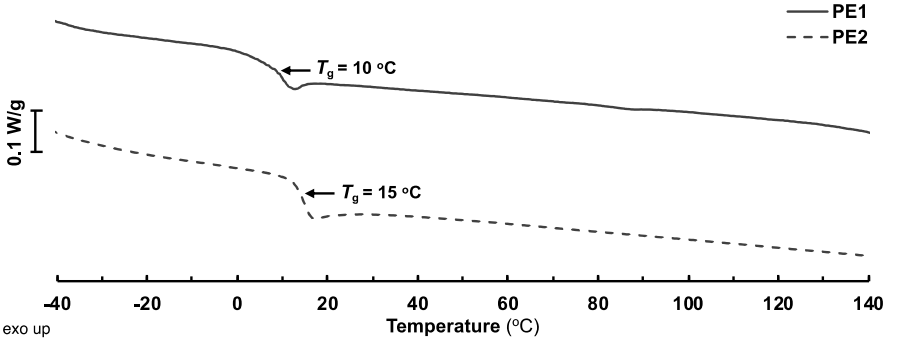

Figure 20. DSC heating curves of polyethers **PE1** and **PE2**.

In the present study, isosorbide-based homopolyethers from 2-*exo*-monoepoxide and 5-*endo*- were prepared. These polymers exhibited relatively high T_g values compared to conventional polyethers. Additionally, isosorbide-based polyethers also have heteroatoms in the main chain of the polymer structure. This feature makes these polyethers enticing also from the degradability aspect,[138] as usually the chain-growth polymers from isosorbide monomers have nondegradable backbone composed of only carbon atoms.

3.2.2. Block copolymers of isosorbide monoepoxides with PEG

In order to show the possibilities how to incorporate isosorbide monoepoxides into different polymer structures, copolymerizations with poly(ethylene glycol) (PEG) were also carried out (Table 4). Two linear difunctional PEG units with average M_n of 3000 (PEG_{3000}) and 6000 g mol^{-1} (PEG_{6000}) were chosen to be macroinitiators. NaH as an activator was added to melted PEG to convert the terminal hydroxyl groups of it to alcoholate anions. Thereafter by the addition of isosorbide monoepoxide, the copolymers with PEG unit as the middle block were obtained.

PEG_{3000} with 30% monoepoxide **E1** afforded block copolymer with M_n of 5.3 kg mol^{-1}, that is slightly higher M_n than expected (Table 4, entry 1). On the contrary, PEG_{6000} with 50% epoxide **E1** gave a copolymer with M_n of 9.6 kg mol^{-1},

a somewhat smaller than the target M_n of 12 kg mol^{-1} (Table 4, entry 2). Similarly, from isosorbide epoxide **E2** (30%) the copolymer with M_n of 5.2 kg mol^{-1} was obtained with PEG_{3000} as macroinitiator, and block copolymer with M_n of 12.8 kg mol^{-1} was achieved with 50% epoxide **E2** content and 50% PEG_{6000} (Table 4, entries 3 and 4). Interestingly, the latter copolymer exhibited a bit higher M_n than expected (12 kg mol^{-1}). The molecular mass distribution was quite narrow for all the synthesized block copolymers, $Đ$ = 1.1.

Table 4. Copolymerization of isosorbide monoepoxides with PEG at 100 °C.

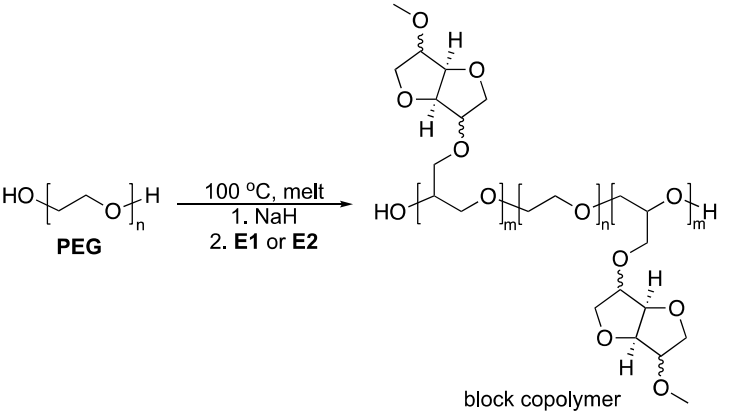

Entry	Epoxide	PEG block	Block copolymer	Aim of epoxide in copolymer by mass	Target M_n (kg mol^{-1})[a]	M_n (kg mol^{-1})[b]	$Đ$[b]
1	**E1**	PEG_{3000}	**PE1-PEG$_{3000}$**	30%	4.3	5.3	1.1
2	**E1**	PEG_{6000}	**PE1-PEG$_{6000}$**	50%	12.0	9.6	1.1
3	**E2**	PEG_{3000}	**PE2-PEG$_{3000}$**	30%	4.3	5.2	1.1
4	**E2**	PEG_{6000}	**PE2-PEG$_{6000}$**	50%	12.0	12.8	1.1

[a]Calculated as $M_n = M_{n,PEG}/(1–x)$, where x is 0.3 or 0.5, according to the aimed epoxide content of 30% or 50%, respectively. [b]Determined by SEC in $CHCl_3$ using poly(ethylene oxide) standards (M_n = 4 250 and 100 900 g mol^{-1}).

Furthermore, the solubility of the obtained block copolymers (Table 9 in Chapter 4.3.) was determined in a similar way as was investigated for the isosorbide polyethers. All the block copolymers were soluble in strongly hydrogen-bond-forming H_2O and MeOH, in moderately hydrogen-bonding DMSO and THF, in poorly H-bond forming $CHCl_3$ and toluene, but insoluble in nonpolar Et_2O. Interestingly, the original PEG block itself is insoluble in toluene, but with the added isosorbide sections, it becomes soluble.

Herein, isosorbide monoepoxides were used to synthesize corresponding isosorbide-based copolyethers with PEG. Therefore, these isosorbide-based monomers have proven to be versatile building blocks for different polymer structures.

3.3. C–C elongated derivatives of isosorbide

Paper III

In most derivatives, isosorbide has been functionalized through its hydroxyl groups at C2 and/or C5 (Scheme 14, left). Less attention has been paid to the chain elongation by a C–C bond at C2/C5 and also, by a C–C bond at positions C1/C6 in isosorbide structure (Scheme 14, right).

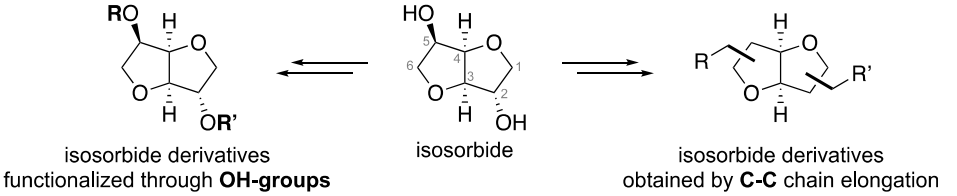

Scheme 14. Different strategies for isosorbide derivatives.

Hydroformylation is an atom-economical method for introducing new C–C bond into a molecule structure through the formation of aldehydes from alkenes.[126] Therefore, this strategy was chosen for the carbon chain elongation in isosorbide to replace the C–O bond with a C–C bond at C5. For this approach, the olefinic derivatives of isosorbide were prepared first, then hydroformylation reaction with corresponding compounds and synthetic gas (syngas, mixture of 1:1 CO/H_2) was carried out. Due to the formation of regioisomers during hydroformylation step, C–C bond elongation at C6 in isosorbide was also achieved.

3.3.1. Synthesis of olefinic derivatives of isosorbide

As hydroformylation requires an alkene as a starting material, then isosorbide-based alkenes were synthesized through β-elimination strategy.

First, isosorbide (**1**) was treated with thionyl chloride ($SOCl_2$) and pyridine at 70 °C for 1.5 h (Scheme 15). Following extractive work-up afforded the mono-chloride derivative of isosorbide (**4**) with clean inversion of configuration and in 93% yield as a beige waxy solid. It could be seen that only *endo*-OH at C5 in isosorbide structure was substituted with chloride.

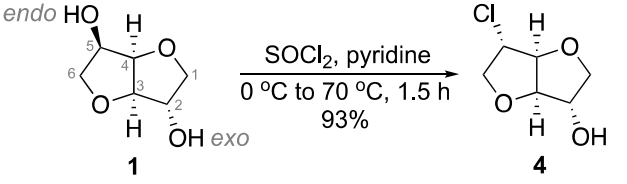

Scheme 15. Chlorination of isosorbide with $SOCl_2$ to monochloride derivative **4**.

The obtained monochloride derivative **4** was thereafter converted to olefinic derivative of isosorbide (**5**, 85%) by elimination with potassium *tert*-butoxide (*t*-BuOK) at 50 °C (Scheme 16, middle). As compound **5** proved to be quite unstable, then three more olefinic derivatives (**6**, **7**, and **8**) with different protective groups were prepared (Schemes 16 and 17).

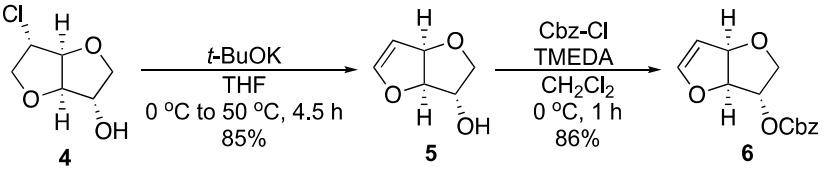

Scheme 16. Synthesis of isosorbide olefinic derivatives **5** and **6**.

Carbobenzyloxy-protected olefinic derivative **6** (86%) was obtained from compound **5** by the treatment of OH-group with benzyl chloroformate (Cbz-Cl) and *N*,*N*,*N*′,*N*′-tetramethylethylenediamine (TMEDA) in CH_2Cl_2 at 0 °C for 1 h (Scheme 16, right).

Additionally, two silyl groups were chosen for protecting the hydroxyl group at C2 in isosorbide structure. Olefinic derivative **4** was treated with *tert*-butyl-diphenylsilyl chloride (TBDPSCl) or *tert*-butyldimethylsilyl chloride (TBDMSCl) in the presence of imidazole (Im), followed by β-elimination with *t*-BuOK to afford olefinic compounds **7** or **8**, correspondingly (Scheme 17).

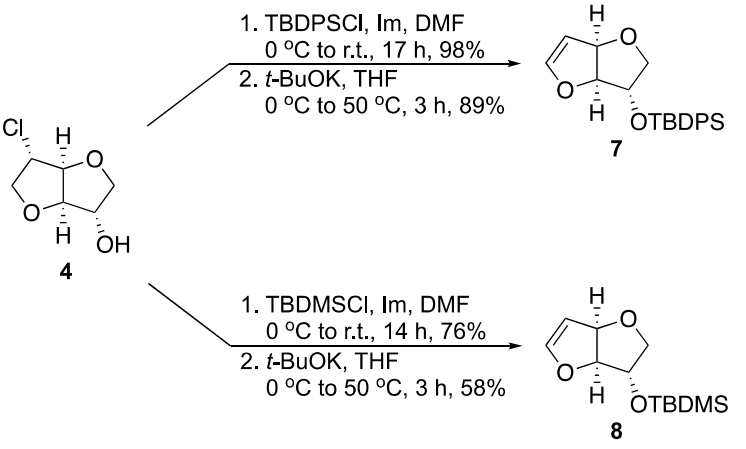

Scheme 17. Synthesis of isosorbide olefinic derivatives **7** and **8** from monochloride **4**.

As already mentioned before, the treatment of isosorbide with $SOCl_2$ afforded monochloride **D1** by the substitution of *endo*-OH. Therefore, it was decided to try the same reaction with isomannide (**2**), as it has two *endo*-OH groups that are also susceptible to same substitution. The reaction between $SOCl_2$ and isomannide afforded dichloride derivative **9**, as expected (Scheme 18).

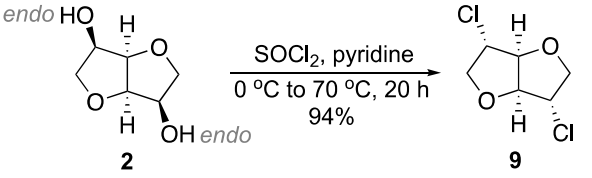

Scheme 18. Chlorination of isomannide with $SOCl_2$ to dichloride derivative **9**.

It was speculated that compound **9** could give dialkene of isomannide by the treatment with *t*-BuOK (Scheme 19). In reality, only one Cl was eliminated under these conditions and therefore the olefinic derivative **10** with Cl-group was obtained in 56% yield. Similarly to isosorbide olefinic derivatives **5**–**8**, isomannide-based alkene **10** also has only one double bond in its structure.

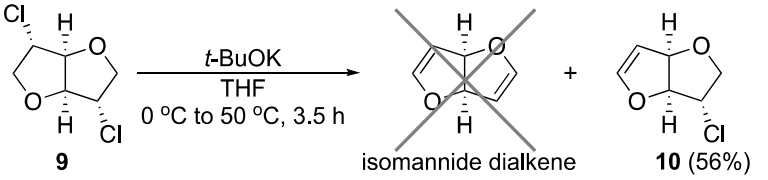

Scheme 19. Reaction between isomannide derivative **9** and *t*-BuOK that only afforded olefinic derivative **10**.

In brief, three different olefinic derivatives of isosorbide were obtained for hydroformylation experiments. In addition, one olefinic derivative of isomannide with Cl-group was also prepared.

3.3.2. Hydroformylation of olefinic derivatives of isosorbide

For hydroformylation of isosorbide-based alkenes two rhodium precursors $Rh(CO)_2acac$ and $[RhCl(cod)]_2$ in combination of various ligands were tested (for more details, please refer to Paper III). The ligands were chosen based on their reported performance in hydroformylation reactions,[139–144] structural diversity, and also commercial availability. Herein only the selected experiments with $Rh(CO)_2acac$ and five ligands are discussed (Figure 21). Additional hydroformylation experiments and corresponding results can be found in Paper III.

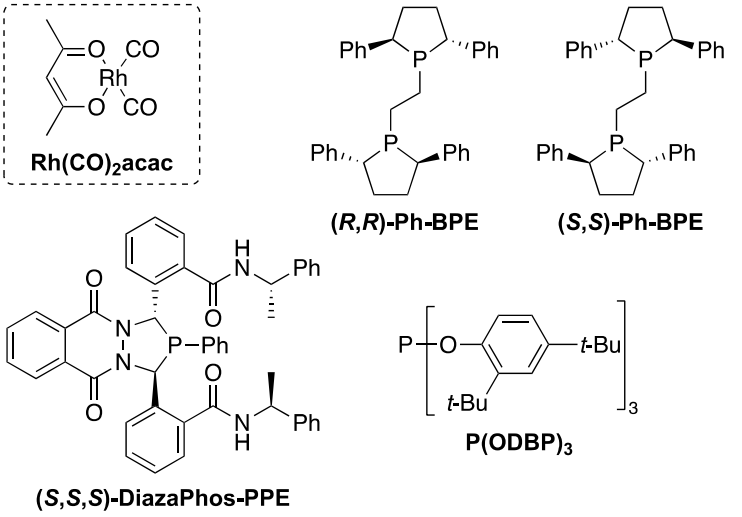

Figure 21. Rhodium precursor and ligands used for hydroformylation reactions.

Hydroformylation with olefinic derivatives of isosorbide **5**–**8** (and isomannide alkene **10**) in toluene using syngas (CO/H_2, 1:1, 10–40 bar) at different temperatures (50–80 °C) afforded the mixture of regioisomeric *endo*-aldehydes **a** and **b** (Scheme 20). The ratio of aldehyde products (**a**:**b**) was determined from crude ^1H NMR spectrum. These aldehydes could also be purified by column chromatography, but some epimerization on silica gel was observed.

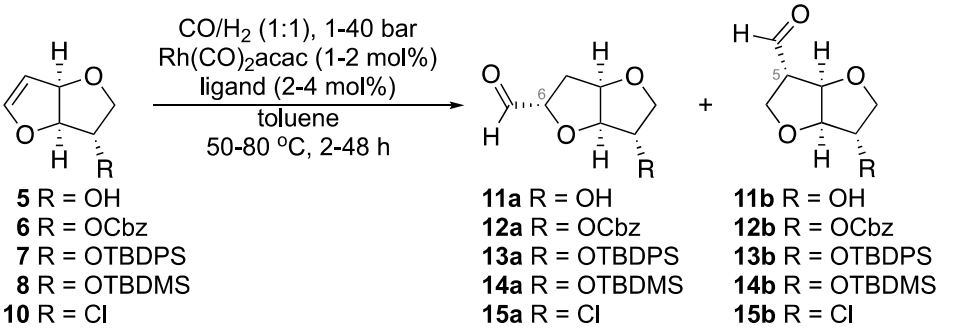

Scheme 20. Hydroformylation of olefinic derivatives **5**–**8** and **10**.

Firstly, hydroformylation of alkene **5** was tested with $P(ODBP)_3$ as ligand, but this compound with free OH-group turned out to be very unstable and in hydroformylation reactions the yield of aldehydes remained very low (up to 30%, Table 5, entries 1 and 2). The best regioselectivity of aldehydes **11a**:**11b** was 1:2 obtained at 60 °C under 40 bar.

Next, Cbz-capped olefin **6** was subjected under similar reaction conditions ($P(ODBP)_3$ as ligand, 60 °C, 40 bar), and the aldehyde ratio remained the same

(**12a**:**12b** as 1:2), but the conversion of starting material and the isolated yield of aldehyde product was much higher, 95% and 79%, respectively (Table 5, entry 3). Conversely, when using the same ligand, but raising temperature to 80 °C, lowering pressure to 10 bar, and shortening reaction time to 2 h, the product ratio was reversed to 3.5:1 favouring the C6-aldehyde, while the isolated yield was still very high, 90% (Table 5, entry 4). However, lowering the pressure even more to 1 bar, yielded only traces of aldehydes determined by ^{1}H NMR spectroscopy, and the conversion of alkene was also very low, <5% (Table 5, entry 5). Therefore, hydroformylation reaction with isosorbide-alkenes needs higher temperature and pressure to produce any aldehydes.

As P(ODBP)$_3$ seemed to give good result at 80 °C under 10 bar, then the same conditions were applied for alkene **6** in combination with another ligand (*S*,*S*)-Ph-BPE (Table 5, entry 6). In this case, the yield was lower (30%), but the ratio of aldehydes **12a**:**12b** was 1:13, favouring the C5 product. Under the same conditions, experiment using a larger amount of starting material was carried out (Table 5, entry 7). Now, the ratio of regioisomeric aldehydes increased to 1:20, even though the yield of aldehydes remained around the same level (38%). Another experiment on larger scale with alkene **6** under comparable conditions, but extending the reaction time to 2.75 h, afforded aldehydes with 1:17.3 ratio, at the same time the product yield increased to 68% (Table 5, entry 8). Peculiarly, very similar ligand (*R*,*R*)-Ph-BPE gave negligible regiopreference towards C5 derivative (Table 5, entry 9). Just like P(ODBP)$_3$, another ligand (*S*,*S*,*S*)-DiazaPhos-PPE afforded aldehydes **12a/b** with 1:2 ratio at 80 °C under 10 bar (Table 5, entry 10).

Turning to silyl-protected alkenes **7** and **8**. Similarly to hydroformylation of **6** (Table 5, entry 4), the reaction with alkene **7** in combination ligand P(ODBP)$_3$ afforded aldehydes **13a/b** with a ratio of 4:1 and in 99% yield, favouring C6 product (Table 5, entry 11). However, hydroformylation using (*S*,*S*)-Ph-BPE as ligand yielded aldehydes **13a/b** with the opposite selectivity 1:20 towards C5 regioisomer **13b** (Table 5, entry 12). But reaction with (*S*,*S*,*S*)-DiazaPhos-PPE provided aldehydes **13a/b** with 1.9:1 regioisomeric ratio and in 75% yield (Table 5, entry 13). Finally, hydroformylation of olefin **8** performed similarly to compound **7** in combination with P(ODBP)$_3$ afforded C6-aldehyde **14a** as the main product (Table 5, entry 14).

Table 5. Hydroformylation of isosorbide-alkenes **5**–**8**.[a]

Entry	Alkene	Ligand	T (°C)	P (bar)	Time (h)	Product	Product ratio (**a**:**b**)[b]	Alkene conv. (%)[b]	Yield **a**+**b** (%)[c]
1	**5**	$P(ODBP)_3$	60	20	2	**11a/b**	1:1.3	50	30
2	**5**	$P(ODBP)_3$	60	40	16	**11a/b**	1:2	50	12
3	**6**	$P(ODBP)_3$	60	40	14	**12a/b**	1:2	95	79
4	**6**	$P(ODBP)_3$	80	10	2	**12a/b**	3.5:1	n.d.[d]	90
5	**6**	$P(ODBP)_3$	80	1	2	**12a/b**	n.d.[d]	<5	traces[e]
6	**6**	(*S*,*S*)-Ph-BPE	80	10	2	**12a/b**	1:13	n.d.	30
7	**6**[f]	(*S*,*S*)-Ph-BPE	80	10	2	**12a/b**	1:20	40	38[e]
8	**6**[f]	(*S*,*S*)-Ph-BPE	80	10	2.75	**12a/b**	1:17.3	70	68[e]
9	**6**	(*R*,*R*)-Ph-BPE	80	40	4	**12a/b**	1:1.2	99	98
10	**6**	(*S*,*S*,*S*)-DiazaPhos-PPE	80	10	2	**12a/b**	1:2	60	54
11	**7**	$P(ODBP)_3$	80	10	2	**13a/b**	4:1	99	99[e]
12	**7**	(*S*,*S*)-Ph-BPE	80	10	2	**13a/b**	1:20	85	70
13	**7**	(*S*,*S*,*S*)-DiazaPhos-PPE	80	10	2	**13a/b**	1.9:1	76	75
14	**8**	$P(ODBP)_3$	80	10	2	**14a/b**	3.7:1	90	86

[a]Reaction conditions: alkene, $Rh(CO)_2acac$ precursor (1–2 mol%) and ligand (2–4 mol%) in toluene (1–1.5 mL) were placed into the high-pressure reactor under synthetic gas environment and then heated to the required temperature. [b]Product ratio (**a**:**b**) and alkene conversion were determined by ^{1}H NMR spectrum of the crude reaction mixture. [c]Isolated yield of aldehyde product. [d]n.d., not determined [e]Yield determined from crude by ^{1}H NMR against tetramethylsilane as internal standard. [f]Large scale (1 g of alkene).

Isomannide-based alkene **10** was also subjected under different hydroformylation conditions (Table 6). Reaction with $P(ODBP)_3$ as ligand favoured the C6-aldehyde **15a** as product (Table 6, entries 1–3). Small scale experiment at 80 °C under 10 bar afforded aldehydes with 4:1 regioisomeric ratio in 93% yield, compared to large scale reaction that gave 3.3:1 ratio of aldehydes **15a/b**. Lowering the temperature from 80 to 60 °C also decreased the ratio of aldehydes (2:1) and product yield to 65%. Hydroformylation of **10** with ligand (*S*,*S*)-Ph-BPE provided C5-aldehyde **15b** as the main product (Table 6, entries 4–6). In case of large scale experiment, the regioisomeric ratio of aldehydes reached 1:46. Interestingly, resembling ligand (*R*,*R*)-Ph-BPE gave a much lower ratio of 1:1.1 in 86% yield (Table 6, entry 7). In hydroformylation reaction with (*S*,*S*,*S*)-DiazaPhos-PPE as ligand, regiopreference towards **15b** was observed (Table 6, entries 8 and 9). Under 10 bar the yield was 50% with 1:2 aldehyde ratio, conversely, under 40 bar the total yield improved to 60%, while the aldehyde ratio decreased to 1:1.6.

Table 6. Hydroformylation of isomannide-alkene **10**.

Entry	Alkene	Ligand	T (°C)	P (bar)	Time (h)	Product	Product ratio (**a**:**b**)[b]	Alkene conv. (%)[b]	Yield **a**+**b** (%)[c]
1	**10**	$P(ODBP)_3$	80	10	2	**15a/b**	4:1	99	93[d]
2	**10**[e]	$P(ODBP)_3$	80	10	2	**15a/b**	3.3:1	99	88[d]
3	**10**	$P(ODBP)_3$	60	10	2	**15a/b**	2:1	99	65
4	**10**	(*S*,*S*)-Ph-BPE	80	10	2	**15a/b**	1:8	73	24
5	**10**	(*S*,*S*)-Ph-BPE	80	40	4	**15a/b**	1:26	75	35[d]
6	**10**[e]	(*S*,*S*)-Ph-BPE	80	30	5	**15a/b**	1:46	70	47[d]
7	**10**	(*R*,*R*)-Ph-BPE	80	30	5	**15a/b**	1:1.1	89	86
8	**10**	(*S*,*S*,*S*)-DiazaPhos-PPE	80	10	2	**15a/b**	1:2	50	50
9	**10**	(*S*,*S*,*S*)-DiazaPhos-PPE	80	40	4	**15a/b**	1:1.6	99	60

[a]Reaction conditions: alkene, $Rh(CO)_2acac$ precursor (1–2 mol%) and ligand (2–4 mol%) in toluene (1–1.5 mL) were placed into the high-pressure reactor under synthetic gas environment and then heated to the required temperature. [b]Product ratio (**a**:**b**) and alkene conversion were determined by ^{1}H NMR spectrum of the crude reaction mixture. [c]Isolated yield of aldehyde product. [d]Yield determined from crude by ^{1}H NMR against tetramethylsilane as internal standard. [e]Large scale (0.8 g of alkene).

Therefore, elongation of isosorbide by a new C–C bond was achieved via hydroformylation method that afforded C5-aldehyde with up to 46:1 and C6-aldehyde with up to 4:1 regioisomeric ratio.

3.3.3. Reduction of isosorbide aldehydes to corresponding alcohols

To prevent the epimerization of aldehyde product during purification step, one-pot procedure of hydroformylation and subsequent reduction was developed (Scheme 21). Large scale hydroformylation experiments of alkenes **6** and **10** demonstrated in the previous chapter (Table 5, entry 8, and Table 6, entries 2 and 6) were used for this approach. Additionally, one smaller scale experiment of OTBDPS-capped alkene **7** (Table 5, entry 11) was also utilized.

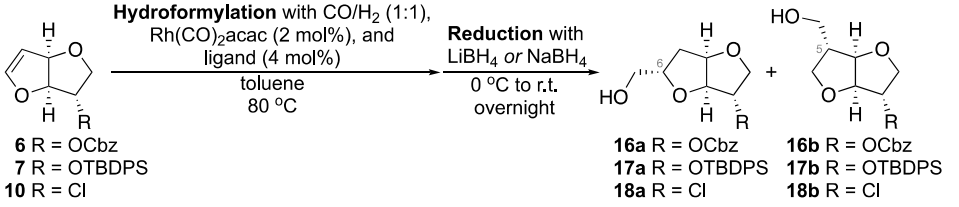

Scheme 21. One-pot hydroformylation and aldehyde reduction sequence for the synthesis of primary alcohols **16a/b**, **17a/b**, and **18a/b**. For reaction conditions see Table 7.

Isosorbide alkene **6** was converted to primary alcohol **16a/b** via the one-pot procedure with a 44% yield over two steps (Table 7, entry 1). Conversely, OTBDPS-capped isosorbide primary alcohol **17a/b** was obtained in 84% yield, but with regioisomeric ratio **a**:**b** of 4:1 (Table 7, entry 2). Two large scale experiments with isomannide alkene **10** afforded primary alcohol **18a/b** with 69% and 37% in yield and regioisomeric ratio **a**:**b** of 3.3:1 and 1:46, respectively (Table 7, entries 3 and 4). The **a**:**b** ratio of regioisomeric product was determined by the hydroformylation conditions and did not change during reduction step.

Table 7. One-pot hydroformylation[a] and aldehyde reduction[b] sequence of alkenes **6**, **7**, and **10**.

Entry	Alkene	Hydro-formylation conditions	Aldehyde product	Aldehyde yield **a**+**b** (%)[c]	Reducing agent, solvent	Alcohol product	Alcohol yield **a**+**b** (%)[d]	Product ratio (**a**:**b**)[c]
1	**6**[e]	(*S*,*S*)-Ph-BPE, 10 bar, 2.75 h	**12a/b**	68	$NaBH_4$ MeOH	**16a/b**	44	1:17.3
2	**7**	$P(ODBP)_3$, 10 bar, 2 h	**13a/b**	99	$LiBH_4$ THF	**17a/b**	84	4:1
3	**10**[e]	$P(ODBP)_3$ 10 bar, 2 h	**15a/b**	93	$LiBH_4$ THF	**18a/b**	69	3.3:1
4	**10**[e]	(*S*,*S*)-Ph-BPE 30 bar, 5 h	**15a/b**	47	$LiBH_4$ THF	**18a/b**	37	1:46

[a]Reaction conditions: alkene, $Rh(CO)_2acac$ precursor and ligand in toluene were placed into the high-pressure reactor under synthetic gas environment and then heated to the required temperature. [b]Reaction conditions: to the crude untreated hydroformylation reaction mixture in toluene was added THF (or MeOH), and then the solution was cooled to 0 °C, the reducing agent was added, and the mixture was stirred overnight at r.t. [c]Aldehyde yield and product ratio (**a**:**b**) were determined by ^1H NMR spectrum of the crude reaction mixture (tetramethylsilane as internal standard). [d]Isolated yield of alcohol product. [e]Large scale (0.8–1 g of alkene).

Primary alcohol preparation from isosorbide alkenes via hydroformylation and subsequent reduction has been demonstrated as a one-pot sequence in order to retain the regioselectivity and diastereomeric ratio over the two reaction steps.

3.3.4. Second hydroformylation of primary alcohol of isosorbide

The sequential chlorination with $SOCl_2$ and β-elimination of isosorbide introduced only one double bond into its structure. Therefore, the hydroformylation could only happen with this one double bond. Additionally, the substitution of OH-groups with chloride in isomannide was successful with both hydroxyls, but the β-elimination still happened only at one site as is shown in Scheme 19 in Chapter 3.3.1. As a result, hydroformylation of these monoalkenes of isosorbide and isomannide have shown to add a new C–C bond into the C5 or C6 position. But, in order to introduce second C–C bond to C2 or C1 position via hydroformylation strategy, a longer reaction sequence is needed.

To use the knowledge already at hand, the primary alcohol **18a/b** with **a**:**b** ratio (C6:C5) of 3.3:1 was chosen for the introduction of the second C–C bond. Firstly, the second β-elimination reaction with *t*-BuOK in THF was carried out to obtain alkene **19a/b** with a free OH-group in 77% yield (Scheme 22, middle). Hydroformylation with alkene **19a/b** was also attempted, but the yield of final aldehyde was only 16%, as most of the starting material decomposed during reaction. It was decided to treat the alkene **19a/b** with TBDMSCl to get silyl-capped olefin **20a/b** (62% in yield, Scheme 22, right).

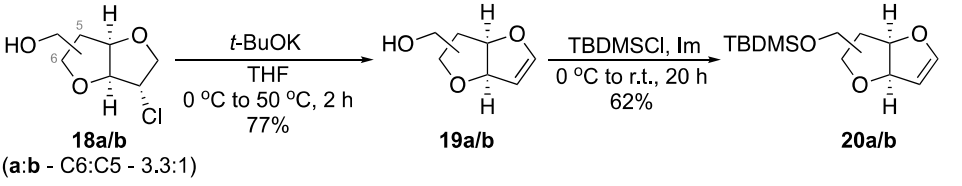

Scheme 22. Synthesis path for alkene **20a/b**.

Subsequently, hydroformylation of alkene **20a/b** with $Rh(CO)_2acac$ and $P(ODBP)_3$ afforded aldehyde **21a–h** (Scheme 23). As a result, a mixture of eight regio- and diastereoisomers was obtained. The aldehydes ratio according to ^1H NMR was 20.39:8.52:7.53:7.51:3.61:3.04:1.97:1.00 as shown in Figure 22.

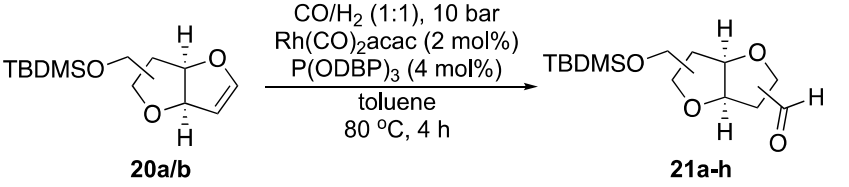

Scheme 23. Hydroformylation of alkene **20a/b** to aldehyde **21a–h**.

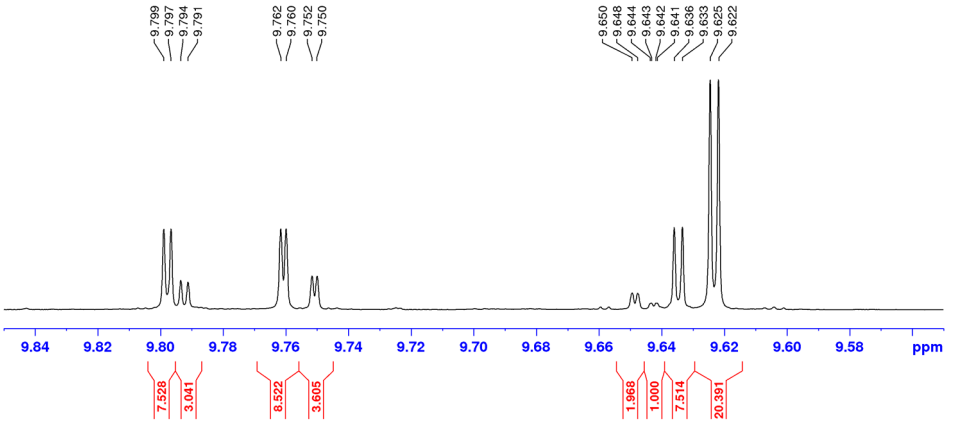

Figure 22. Enlargement of aldehyde proton region in ^{1}H NMR spectrum of compound **21a–h**.

Because the mixture contains so many isomers, and is very complicated, the exact structures of all the isomers were not determined. Possible aldehyde structures are illustrated in Figure 23.

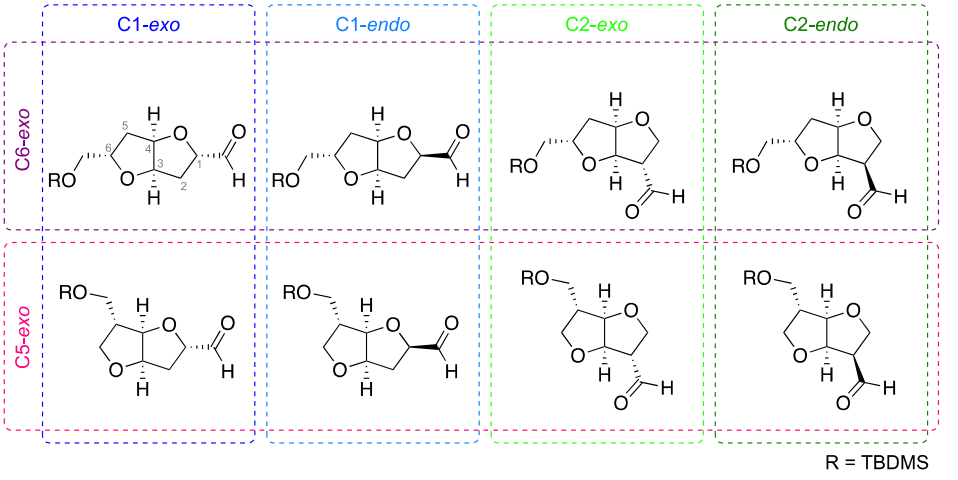

Figure 23. Eight possible regio- and diastereoisomers of aldehyde **21a–h**.

Hydroformylation has proven to be an efficient method for the carbon chain elongation at the positions C5 or C6 in isosorbide and isomannide structures. The large-scale experiments of the sequential hydroformylation and reduction reactions were also successful, preserving the regioisomeric ratio of the C5 and C6 products in both steps. Furthermore, it was shown that a second C–C bond at C1 or C2 can also be introduced into isomannide structure by a longer synthesis path with two hydroformylation steps. This strategy opens up many new possibilities for isosorbide-based derivatives as appealing building blocks in polymer structures.

4. MATERIALS, METHODS, AND EXPERIMENTAL DETAILS

A detailed descriptions of the used materials and chemicals, synthesis and characterization methods, experimental details, and other necessary information can be found in the Papers I–III:

- synthesis and characterization of isosorbide polymethacrylates (Paper I),
- synthesis and characterization of isosorbide polyethers (Paper II),
- synthesis and hydroformylation of isosorbide olefinic derivatives (Paper III).

Additional descriptions of experiments that were not included in the Publications I–III can be found in the following Chapters 4.1.–4.4. All the reagents and solvents used were obtained from commercial sources and were used without further purification, if not stated otherwise.

^{1}H and ^{13}C NMR spectra were recorded at 400.1 and 100.6 MHz, respectively. For compounds **19a/b** and **21a–h** ^{1}H NMR spectra were recorded at 700.1 MHz, and for compound **19a/b** ^{13}C NMR spectra were recorded at 176.0 MHz. The chemical shifts for the ^{1}H and ^{13}C NMR spectra are given in ppm and are calibrated using residual solvent signals (e.g., for ^{1}H, $CDCl_3$: δ = 7.26 ppm and DMSO-d_6: δ = 2.50 ppm, for ^{13}C, $CDCl_3$: δ = 77.0 ppm and DMSO-d_6: δ = 39.53 ppm). The following abbreviations are used for multiplicities: s, singlet; d, doublet; t, triplet; q, quartet; m, multiplet; b, broadened. Purification of reaction products was done by flash chromatography using silica gel 60 (0.040–0.063 mm, 230–400 mesh). For HRMS analysis, a Thermo Electron LTQ Orbitrap XL analyzer was used. An FTIR (ATR) spectrophotometer Shimadzu IRAffinity-1 was used for IR analysis. The molecular weights of the polymers were determined by SEC in THF or in $CHCl_3$. The SEC setup included three Shodex columns coupled in series (KF-805, -804, and -802.5) situated in a Shimadzu CTO-20A prominence column oven, a Shimadzu RID-20A refractive index detector, with Shimadzu LabSolution software. All samples were run at 40 °C in THF or in $CHCl_3$ and at an elution rate of 1 mL/min. Calibration was done by using poly(ethylene oxide) standards (M_n = 3860, 12 600, 49 640, and 96 100 g mol^{-1}).

4.1. General procedure for cationic polymerization of isosorbide monoepoxides

The details of the CROP experiments are presented in Table 8 below.

Isosorbide monoepoxide (**E1** or **E2**) was dried carefully prior to the polymerization.

Firstly, all the flasks used in the experiments were set up beforehand. The flasks were flamed with a hot-gun, equipped with magnetic stirrer bars, fitted with rubber septa, and degassed with vacuum/argon-cycle. After degassing, inert gas atmosphere was assured with Ar-balloons connected through the septum with a syringe needle.

Stock solutions of initiator, catalyst, and monomer in appropriate solvents were also prepared beforehand.

Then the right amount of initiator and catalyst solutions were transferred into the reaction mixture with syringes and left to react for a certain period of time (from 10 min up to 2 h, depending on the reagents used). Thereafter, reaction flask was cooled down on an ice bath and the right amount of monomer solution was added. The temperature of the mixture was slowly increased to room temperature (21 °C) and the polymerization was allowed to proceed for a certain period of time at this temperature (0.5–24 h). Then the conversion of epoxide was determined by ^{1}H NMR spectrum with the sample dissolved in a suitable deuterated solvent (e.g., $CDCl_3$, DMSO-d_6).

Table 8. Cationic ring-opening polymerization of isosorbide monoepoxides **E1** and **E2**.[a]

Entry	Epoxide	Initiator	Catalyst	Solvent	Epoxide conc. (mol L^{-1})	[epoxide]/ [I]/[C]	Time (h)	Epoxide conv.[b]
1	**E1**[c]	BD	BF_3OEt_2	toluene	1.5	100/6/1	0.5	n.d.[d]
2	**E2**[c]	BD	BF_3OEt_2	toluene	1.5	100/1/1	0.5	n.d.[d]
3	**E2**	BD	CF_3SO_3H	CH_2Cl_2	1.4	100/1/1	19	60%
4	**E2**	BD	$SnCl_4$	CH_2Cl_2	1.0	100/1/0.25	24[e]	10%
5	**E2**	BD	$AlCl_3$	CH_2Cl_2	0.6	100/1/0.25	24	10%
6[f]	**E2**	PO	$Sc(OTf)_3$	ACN	0.8	100/5/1	24	0%

[a]Reaction conditions: temperature 0 °C to r.t. [b]Determined by ^{1}H NMR spectroscopy. [c]Solid precipitate formed during reaction. [d]n.d., not determined (products of entries 1 and 2 were found insoluble in common deuterated solvents). [e]After 24 h the reaction mixture was heated to 50 °C and let to stir at this temperature for 72 h, but still no polymer was detected in ^{1}H NMR spectrum after heating. [f]Carried out according to a reported procedure.[96]

4.2. General procedure for anionic polymerization of isosorbide monoepoxides with phosphazene bases or MeMgBr as deprotonating agent

The details of the AROP experiments are presented in Table 2 in Chapter 3.2.1.

Isosorbide monoepoxide (**E1** or **E2**) was dried carefully prior to the polymerization.

Similarly to cationic ring-opening polymerizations, all the flasks used in the experiments were set up beforehand. The flasks were flamed with a hot-gun or dried prior to reaction in an over at 150 °C for 2 h, equipped with magnetic stirrer bars, fitted with rubber septa, and degassed with vacuum/argon-cycle. After degassing, inert gas atmosphere was assured with Ar-balloons connected through the septum with a syringe needle.

When PB_4 or MeMgBr was used, then the reaction flask was cooled down to –30 °C on ACN/liquid N_2 bath before the addition of any reagents.

Stock solutions of initiator, deprotonating agent, and monomer in appropriate solvents were also prepared beforehand (1 M solution of Et_3B in hexane, 1.1 M solution of *i*-Bu_3Al in toluene, and 1.4 M solution of MeMgBr in 1:3 THF/toluene were purchased from commercial sources).

Next, the right amount of initiator and deprotonating agent solutions were transferred into the reaction mixture with syringes and left to react for a certain period of time (from 10 min up to 1.5 h, depending on the reagents used). Thereafter, catalyst solution and monomer solutions were added into the mixture which was then let to stir at r.t. for 24 h. When PB_4 or MeMgBr was used, then the temperature of the mixture was slowly increased to r.t. and the polymerization was allowed to proceed at r.t. for 24 h. The polymerization was stopped by adding a drop of acetic acid (or MeOH in case of MeMgBr) into the reaction mixture. Subsequently, the conversion of epoxide was determined by ^{1}H NMR spectrum with the sample dissolved in a suitable deuterated solvent (e.g., $CDCl_3$, DMSO-d_6, etc).

4.3. General procedure for anionic copolymerization of isosorbide monoepoxides with poly(ethylene glycol)

Isosorbide monoepoxide (**E1** or **E2**) and PEG precursor block (PEG_{3000}, average M_n = 3000 g mol^{-1}, actual M_n = 2700–3300 g mol^{-1}, or PEG_{6000}, average M_n = 6000 g mol^{-1}, actual M_n = 5700–7000 g mol^{-1}) were dried carefully prior to the polymerization reaction.

The PEG precursor block was charged to a 10 mL two-neck round-bottom flask equipped with a reflux condenser, magnetic stirrer, and fitted with rubber septa. The flask was heated up to 100 °C, the PEG was kept in the melt state at this temperature, and it was degassed with Ar for 1 h. Sodium hydride (60% in mineral oil) was then quickly transferred to the melt and was left to react for 1 h to partly convert the terminal hydroxyl groups of the PEG to alcoholate anions ([NaH]/[OH] = 1:2). Next, isosorbide monoepoxide was added via syringe to start the polymerization, which was allowed to proceed for 24–72 h at 100 °C under slow Ar-flow. The copolymer was then precipitated in Et_2O from MeOH solutions to remove any residual monomer and filtered from Et_2O three times. After the final filtration, a solid product was collected and carefully dried under vacuum.

For all the dried copolymers NMR and SEC measurements were carried out, additionally the solubility of the polymers in selected solvents was determined (Table 9 below). No further measurements were conducted, as the aim was just to show the versatility of isosorbide monoepoxides in different polymer structures. For NMR figures, please refer to Appendix 1 Figures A1–A4. For SEC results, please refer to Table 4 in Chapter 3.2.2.

The solubility of the block copolymers of isosorbide monoepoxides and PEG was investigated by mixing small samples (about 5 mg) with a range of selected solvents (1 mL). The mixture was stirred for 24 h at room temperature. The results of the dissolution tests were divided into two categories, soluble and insoluble, based on visual inspection. If the samples were found to be completely dissolved, they were considered as soluble; if not, they were considered as insoluble.

Table 9. Solubility of PEG_{6000} and block copolymers of PEG and isosorbide monoepoxides at 21 °C.

Polymer	Solvent[a]						
	H_2O $\delta = 48$ (s)	MeOH $\delta = 30$ (s)	DMSO $\delta = 25$ (m)	THF $\delta = 19$ (m)	Et_2O $\delta = 15$ (m)	$CHCl_3$ $\delta = 19$ (p)	toluene $\delta = 18$ (p)
PEG_{6000}	+	+	+	+	–	+	–
PE1-PEG_{3000}	+	+	+	+	–	+	+
PE1-PEG_{6000}	+	+	+	+	–	+	+
PE2-PEG_{3000}	+	+	+	+	–	+	+
PE2-PEG_{6000}	+	+	+	+	–	+	+

[a]The symbols "+" and "–" indicate solubility and insolubility, respectively. Solubility parameters (δ, $MPa^{½}$) were obtained from the Polymer Handbook (J. Brandrup, E. H. Immergut, E. A. Grulke, A. Abe, D. Bloch. *Polymer Handbook, 4th ed.*, John Wiley and Sons, New York, 1999), and the letters s, m, and p denote strongly, moderately, and poorly hydrogen-bond-forming solvents, respectively.

4.4. Experimental details of the synthesis of isomannide aldehyde with two C–C bond elongations

In this chapter the synthesis of aldehyde derivative **21a–h** of isomannide starting from primary alcohol **18a/b** with the **a**:**b** (C6:C5) regioisomeric ratio of 3.3:1 is presented (please also refer to Scheme 22 and 23 in Chapter 3.3.4).

Alkene **19a/b**

To the compound **18a/b** (110 mg, 0.6 mmol) in THF (0.8 mL) was added *t*-BuOK (173 mg, 1.5 mmol) in THF (4 mL) dropwise at 0 °C under argon atmosphere. Then the reaction was brought to 50 °C and stirred for 2 h. After that the reaction was quenched with H_2O (10 mL) at 0 °C. Next, the mixture was diluted with EtOAc (12 mL) and sat. aq. NaCl (10 mL). The phases were separated, and the aqueous phase was extracted with EtOAc (3 × 12 mL). The collected organic phases were dried over $MgSO_4$, filtrated, and carefully concentrated to dryness in vacuo. The crude was purified by column chromatography on silica (1% MeOH/CH_2Cl_2) to afford the product **19a/b** as a clear colourless oil (67.4 mg, 77%, **a**:**b** ratio 3.3:1). Isomer **19a**: ^{1}H NMR (700.1 MHz, $CDCl_3$) δ 6.57 (d, J = 2.7 Hz, 1H), 5.39 (dd,

J = 6.3, 2.6 Hz, 1H), 5.03 (dd, *J* = 6.3, 5.8 Hz, 1H), 5.01 (dd, *J* = 2.7, 2.6 Hz, 1H), 3.91 (dddd, *J* = 11.1, 4.7, 4.5, 3.0 Hz, 1H), 3.88 (ddd, *J* = 11.9, 4.6, 3.0 Hz, 1H), 3.60 (ddd, *J* = 11.9, 6.8, 4.5 Hz, 1H), 2.07 (dd, *J* = 13.4, 4.7 Hz, 1H), 2.00 (dd, *J* = 6.8, 4.6 Hz, 1H), 1.95 (ddd, *J* = 13.4, 11.1, 5.8 Hz, 1H) ppm; ^{13}C NMR (176.0 MHz, $CDCl_3$) δ 150.9, 100.0, 85.0, 84.9, 75.7, 63.0, 35.4 ppm. Isomer **19b**: ^{1}H NMR (700.1 MHz, $CDCl_3$) δ 6.56 (d, *J* = 2.7 Hz, 1H), 5.34 (dd, *J* = 6.5, 2.6 Hz, 1H), 5.00 (dd, *J* = 2.7, 2.6 Hz, 1H), 4.83 (d, *J* = 6.5 Hz, 1H), 3.80 (dd, *J* = 9.2, 1.3 Hz, 1H), 3.63 (overlapping m and dd, *J* = 9.2, 5.0 Hz, 3H), 2.48 (m, 1H), 1.73 (bs, 1H) ppm; ^{13}C NMR (176.0 MHz, $CDCl_3$) δ 150.5, 99.5, 86.0, 84.5, 66.1, 62.8, 49.3 ppm. IR (ATR) ν_{max} (cm^{-1}): 3399, 2874, 1609, 1146, 1045, 1015. HRMS (ESI): calculated for $C_7H_{11}O_3$ $[M+Na]^+$ 165.0522, found 165.0515.

TBDMSO-alkene **20a/b**

To a solution of **19a/b** (50 mg, 0.4 mmol) in DMF (0.5 mL) was added imidazole (60 mg, 0.9 mmol) and *tert*-butyldimethylsilyl chloride (63 mg, 0.4 mmol) at 0 °C. Then the reaction was brought to room temperature and stirred for 20 h. After the mixture was diluted with EtOAc (7 mL) and aq. sat. NaCl (7 mL), the phases were separated, and the aqueous phase was extracted with EtOAc (3 × 6 mL). The collected organic phases were dried over $MgSO_4$, filtrated, and concentrated to dryness in vacuo. The crude was purified by column chromatography on silica (5% EtOAc/p.ether) to afford a clear colourless oily product **20a/b** (56 mg, 62%, **a**:**b** ratio 3.3:1). Isomer **20a**: ^{1}H NMR (400.1 MHz, $CDCl_3$) δ 6.54 (d, *J* = 2.7 Hz, 1H), 5.36 (dd, *J* = 6.4, 2.6 Hz, 1H), 5.01 (dd, *J* = 2.7, 2.6 Hz, 1H), 4.99 (dm, *J* = 6.4 Hz, 1H), 3.86 (dddd, *J* = 10.3, 4.7, 4.6, 4.3 Hz, 1H), 3.75 (dd, *J* = 10.8, 4.3 Hz, 1H), 3.72 (dd, *J* = 10.8, 4.6 Hz, 1H), 2.12 (dd, *J* = 13.5, 4.7 Hz, 1H), 1.89 (ddd, *J* = 13.5, 10.3, 6.0 Hz, 1H), 0.89 (s, 9H), 0.05 (s, 6H) ppm; ^{13}C NMR (100.6 MHz, $CDCl_3$) δ 150.5, 100.3, 85.0, 84.8, 76.2, 64.6, 36.9, 25.92, 18.4, -5.32, -5.35 ppm. Isomer **20b**: ^{1}H NMR (400.1 MHz, $CDCl_3$) δ 6.55 (m, 1H), 5.30 (dd, *J* = 6.5, 2.6 Hz, 1H), 5.00 (m, 1H), 4.78 (dm, *J* = 6.5 Hz, 1H), 3.71 (dd, *J* = 9.1, 1.8 Hz, 1H), 3.59 (dd, *J* = 9.1, 5.2 Hz, 1H), 3.57 (dd, *J* = 10.2, 7.7 Hz, 1H), 3.52 (dd, *J* = 10.2, 8.0 Hz, 1H), 2.48 (m, 1H), 1.65 (bs, 1H), 0.90 (s, 9H), 0.06 (s, 6H) ppm; ^{13}C NMR (100.6 MHz, $CDCl_3$) δ 150.3, 99.8, 85.8, 84.1, 65.7, 62.3, 49.9, 25.85, 18.2, -5.40, -5.44 ppm. IR (ATR) ν_{max} (cm^{-1}): 2928, 1612, 1254, 1146, 1053, 837. HRMS (ESI): calculated for $C_{13}H_{25}O_3Si$ $[M+H]^+$ 257.1567, found 257.1563.

Aldehyde **21a–h**

The mixture of an alkene **20a/b** (14.7 mg, 0.06 mmol), $Rh(CO)_2acac$ (1.6 mg, 0.006 mmol) and ligand $P(ODBP)_3$ (21.5 mg, 0.03 mmol) in toluene (1 mL) was placed into the high-pressure reactor in a 4 mL open glass vial. After degassing with water jet vacuum pump, the reactor was filled with syngas (CO/H_2, 1:1, 10 bar). The reaction was stirred 4 h under rapid stirring (500–600 rpm) at 80 °C. Then the pressure was reduced to atmospheric level and the heater was turned

off. The crude NMR spectra were taken directly from the cooled and aired reaction mixture. The crude mixture was purified by column chromatography on silica (20% EtOAc/p.ether) to afford a clear yellow oil as a mixture of eight regio- and diastereoisomers (**21a–h**, 12.1 mg, 74%). Ratio of the 8 isomers according to ^{1}H NMR was 20.39:8.52:7.53:7.51:3.61:3.04:1.97:1.00. Major isomer **21a**: ^{1}H NMR (700.1 MHz, $CDCl_3$) δ 9.62 (d, J = 1.9 Hz, 1H), 4.81 (dm, J = 4.1 Hz, 1H), 4.72 (dd, J = 4.8, 4.1 Hz, 1H), 4.45 (dddd, J = 9.7, 6.7, 1.9, 0.7 Hz, 1H), 4.20 (m, 1H), 3.67 (m, 1H), 3.59 (m, 1H), 2.35 (ddm, J = 13.6, 6.7 Hz, 1H), 2.15 (dm, J = 13.6 Hz, 1H), 1.98 (ddd, J = 13.6, 10.2, 4.9 Hz, 1H), 1.97 (ddd, J = 13.6, 9.7, 4.8 Hz, 1H) ppm, TBDMS signals were not assigned due to overlap; ^{13}C NMR (100.6 MHz, $CDCl_3$) δ 201.0, 86.0, 83.4, 83.3, 80.6, 65.3, 36.1, 35.9 ppm, TBDMS signals were not assigned due to overlap. For full NMR figures, please refer to Appendix 1 Figures A5 and A6. IR (ATR) ν_{max} (cm^{-1}): 2932, 1732, 1389, 1253, 1096, 837. HRMS (ESI): calculated for $C_{14}H_{27}O_4Si$ $[M+H]^+$ 287.1673, found 287.1667.

SUMMARY

The current tendency of moving towards a more sustainable economy comprehends the substitution of materials from non-renewable fossil resources with biobased alternatives. This also includes the replacement of oil-derived polymers, that are the main components of plastics, with biobased polymeric materials.

Isosorbide, a well-known rigid diol from biomass has appeared to be an interesting component in polymers. Its appealing properties are not only caused by the *exo*/*endo* difference of its two hydroxyl groups, but also by its stiff structure that is rare among bio-derived compounds. Hence, in this study isosorbide was used as a starting material for the preparation of smaller building blocks and novel biobased polymers.

Firstly, linear polymethacrylates with isosorbide unit as a pendant group were prepared by conventional radical polymerization of both, *exo*- and *endo*-monomethacrylic derivatives. Additionally, these methacrylic monomers had different substituents attached to the free OH-group in isosorbide structure. Number average molecular weight (M_n) of the prepared polymethacrylates varied between 26 and 48 kg mol^{-1} with the polydispersity indexes ($Đ$) fluctuating from 2.4 to 2.9. No considerable impact by the *exo*/*endo* configuration and the different substituents was seen in case of molecular weights. The effect of the substituents was clearly seen in case of solubility, e.g., OH-functional polymers were only soluble in dimethyl sulfoxide, but polymers with alkyl chains were also soluble in tetrahydrofuran and chloroform. Besides, polymers with acetate group were soluble in acetonitrile and polymethacrylates with larger alkyl units in toluene. The values of intrinsic viscosity of the isosorbide polymethacrylates were also quite unified with only one exception: the polymer with *exo*-OH exhibited much higher intrinsic viscosity, which is supposedly caused by the additional hydrogen bonding between the polymer chains. Further, isosorbide polymethacrylates were thermally very stable, on the heating curve the 5% weight loss was noticed varying between 208 and 240 °C for polymers with different substituents. The influence of the substitute group was also noticed in case of the glass transition temperatures (T_g). Polymers with OH-groups had very high T_g of 167 °C and with shorter alkyl chains around 130 °C. Interestingly, polymethacrylates with longer carbon side chains had lower T_g-s of 54 and 66 °C for *endo*- and *exo*-dodeconoate polymethacrylate, respectively. Additionally, the latter polymer also exhibited a small order-to-disorder transition in its differential scanning calorimetry (DSC) curve.

Secondly, linear polyethers were prepared from two regioisomeric isosorbide monoepoxides by anionic ring-opening polymerization with tetraocylammonium bromide as initiator and triisobutylaluminium as activator. This method provided polyethers with M_n of 13.2 kg mol^{-1} ($Đ$ = 1.7) and 17.8 kg mol^{-1} ($Đ$ = 2.1). Thermal stability of these polymers with isosorbide units as pendant groups were high, up to 300 °C. DSC curves revealed glass transitions below room temperature (10 and 15 °C), but the values are higher compared to T_g-s of other

commonly known polyethers. No significant impact by the regioisomeric isosorbide epoxy-monomers was seen in case of the properties of the two corresponding polyethers. Additionally, it was shown that the monoepoxides of isosorbide can successfully be used in the composition of copolymers, e.g., with poly(ethylene glycol).

Thirdly, novel isosorbide derivatives with carbon-carbon bond elongation were demonstrated. Hydroformylation of isosorbide alkene-derivatives was used for this approach. Thus, regioisomeric mixtures of isosorbide C5- and C6-aldehydes were obtained. The preference towards position C5 in isosorbide structure was achieved with the regioisomeric ratio up to 46:1 and towards position C6 with the ratio up to 4:1. The synthesis was also carried out on larger scale and the one-pot hydroformylation-reduction sequence was demonstrated. Moreover, a longer synthesis sequence provided a building block with carbon chain elongations by two carbon atoms at both tetrahydrofuran rings in isosorbide structure.

The linear isosorbide-based polymers synthesized in this study have once again proved the suitability of isosorbide structure in polymeric materials. The rigidity of isosorbide gives high thermal stability to polymers and increases their T_g values. Additionally, the diol functionality enables the attachment of different substituents to the other OH-group and this, in turn, allows the variation of the final polymer properties. On top of that, the C–C elongated isosorbide derivatives prepared through hydroformylation strategy, make it possible to design new biobased monomers for polymeric materials.

SUMMARY IN ESTONIAN

Uudsed isosorbiidil baseeruvad polümeerid

Nüüdisaja suundumus jätkusuutlikuma majanduse poole hõlmab mitte-taastuvatest fossiilsetest allikatest saadud materjalide asendamist biopõhiste alternatiividega. Selle hulka kuulub ka naftal baseeruvate polümeeride, mis on plastikute peamine koostisosa, välja vahetamine biopõhiste polümeersete materjalide vastu.

Isosorbiid, mis on tuntud biomassist saadav dialkohol, on polümeeride koostisosana andnud neile väga huvipakkuvaid omadusi. Need omadused ei ole põhjustatud ainult isosorbiidi hüdroksüülrühmade *ekso*/*endo* konfiguratsioonist, vaid ka molekuli jäigast struktuurist, mis on küllaltki haruldane kõigi biopõhiste ühendite hulgas. Seetõttu kasutati ka käesolevas uurimistöös isosorbiidi kui lähteainet uudsete väiksemate molekulide ja biopõhiste polümeeride valmistamisel.

Esmalt sünteesiti vabaradikaalse polümerisatsioonimeetodil *ekso*- ja *endo*-mono-metakrüülsetest isosorbiidi derivaatidest lineaarsed polümetakrülaadid, milles isosorbiidi struktuuriühikud esinevad külgrühmades. Lisaks olid nendel mono-metakrüülsetel ühenditel erinevad asendajad isosorbiidi vaba hüdroksüülrühma küljes. Arvkeskmistatud molekulmass nende polümeeride puhul varieerus vahemikus 26 kuni 48 kg mol^{-1} ja polüdisperssusindeks ($Đ$) 2.4 kuni 2.9. *Ekso*/*endo* konfiguratsioon ja erinevad asendusrühmad ei avaldanud suurt mõju molekulmassidele, kuid asendajate mõju oli selgelt märgata lahustuvusomaduste puhul. Näiteks vabade OH-gruppidega polümeerid lahustusid ainult dimetüülsulfoksiidis, kuid alküülrühmadega polümeerid olid lahustuvad ka tetrahüdrofuraanis ja kloroformis. Sealjuures atsetaat-gruppidega polümeerid lahustusid ka atsetonitriilis ja polümetakrülaadid, millel olid suuremad C12-alküülrühmad, lahustusid tolueenis. Isosorbiidi polümetakrülaatide piirviskoossuste väärtused olid küllaltki ühtsed, ent esines üks erand: *ekso*-OH-rühma sisaldaval polümeeril oli palju suurem piirviskoossus. Arvatavasti on selle nähtuse põhjuseks täiendavad vesiniksidemed polümeeriahelate vahel. Kõik isosorbiidi polümetakrülaadid osutusid termiliselt väga stabiilseteks, kuna kuumutuskõveratelt leitud 5%-line massikadu esines neil vahemikus 208–240 °C. Erinevate asendusrühmade mõju võis veel märgata klaasistumistemperatuuride (T_g) määramisel. Polümeeridel, millel esinevad OH-rühmad, oli T_g väga kõrge (167 °C), ent lühemate alküülrühmadega polümeeridel oli see madalam, 130 °C juures. Sealjuures polümetakrülaadid, millel olid pikad külgahelad, esines T_g veelgi madalamal, 54 °C juures *endo*-C12 polümetakrülaadil ja 66 °C juures *ekso*-C12 polümetakrülaadil. Lisaks oli viimasel polümeeril ka väike üleminek korrastatud olekust vähem korrastatud olekusse, mida võis täheldada diferentsiaalse kalorimeetria (DSC) mõõtmisgraafikutelt.

Järgnevalt valmistati kahest regioisomeersest isosorbiidi monoepoksiidist anioonse ringi-avava polümerisatsioonimeetodi abil lineaarsed polüeetrid, kasutades selleks initsiaatorina tetraoktüülammoniumbromiidi ja aktivaatorina triisobütüülalumiiniumi. See meetod andis tulemusena polüeetrid, mille arvkeskmistatud molekulmassid olid 13.2 kg mol^{-1} ($Đ$ = 1.7) ja 17.8 kg mol^{-1} ($Đ$ = 2.1). Nende polümeeride, milles samuti isosorbiidi struktuuriühikud asetsevad külgahelas,

termiline stabiilsus oli kõrge, ulatudes 300 °C-ni. DSC graafikutelt määrati T_g väärtused, mis osutusid toatemperatuurist madalamaks (10 ja 15 °C), kuid vastavad väärtused on siiski kõrgemad kui teistel laialdaselt tuntud polüeetritel. Kahe lineaarse isosorbiidi polüeetri omadustes ei märgatud silmnähtavaid erinevusi, mille oleks põhjustanud regioisomeersed epoksü-monomeerid. Veel näidati antud töös, et isosorbiidi monoepoksiide saab edukalt kasutada ka kopolümeeride koostises, näiteks koos polüetüleenglükooliga.

Täiendavalt sünteesiti antud uurimistöös isosorbiidi derivaadid, mis on ühe süsinik-süsinik sideme võrra pikendatud. Selleks transformatsiooniks kasutati vastavate alkeenide hüdroformüleerimist. Tulemusena saadi regioisomeersete isosorbiidi C5- ja C6-aldehüüdide segu. Kõrgeim regioselektiivsus positsiooni C5 suhtes oli 46:1 ja positsiooni C6 puhul 4:1. Vastavat meetodit katsetati ka suuremal skaalal ja näidati järjestikust hüdroformüleerimise-redutseerimise teostamist samas kolvis. Peale selle demonstreeriti ka pikemat sünteesirada, mille tulemusena lisati kaks uut süsinik-süsinik sidet isosorbiidi molekulisse.

Antud doktoritöös raames valmistatud isosorbiidil baseeruvad polümeerid on taaskord tõestanud isosorbiidi kui struktuuriühiku sobivust polümeeride koostises. Isosorbiidi jäikus annab polümeeridele kõrge termilise stabiilsuse ja tõstab nende klaasistumistemperatuuri. Veel võimaldavad isosorbiidi struktuuris olevad kaks hüdroksüülrühma molekuli funktsionaliseerimist mitmete asendusrühmadega ja selle kaudu saab omakorda varieerida polümeeri omadusi. Lisaks eelnevale, selles töös saadud C–C sideme võrra pikendatud isosorbiidi derivaadid, mis valmistati hüdroformüleerimismeetodi abil, võimaldavad samuti uudsete biopõhiste monomeeride kujundamist polümeersete materjalide jaoks.

REFERENCES

(1) Odian, G. *Principles of Polymerization*, 4th ed.; John Wiley & Sons, Inc., Hoboken, New Jersey, USA, 2004. https://doi.org/10.1002/047147875X

(2) Vert, M.; Doi, Y.; Hellwich, K.-H.; Hess, M.; Hodge, P.; Kubisa, P.; Rinaudo, M.; Schué, F. Terminology for biorelated polymers and applications (IUPAC Recommendations 2012). *Pure Appl. Chem.* **2012**, *84* (2), 377–410. https://doi.org/10.1351/PAC-REC-10-12-04

(3) Jenkins, A. D.; Kratochvíl, P.; Stepto, R. F. T.; Suter, U. W. Glossary of basic terms in polymer science (IUPAC Recommendations 1996). *Pure Appl. Chem.* **1996**, *68* (12), 2287–2311. https://doi.org/10.1351/pac199668122287

(4) Geyer, R.; Jambeck, J. R.; Law, K. L. Production, use, and fate of all plastics ever made. *Sci. Adv.* **2017**, *3* (7), e1700782. https://doi.org/10.1126/sciadv.1700782

(5) Hockett, R. C.; Fletcher, H. G.; Sheffield, E. L.; Goepp, R. M. Hexitol Anhydrides. The Structure of Isosorbide, a Crystalline Dianhydrosorbitol. *J. Am. Chem. Soc.* **1946**, *68* (6), 927–930. https://doi.org/10.1021/ja01210a003

(6) Fenouillot, F.; Rousseau, A.; Colomines, G.; Saint-Loup, R.; Pascault, J.-P. Polymers from renewable 1,4:3,6-dianhydrohexitols (isosorbide, isomannide and isoidide): A review. *Prog. Polym. Sci.* **2010**, *35* (5), 578–622. https://doi.org/10.1016/j.progpolymsci.2009.10.001

(7) Wu, J.; Eduard, P.; Jasinska-Walc, L.; Rozanski, A.; Noordover, B. A. J.; van Es, D. S.; Koning, C. E. Fully Isohexide-Based Polyesters: Synthesis, Characterization, and Structure-Properties Relations. *Macromolecules* **2013**, *46* (2), 384–394. https://doi.org/10.1021/ma302209f

(8) Isikgor, F. H.; Becer, C. R. Lignocellulosic biomass: a sustainable platform for the production of bio-based chemicals and polymers. *Polym. Chem.* **2015**, *6* (25), 4497–4559. https://doi.org/10.1039/C5PY00263J

(9) Delidovich, I.; Hausoul, P. J. C.; Deng, L.; Pfützenreuter, R.; Rose, M.; Palkovits, R. Alternative Monomers Based on Lignocellulose and Their Use for Polymer Production. *Chem. Rev.* **2016**, *116* (3), 1540–1599. https://doi.org/10.1021/acs.chemrev.5b00354

(10) Al-Naji, M.; Schlaad, H.; Antonietti, M. New (and Old) Monomers from Biorefineries to Make Polymer Chemistry More Sustainable. *Macromol. Rapid Commun.* **2021**, *42* (3), 2000485. https://doi.org/10.1002/marc.202000485

(11) Luterbacher, J. S.; Martin Alonso, D.; Dumesic, J. A. Targeted chemical upgrading of lignocellulosic biomass to platform molecules. *Green Chem.* **2014**, *16* (12), 4816–4838. https://doi.org/10.1039/C4GC01160K

(12) Masutani, K.; Kimura, Y. Biobased Polymers. In *Encyclopedia of Polymeric Nanomaterials*, Kobayashi, S., Müllen, K., Eds.; Springer-Verlag, Berlin, Heidelberg, Germany, 2015; pp 1–7. https://doi.org/10.1007/978-3-642-36199-9_390-1

(13) García-Depraect, O.; Bordel, S.; Lebrero, R.; Santos-Beneit, F.; Börner, R. A.; Börner, T.; Muñoz, R. Inspired by nature: Microbial production, degradation and valorization of biodegradable bioplastics for life-cycle-engineered products. *Biotechnol. Adv.* **2021**, 107772. https://doi.org/10.1016/j.biotechadv.2021.107772

(14) Siracusa, V.; Blanco, I. Bio-Polyethylene (Bio-PE), Bio-Polypropylene (Bio-PP) and Bio-Poly(ethylene terephthalate) (Bio-PET): Recent Developments in Bio-Based Polymers Analogous to Petroleum-Derived Ones for Packaging and Engineering Applications. *Polymers* **2020**, *12* (8), 1641. https://doi.org/10.3390/polym12081641

(15) Kabasci, S. Chapter 4 – Biobased plastics. In *Plastic Waste and Recycling*, Letcher, T. M., Ed.; Academic Press, 2020; pp 67–96. https://doi.org/10.1016/B978-0-12-817880-5.00004-9
(16) Ahmed, T.; Shahid, M.; Azeem, F.; Rasul, I.; Shah, A. A.; Noman, M.; Hameed, A.; Manzoor, N.; Manzoor, I.; Muhammad, S. Biodegradation of plastics: current scenario and future prospects for environmental safety. *Environ. Sci. Pollut. Res.* **2018**, *25* (8), 7287–7298. https://doi.org/10.1007/s11356-018-1234-9
(17) Karlsson, S.; Albertsson, A.-C. Biodegradable polymers and environmental interaction. *Polym. Eng. Sci.* **1998**, *38* (8), 1251–1253. https://doi.org/10.1002/pen.10294
(18) European Bioplastics: What are bioplastics? https://www.european-bioplastics.org/bioplastics/ (accessed August 6, 2021).
(19) European Environment Agency: Biodegradable and compostable plastics – challenges and opportunities. https://www.eea.europa.eu/publications/biodegradable-and-compostable-plastics/biodegradable-and-compostable-plastics-challenges (accessed August 6, 2021).
(20) Zhu, Y.; Romain, C.; Williams, C. K. Sustainable polymers from renewable resources. *Nature* **2016**, *540* (7633), 354–362. https://doi.org/10.1038/nature21001
(21) Gallezot, P. Conversion of biomass to selected chemical products. *Chem. Soc. Rev.* **2012**, *41* (4), 1538–1558. https://doi.org/10.1039/C1CS15147A
(22) Nguyen, H. T. H.; Qi, P.; Rostagno, M.; Feteha, A.; Miller, S. A. The quest for high glass transition temperature bioplastics. *J. Mater. Chem. A* **2018**, *6* (20), 9298–9331. https://doi.org/10.1039/C8TA00377G
(23) Rose, M.; Palkovits, R. Isosorbide as a Renewable Platform chemical for Versatile Applications – Quo Vadis? *ChemSusChem* **2012**, *5* (1), 167–176. https://doi.org/10.1002/cssc.201100580
(24) Müller, J.; Hoffmann, U. Verfahren zur Herstellung wertvoller Produkte aus Sorbit. DE488602C, 1927.
(25) Flèche, G.; Huchette, M. Isosorbide. Preparation, Properties and Chemistry. *Starch/Staerke* **1986**, *38* (1), 26–30. https://doi.org/10.1002/star.19860380107
(26) Diuretic compositions. GB1067298A, 1967.
(27) Cope, A. C.; Shen, T. Y. The Stereochemistry of 1,4:3,6-Dianhydrohexitol Derivatives. *J. Am. Chem. Soc.* **1956**, *78* (13), 3177–3182. https://doi.org/10.1021/ja01594a055
(28) Bell, F. K.; Carr, C. J.; Krantz, J. C. Sugar Alcohols. XXI. A Study of the Effect of the Anhydrides of Sorbitol on the Dissociation Constant of Boric Acid. *J. Phys. Chem.* **1940**, *44* (7), 862–865. https://doi.org/10.1021/j150403a004
(29) Wiggins, L. F. The anhydrides of polyhydric alcohols. Part I. The constitution of *iso*mannide. *J. Chem. Soc.* **1945**, 4–7. https://doi.org/10.1039/JR9450000004
(30) Fauconnier, A. Sur le second ahydride de la mannite. *Bull. Soc. Chim. Fr.* **1884**, *41*, 119–125.
(31) Fletcher, H. G.; Goepp, R. M. 1,4;3,6-Hexitol dianhydride L-isodide. *J. Am. Chem. Soc.* **1945**, *67* (6), 1042–1043. https://doi.org/10.1021/ja01222a513
(32) Fletcher, H. G.; Goepp, R. M. Hexitol Anhydrides. 1,4,3,6-Dianhydro-L-iditol and the Structures of Isomannide and Isosorbide. *J. Am. Chem. Soc.* **1946**, *68* (6), 939–941. https://doi.org/10.1021/ja01210a007

(33) Mills, J. A. The Stereochemistry of Cyclic Derivatives of Carbohydrates. In *Advances in Carbohydrate Chemistry*, Wolfrom, M. L., Ed.; Academic Press, 1955; Vol. 10, pp 1–53. https://doi.org/10.1016/s0096-5332(08)60389-6
(34) Stoss, P.; Hemmer, R. 1,4:3,6-dianhydrohexitols. In *Advances in Carbohydrate Chemistry and Biochemistry*, Horton, D., Ed.; Academic Press, 1991; Vol. 49, pp 93–173. https://doi.org/10.1016/s0065-2318(08)60182-1
(35) Brimacombe, J. S.; Foster, A. B.; Stacey, M.; Whiffen, D. H. Aspects of stereochemistry – I: Properties and reactions of some diols. *Tetrahedron* **1958**, *4* (3), 351–360. https://doi.org/10.1016/0040-4020(58)80056-3
(36) Muller, P. Glossary of terms used in physical organic chemistry (IUPAC Recommendations 1994). *Pure Appl. Chem.* **1994**, *66* (5), 1077–1184. https://doi.org/10.1351/pac199466051077
(37) Lemieux, R. U.; McInnes, A. G. The Preferential tosylation of the endo-5-hydroxyl group of 1,4:3,6-dianhydro-D-glucitol. *Can. J. Chem.* **1960**, *38*, 136–140. https://doi.org/10.1139/v60-015
(38) Buck, K. W.; Duxbury, J. M.; Foster, A. B.; Perry, A. R.; Webber, J. M. Observations on esterification reactions. *Carbohydr. Res.* **1966**, *2* (2), 122–131. https://doi.org/10.1016/S0008-6215(00)81476-7
(39) Stoss, P.; Merrath, P.; Schlüter, G. Regioselektive Acylierung von 1,4:3,6-Dianhydro-D-glucit. *Synthesis* **1987**, No. 2, 174–176. https://doi.org/10.1055/s-1987-27878
(40) Abenhaïm, D.; Loupy, A.; Munnier, L.; Tamion, R.; Marsais, F.; Quéguiner, G. Selective alkylations of 1,4:3,6-dianhydro-D-glucitol (isosorbide). *Carbohydr. Res.* **1994**, *261* (2), 255–266. https://doi.org/10.1016/0008-6215(94)84022-9
(41) Loupy, A.; Monteux, D. A. Isomannide and isosorbide as new chiral auxiliaries for the stereoselective synthesis of tertiary α-hydroxy acids. *Tetrahedron* **2002**, *58*, 1541–1549. https://doi.org/10.1016/S0040-4020(02)00024-8
(42) Dussenne, C.; Delaunay, T.; Wiatz, V.; Wyart, H.; Suisse, I.; Sauthier, M. Synthesis of isosorbide: an overview of challenging reactions. *Green Chem.* **2017**, *19* (22), 5332–5344. https://doi.org/10.1039/C7GC01912B
(43) Delbecq, F.; Khodadadi, M. R.; Rodriguez Padron, D.; Varma, R.; Len, C. Isosorbide: Recent advances in catalytic production. *Mol. Catal.* **2020**, *482*, 110648. https://doi.org/10.1016/j.mcat.2019.110648
(44) Huang, Y.-B.; Fu, Y. Hydrolysis of cellulose to glucose by solid acid catalysts. *Green Chem.* **2013**, *15* (5), 1095–1111. https://doi.org/10.1039/C3GC40136G
(45) Bozell, J. J.; Petersen, G. R. Technology development for the production of biobased products from biorefinery carbohydrates – the US Department of Energy's "Top 10" revisited. *Green Chem.* **2010**, *12* (4), 539–554. https://doi.org/10.1039/B922014C
(46) Zhang, J.; Li, J.-b.; Wu, S.-B.; Liu, Y. Advances in the Catalytic Production and Utilization of Sorbitol. *Ind. Eng. Chem. Res.* **2013**, *52* (34), 11799–11815. https://doi.org/10.1021/ie4011854
(47) Yuan, D.; Li, L.; Li, F.; Wang, Y.; Wang, F.; Zhao, N.; Xiao, F. Solvent-Free Production of Isosorbide from Sorbitol Catalyzed by a Polymeric Solid Acid. *ChemSusChem* **2019**, *12* (22), 4986–4995. https://doi.org/10.1002/cssc.201901922
(48) Le Nôtre, J.; van Haveren, J.; van Es, D. S. Synthesis of Isoidide through Epimerization of Isosorbide using Ruthenium on Carbon. *ChemSusChem* **2013**, *6* (4), 693–700. https://doi.org/10.1002/cssc.201200714

(49) Vanbésien, T.; Delaunay, T.; Wiatz, V.; Bigot, S.; Bricout, H.; Tilloy, S.; Monflier, E. Epimerization of isosorbide catalyzed by homogeneous ruthenium-phosphine complexes: A new step towards an industrial process. *Inorg. Chim. Acta* **2021**, *515*, 120094. https://doi.org/10.1016/j.ica.2020.120094
(50) Roquette launches 'world's largest' isosorbide production unit. *Additives for Polymers* **2015**, No. 6, 8–9. https://doi.org/10.1016/S0306-3747(15)30073-7
(51) Bonnin, I.; Mereau, R.; Tassaing, T.; De Oliveira Vigier, K. One-pot synthesis of isosorbide from cellulose or lignocellulosic biomass: a challenge? *Beilstein J. Org. Chem.* **2020**, *16*, 1713–1721. https://doi.org/10.3762/bjoc.16.143
(52) Caiti, M.; Tarantino, G.; Hammond, C. Developing a Continuous Process for Isosorbide Production from Renewable Sources. *ChemCatChem* **2020**, *12* (24), 6393–6400. https://doi.org/10.1002/cctc.202001278
(53) Brandi, F.; Khalil, I.; Antonietti, M.; Al-Naji, M. Continuous-Flow Production of Isosorbide from Aqueous-Cellulosic Derivable Feed over Sustainable Heterogeneous Catalysts. *ACS Sustainable Chem. Eng.* **2021**, *9* (2), 927–935. https://doi.org/10.1021/acssuschemeng.0c08167
(54) Bloom, P. D.; Tabuena-Salyers, T. Waterborne film-forming compositions containing reactive surfactants and/or humectants. US2011166287A1, 2011.
(55) Wils, D.; Mentink, L. 1,4:3,6 Dianhydrohexitols for moisturising the skin. US2020230042A1, 2020.
(56) Joseph, L. G.; Mancini, A. Isosorbide Dinitrate in Angina Pectoris. *Angiology* **1961**, *12* (6), 264–266. https://doi.org/10.1177/000331976101200609
(57) Stoss, P.; Leitold, M. Pharmaceuticals. EP0361156A2, 1990.
(58) Lynch, M. J. Dentifrice formulation and method of treating teeth, mouth and throat therewith to reduce plaque accumulation and irritation. US4585649A, 1968.
(59) SpecialChem: dimethyl isosorbide. https://cosmetics.specialchem.com/inci/dimethyl-isosorbide# (accessed August 6, 2021).
(60) Zhang, Z.; Ganzuo, L.; Patel, R.; Friberg, S. E.; Aikens, P. A. Formation kinetics and stability of surfactant vesicles. *J. Surfactants Deterg.* **1998**, *1* (3), 393–398. https://doi.org/10.1007/s11743-998-0041-3
(61) Russo, F.; Galiano, F.; Pedace, F.; Aricò, F.; Figoli, A. Dimethyl Isosorbide As a Green Solvent for Sustainable Ultrafiltration and Microfiltration Membrane Preparation. *ACS Sustainable Chem. Eng.* **2020**, *8* (1), 659–668. https://doi.org/10.1021/acssuschemeng.9b06496
(62) Kadraoui, M.; Maunoury, T.; Derriche, Z.; Guillarme, S.; Saluzzo, C. Isohexides as Versatile Scaffolds for Asymmetric Catalysis. *Eur. J. Org. Chem.* **2015**, No. 3, 441–457. https://doi.org/10.1002/ejoc.201402851
(63) Diéguez, M.; Pàmies, O.; Claver, C. Palladium-Diphosphite Catalysts for the Asymmetric Allylic Substitution Reactions. *J. Org. Chem.* **2005**, *70* (9), 3363–3368. https://doi.org/10.1021/jo0480904
(64) Van Buu, O. N.; Vo-Thanh, G. Synthesis of Novel Chiral Ammonium-Based Ionic Liquids Derived from Isosorbide and their Applications in an Asymmetric Aza Diels-Alder Reaction. *Lett. Org. Chem.* **2007**, *4* (3), 158–167. https://doi.org/10.2174/157017807780737219
(65) Van Buu, O. N.; Aupoix, A.; Hong, N. D. T.; Vo-Thanh, G. Chiral ionic liquids derived from isosorbide: synthesis, properties and applications in asymmetric synthesis. *New J. Chem.* **2009**, *33* (10), 2060–2072. https://doi.org/10.1039/B902956G

(66) Van Buu, O. N.; Aupoix, A.; Vo-Thanh, G. Synthesis of novel chiral imidazolium-based ionic liquids derived from isosorbide and their applications in asymmetric aza Diels-Alder reaction. *Tetrahedron* **2009**, *65* (11), 2260–2265. https://doi.org/10.1016/j.tet.2009.01.055

(67) Suzuki, T.; Koizumi, K.; Suzuki, M.; Kurosawa, E. Kumausallene, a new bromoallene from the marine red alga *Laurencia nipponica* Yamada. *Chem. Lett.* **1983**, *12* (10), 1639–1642. https://doi.org/10.1246/cl.1983.1639

(68) Pinacho Crisóstomo, F. R.; Padrón, J. M.; Martín, T.; Villar, J.; Martín, V. S. A Short and Efficient Enantiomeric Synthesis of Antitumor Fused Tetrahydrofurans. *Eur. J. Org. Chem.* **2006**, No. 8, 1910–1916. https://doi.org/10.1002/ejoc.200500842

(69) Saxon, D. J.; Luke, A. M.; Sajjad, H.; Tolman, W. B.; Reineke, T. M. Next-generation polymers: Isosorbide as a renewable alternative. *Prog. Polym. Sci.* **2020**, *101*, 101196. https://doi.org/10.1016/j.progpolymsci.2019.101196

(70) Storbeck, R.; Rehahn, M.; Ballauff, M. Synthesis and properties of high-molecular-weight polyesters based on 1,4:3,6-dianhydrohexitols and terephthalic acid. *Makromol. Chem.* **1993**, *194* (1), 53–64. https://doi.org/10.1002/macp.1993.021940104

(71) Storbeck, R.; Ballauff, M. Synthesis and thermal analysis of copolyesters deriving from 1,4:3,6-dianhydrosorbitol, ethylene glycol, and terephthalic acid. *J. Appl. Polym. Sci.* **1996**, *59* (7), 1199–1202. https://doi.org/10.1002/(SICI)1097-4628(19960214)59:7<1199::AID-APP19>3.0.CO;2-0

(72) Kricheldorf, H. R.; Behnken, G.; Sell, M. Influence of Isosorbide on Glass-Transition Temperature and Crystallinity of Poly(butylene terephthalate). *J. Macromol. Sci, Part A: Pure Appl. Chem.* **2007**, *44* (7), 679–684. https://doi.org/10.1080/10601320701351128

(73) Polymer Properties Database: Glass Transition Temperatures. https://polymerdatabase.com/polymer%20physics/Polymer%20Tg%20C.html (accessed August 6, 2021).

(74) Cognet-Georjon, E.; Méchin, F.; Pascault, J.-P. New polyurethanes based on diphenylmethane diisocyanate and 1,4:3,6-dianhydrosorbitol, 1. Model kinetic studies and characterization of the hard segment. *Macromol. Chem. Phys.* **1995**, *196* (11), 3733–3751. https://doi.org/10.1002/macp.1995.021961125

(75) Beldi, M.; Medimagh, R.; Chatti, S.; Marque, S.; Prim, D.; Loupy, A.; Delolme, F. Characterization of cyclic and non-cyclic poly-(ether-urethane)s bio-based sugar diols by a combination of MALDI-TOF and NMR. *Eur. Polym. J.* **2007**, *43* (8), 3415–3433. https://doi.org/10.1016/j.eurpolymj.2007.06.003

(76) Thiem, J.; Lüders, H. Synthesis and properties of polyurethanes derived from diaminodianhydroalditols. *Makromol. Chem.* **1986**, *187* (12), 2775–2785. https://doi.org/10.1002/macp.1986.021871204

(77) Bachmann, F.; Reimer, J.; Ruppenstein, M.; Thiem, J. Synthesis of Novel Polyurethanes and Polyureas by Polyaddition Reactions of Dianhydrohexitol Configurated Diisocyanates. *Macromol. Chem. Phys.* **2001**, *202* (17), 3410–3419. https://doi.org/10.1002/1521-3935(20011101)202:17<3410::AID-MACP3410>3.0.CO;2-Q

(78) Ma, Y.; Liu, J.; Luo, M.; Xing, J.; Wu, J.; Pan, H.; Ruan, C.; Luo, Y. Incorporating isosorbide as the chain extender improves mechanical properties of linear biodegradable polyurethanes as potential bone regeneration materials. *RSC Adv.* **2017**, *7* (23), 13886–13895. https://doi.org/10.1039/C6RA28826J

(79) Zenner, M. D.; Xia, Y.; Chen, J. S.; Kessler, M. R. Polyurethanes from Isosorbide-Based Diisocyanates. *ChemSusChem* **2013**, *6* (7), 1182–1185. https://doi.org/10.1002/cssc.201300126
(80) Bachmann, F.; Reimer, J.; Ruppenstein, M.; Thiem, J. Synthesis of a novel starch-derived AB-type polyurethane. *Macromol. Rapid Commun.* **1998**, *19* (1), 21–26. https://doi.org/10.1002/(SICI)1521-3927(19980101)19:1<21::AID-MARC21>3.0.CO;2-T
(81) Steinmetz, R.; Mitchner, N. A.; Grant, A.; Allen, D. L.; Bigsby, R. M.; Ben-Jonathan, N. The Xenoestrogen Bisphenol A Induces Growth, Differentiation, and c-fos Gene Expression in the Female Reproductive Tract. *Endocrinology* **1998**, *139* (6), 2741–2747. https://doi.org/10.1210/endo.139.6.6027
(82) Chatti, S.; Kricheldorf, H. R.; Schwarz, G. Copolycarbonates of isosorbide and various diols. *J. Polym. Sci., Part A: Polym. Chem.* **2006**, *44* (11), 3616–3628. https://doi.org/10.1002/pola.21444
(83) Noordover, B. A. J.; Haveman, D.; Duchateau, R.; van Benthem, R. A. T. M.; Koning, C. E. Chemistry, functionality, and coating performance of biobased copolycarbonates from 1,4:3,6-dianhydrohexitols. *J. Appl. Polym. Sci.* **2011**, *121* (3), 1450–1463. https://doi.org/10.1002/app.33660
(84) Mitsucishi Chemical Corporation: DURABIO – Bio base engineering polymer. https://www.mcpp-global.com/en/asia/products/brand/durabiotm/ (accessed August 6, 2021).
(85) Zech, J. D.; Le Maistre, J. W. Bisglycidyl ethers of isohexides. US3272845A, 1966.
(86) Feng, X.; East, A. J.; Hammond, W. B.; Zhang, Y.; Jaffe, M. Overview of advances in sugar-based polymers. *Polym. Adv. Technol.* **2011**, *22* (1), 139–150. https://doi.org/10.1002/pat.1859
(87) Lorenzini, C.; Versace, D. L.; Renard, E.; Langlois, V. Renewable epoxy networks by photoinitiated copolymerization of poly(3-hydroxyalkanoate)s and isosorbide derivatives. *React. Funct. Polym.* **2015**, *93*, 95–100. https://doi.org/10.1016/j.reactfunctpolym.2015.06.007
(88) Cheng, J.; Zhang, P.; Liu, T.; Zhang, J. Preparation and properties of hydrogels based on PEG and isosorbide building blocks with phosphate linkages. *Polymer* **2015**, *78*, 212–218. https://doi.org/10.1016/j.polymer.2015.10.009
(89) Hong, J.; Radojčić, D.; Ionescu, M.; Petrović, Z. S.; Eastwood, E. Advanced materials from corn: isosorbide-based epoxy resins. *Polym. Chem.* **2014**, *5* (18), 5360–5368. https://doi.org/10.1039/C4PY00514G
(90) Li, C.; Dai, J.; Liu, X.; Jiang, Y.; Ma, S.; Zhu, J. Green Synthesis of a Bio-Based Epoxy Curing Agent from Isosorbide in Aqueous Condition and Shape Memory Properties Investigation of the Cured Resin. *Macromol. Chem. Phys.* **2016**, *217* (13), 1439–1447. https://doi.org/10.1002/macp.201600055
(91) Morrison, J. G. Polyglycidyl ethers of ether anhydro hexitols, method of production, and aqueous solutions thereof. US3041300A, 1962.
(92) Chrysanthos, M.; Galy, J.; Pascault, J.-P. Preparation and properties of bio-based epoxy networks derived from isosorbide diglycidyl ether. *Polymer* **2011**, *52* (16), 3611–3620. https://doi.org/10.1016/j.polymer.2011.06.001
(93) Majdoub, M.; Loupy, A.; Flèche, G. Nouveaux polyéthers et polyesters à base d'isosorbide: synthèse et caractérisation. *Eur. Polym. J.* **1994**, *30* (12), 1431–1437. https://doi.org/10.1016/0014-3057(94)90274-7

(94) Chatti, S.; Bortolussi, M.; Loupy, A.; Blais, J. C.; Bogdal, D.; Majdoub, M. Efficient synthesis of polyethers from isosorbide by microwave-assisted phase transfer catalysis. *Eur. Polym. J.* **2002**, *38* (9), 1851–1861. https://doi.org/10.1016/S0014-3057(02)00071-X

(95) Medimagh, R.; Chatti, S.; Alves, S.; Hammed, N.; Loupy, A.; Zarrouk, H. Caractérisation par spectrométrie de masse MALDI-TOF de poly(isosorbide-éther)s cycliques et linéaires obtenus sous irradiation microondes. *C. R. Chimie* **2007**, *10* (3), 234–250. https://doi.org/10.1016/j.crci.2006.11.002

(96) Saxon, D. J.; Nasiri, M.; Mandal, M.; Maduskar, S.; Dauenhauer, P. J.; Cramer, C. J.; LaPointe, A. M.; Reineke, T. M. Architectural Control of Isosorbide-Based Polyethers via Ring-Opening Polymerization. *J. Am. Chem. Soc.* **2019**, *141* (13), 5107–5111. https://doi.org/10.1021/jacs.9b00083

(97) Gallagher, J. J.; Hillmyer, M. A.; Reineke, T. M. Acrylic Triblock Copolymers Incorporating Isosorbide for Pressure Sensitive Adhesives. *ACS Sustainable Chem. Eng.* **2016**, *4* (6), 3379–3387. https://doi.org/10.1021/acssuschemeng.6b00455

(98) Baek, S.-S.; Jang, S.-H.; Hwang, S.-H. Sustainable isosorbide-based transparent pressure-sensitive adhesives for optically clear adhesive and their adhesion performance. *Polym. Int.* **2017**, *66* (12), 1834–1840. https://doi.org/10.1002/pi.5450

(99) Nasiri, M.; Saxon, D. J.; Reineke, T. M. Enhanced Mechanical and Adhesion Properties in Sustainable Triblock Copolymers via Non-covalent Interactions. *Macromolecules* **2018**, *51* (7), 2456–2465. https://doi.org/10.1021/acs.macromol.7b02248

(100) Mansoori, Y.; Hemmati, S.; Eghbali, P.; Zamanloo, M. R.; Imanzadeh, G. Nanocomposite materials based on isosorbide methacrylate/Cloisite 20A. *Polym. Int.* **2013**, *62* (2), 280–288. https://doi.org/10.1002/pi.4297

(101) Gallagher, J. J.; Hillmyer, M. A.; Reineke, T. M. Isosorbide-based Polymethacrylates. *ACS Sustainable Chem. Eng.* **2015**, *3* (4), 662–667. https://doi.org/10.1021/sc5008362

(102) Beghdadi, S.; Abdelhedi Miladi, I.; Ben Romdhane, H.; Bernard, J.; Drockenmuller, E. RAFT Polymerization of Bio-Based 1-Vinyl-4-dianhydrohexitol-1,2,3-triazole Stereoisomers Obtained via Click Chemistry. *Biomacromolecules* **2012**, *13* (12), 4138–4145. https://doi.org/10.1021/bm301435e

(103) Kieber, R. J.; Ozkardes, C.; Sanchez, N.; Kennemur, J. G. Cationic copolymerization of isosorbide towards value-added poly(vinyl ethers). *Polym. Chem.* **2019**, *10* (25), 3514–3524. https://doi.org/10.1039/C9PY00590K

(104) Mülhaupt, R. Hermann Staudinger and the Origin of Macromolecular Chemistry. *Angew. Chem., Int. Ed.* **2004**, *43* (9), 1054–1063. https://doi.org/10.1002/anie.200330070

(105) Carraher, C. E. J. *Introduction to Polymer Chemistry*, 4th ed.; CRC Press, Taylor & Francis Group, LLC, Boca Ration, Florida, USA, 2017. https://doi.org/10.1201/9781315369488

(106) Polymer Properties Database: Chain-Growth versus Step-Growth Polymerization. https://polymerdatabase.com/polymer%20chemistry/Chain%20versus%20Step%20Growth.html (accessed August 6, 2021).

(107) Nesvadba, P. Radical Polymerization in Industry. In *Encyclopedia of Radicals in Chemistry, Biology and Materials*, 1st ed.; Chatgilialoglu, C., Studer, A., Eds.; John Wiley & Sons, Ltd., 2012. https://doi.org/10.1002/9781119953678.rad080
(108) Simpkins, N. S. Azobisisobutyronitrile. In *e-EROS: Encyclopedia of Reagents for Organic Synthesis*. John Wiley & Sons, Ltd., 2001. https://doi.org/10.1002/047084289X.ra121
(109) Sherburn, M. S. Basic Concepts on Radical Chain Reactions. In *Encyclopedia of Radicals in Chemistry, Biology and Materials*, 1st ed.; Chatgilialoglu, C., Studer, A., Eds.; John Wiley & Sons, Ltd., 2012. https://doi.org/10.1002/9781119953678.rad017
(110) Jenkins, A. D.; Jones, R. G.; Moad, G. Terminology for reversible-deactivation radical polymerization previously called "controlled" radical or "living" radical polymerization (IUPAC Recommendations 2010). *Pure Appl. Chem.* **2009**, *82* (2), 483–491. https://doi.org/10.1351/PAC-REP-08-04-03
(111) Matyjaszewski, K. Atom Transfer Radical Polymerization (ATRP): Current Status and Future Perspectives. *Macromolecules* **2012**, *45* (10), 4015–4039. https://doi.org/10.1021/ma3001719
(112) Perrier, S. 50th Anniversary Perspective: RAFT Polymerization – A User Guide. *Macromolecules* **2017**, *50* (19), 7433–7447. https://doi.org/10.1021/acs.macromol.7b00767
(113) Lligadas, G.; Grama, S.; Percec, V. Single-Electron Transfer Living Radical Polymerization Platform to Practice, Develop, and Invent. *Biomacromolecules* **2017**, *18* (10), 2981–3008. https://doi.org/10.1021/acs.biomac.7b01131
(114) Childers, M. I.; Longo, J. M.; Van Zee, N. J.; LaPointe, A. M.; Coates, G. W. Stereoselective Epoxide Polymerization and Copolymerization. *Chem. Rev.* **2014**, *114* (16), 8129–8152. https://doi.org/10.1021/cr400725x
(115) Brocas, A.-L.; Mantzaridis, C.; Tunc, D.; Carlotti, S. Polyether synthesis: From activated or metal-free anionic ring-opening polymerization of epoxides to functionalization. *Prog. Polym. Sci.* **2013**, *38* (6), 845–873. https://doi.org/10.1016/j.progpolymsci.2012.09.007
(116) Du Prez, F. E.; Goethals, E. J.; Hoogenboom, R. Cationic Polymerizations. In *Handbook of Polymer Synthesis, Characterization, and Processing*, Salvadívar-Guerra, E., Vivaldo-Lima, E., C., Eds.; John Wiley & Sons, Inc., 2013; pp 163–185. https://doi.org/10.1002/9781118480793.ch8
(117) Penczek, S. Cationic ring-opening polymerization (CROP) major mechanistic phenomena. *J. Polym. Sci., Part A: Polym. Chem.* **2000**, *38* (11), 1919–1933. https://doi.org/10.1002/(SICI)1099-0518(20000601)38:11<1919::AID-POLA10>3.0.CO;2-W
(118) Herzberger, J.; Niederer, K.; Pohlit, H.; Seiwert, J.; Worm, M.; Wurm, F. R.; Frey, H. Polymerization of Ethylene Oxide, Propylene Oxide, and Other Alkylene Oxides: Synthesis, Novel Polymer Architectures, and Bioconjugation. *Chem. Rev.* **2016**, *116* (4), 2170–2243. https://doi.org/10.1021/acs.chemrev.5b00441
(119) Labbé, A.; Carlotti, S.; Billouard, C.; Desbois, P.; Deffieux, A. Controlled High-Speed Anionic Polymerization of Propylene Oxide Initiated by Onium Salts in the Presence of Triisobutylaluminum. *Macromolecules* **2007**, *40* (22), 7842–7847. https://doi.org/10.1021/ma070288d
(120) Rejsek, V.; Sauvanier, D.; Billouard, C.; Desbois, P.; Deffieux, A.; Carlotti, S. Controlled Anionic Homo- and Copolymerization of Ethylene Oxide and Propylene Oxide by Monomer Activation. *Macromolecules* **2007**, *40* (18), 6510–6514. https://doi.org/10.1021/ma070450c

(121) Francis, A. U.; Venkatachalam, S.; Kanakavel, M.; Ravindran, P. V.; Ninan, K. N. Structural characterization of hydroxyl terminated polyepichlorohydrin obtained using boron trifluoride etherate and stannic chloride as initiators. *Eur. Polym. J.* **2003**, *39* (4), 831–841. https://doi.org/10.1016/S0014-3057(02)00302-6
(122) Wiese, K.-D.; Obst, D. Hydroformylation. In *Catalytic Carbonylation Reactions*, Beller, M., Ed.; Springer, Berlin, Heidelberg, 2006; pp 1–33. https://doi.org/10.1007/3418_015
(123) Cornils, B.; Börner, A.; Franke, R.; Zhang, B.; Wiebus, E.; Schmid, K. Hydroformylation. In *Applied Homogeneous Catalysis with Organometallic Compounds*, 3rd ed.; Cornils, B., Herrmann, W. A., Beller, M., Paciello, R., Eds.; Wiley-VCH Verlag GmbH & Co. KGaA, 2017; pp 23–90. https://doi.org/10.1002/9783527651733.ch2
(124) Roelen, O. Verfahren zur Herstellung von sauerstoffhaltigen Verbindungen. DE849548C, 1938/1952.
(125) Evans, D.; Osborn, J. A.; Wilkinson, G. Hydroformylation of alkenes by use of rhodium complex catalysts. *J. Chem. Soc. A* **1968**, 3133–3142. https://doi.org/10.1039/J19680003133
(126) Franke, R.; Selent, D.; Börner, A. Applied Hydroformylation. *Chem. Rev.* **2012**, *112* (11), 5675–5732. https://doi.org/10.1021/cr3001803
(127) Claver, C.; Diéguez, M.; Pàmies, O.; Castillón, S. Asymmetric Hydroformylation. In *Catalytic Carbonylation Reactions*, Beller, M., Ed.; Springer, Berlin, Heidelberg, 2006; pp 35–64. https://doi.org/10.1007/3418_016
(128) Pospech, J.; Fleischer, I.; Franke, R.; Buchholz, S.; Beller, M. Alternative Metals for Homogeneous Catalyzed Hydroformylation Reactions. *Angew. Chem., Int. Ed.* **2013**, *52* (10), 2852–2872. https://doi.org/10.1002/anie.201208330
(129) Gorbunov, D. N.; Nenasheva, M. V.; Kardasheva, Y. S.; Karakhanov, E. A. Alternative sources of syngas for hydroformylation of unsaturated compounds. *Russ. Chem. Bull.* **2020**, *69* (4), 625–634. https://doi.org/10.1007/s11172-020-2810-y
(130) Sparta, M.; Børve, K. J.; Jensen, V. R. Activity of Rhodium-Catalyzed Hydroformylation: Added Insight and Predictions from Theory. *J. Am. Chem. Soc.* **2007**, *129* (27), 8487–8499. https://doi.org/10.1021/ja070395n
(131) Chen, Y.; Shen, J.; Liu, S.; Zhao, J.; Wang, Y.; Zhang, G. High Efficiency Organic Lewis Pair Catalyst for Ring-Opening Polymerization of Epoxides with Chemoselectivity. *Macromolecules* **2018**, *51* (20), 8286–8297. https://doi.org/10.1021/acs.macromol.8b01852
(132) Brocas, A.-L.; Deffieux, A.; Le Malicot, N.; Carlotti, S. Combination of phosphazene base and triisobutylaluminum for the rapid synthesis of polyhydroxy telechelic poly(propylene oxide). *Polym. Chem.* **2012**, *3* (5), 1189–1195. https://doi.org/10.1039/C2PY20014G
(133) Roos, K.; Carlotti, S. Grignard-based anionic ring-opening polymerization of propylene oxide activated by triisobutylaluminum. *Eur. Polym. J.* **2015**, *70*, 240–246. https://doi.org/10.1016/j.eurpolymj.2015.07.016
(134) Carlotti, S.; Labbe, A.; Rejsek, V.; Doutaz, S.; Gervais, M.; Deffieux, A. Living/Controlled Anionic Polymerization and Copolymerization of Epichlorohydrin with Tetraoctylammonium Bromide–Triisobutylaluminum Initiating Systems. *Macromolecules* **2008**, *41* (19), 7958–7062. https://doi.org/10.1021/ma801422c
(135) Gervais, M.; Brocas, A.-L.; Cendejas, G.; Deffieux, A.; Carlotti, S. Synthesis of Linear High Molar Mass Glycidol-Based Polymers by Monomer-Activated Anionic Polymerization. *Macromolecules* **2010**, *43* (4), 1778–1784. https://doi.org/10.1021/ma902286a

(136) Herzberger, J.; Leibig, D.; Liermann, J. C.; Frey, H. Conventional Oxyanionic versus Monomer-Activated Anionic Copolymerization of Ethylene Oxide with Glycidyl Ethers: Striking Differences in Reactivity Ratios. *ACS Macro Lett.* **2016**, *5* (11), 1206–1211. https://doi.org/10.1021/acsmacrolett.6b00701
(137) Heinen, S.; Rackow, S.; Schäfer, A.; Weinhart, M. A Perfect Match: Fast and Truly Random Copolymerization of Glycidyl Ether Monomers to Thermo-responsive Copolymers. *Macromolecules* **2017**, *50* (1), 44–53. https://doi.org/10.1021/acs.macromol.6b01904
(138) Okada, M. Chemical syntheses of biodegradable polymers. *Prog. Polym. Sci.* **2002**, *27* (1), 87–133. https://doi.org/10.1016/S0079-6700(01)00039-9
(139) Sakai, N.; Mano, S.; Nozaki, K.; Takaya, H. Highly enantioselective hydroformylation of olefins catalyzed by new phosphine phosphite-rhodium(I) complexes. *J. Am. Chem. Soc.* **1993**, *115* (15), 7033–7034. https://doi.org/10.1021/ja00068a095
(140) Lambers-Verstappen, M. M. H.; de Vries, J. G. Rhodium-Catalysed Asymmetric Hydroformylation of Unsaturated Nitriles. *Adv. Synth. Catal.* **2003**, *345* (4), 478–482. https://doi.org/10.1002/adsc.200390053
(141) Axtell, A. T.; Cobley, C. J.; Klosin, J.; Whiteker, G. T.; Zanotti-Gerosa, A.; Abboud, K. A. Highly Regio- and Enantioselective Asymmetric Hydroformylation of Olefins Mediated by 2,5-Disubstituted Phospholane Ligands. *Angew. Chem., Int. Ed.* **2005**, *44* (36), 5834–5838. https://doi.org/10.1002/anie.200501478
(142) Klosin, J.; Landis, C. R. Ligands for Practical Rhodium-Catalyzed Asymmetric Hydroformylation. *Acc. Chem. Res.* **2007**, *40* (12), 1251–1259. https://doi.org/10.1021/ar7001039
(143) Makado, G.; Morimoto, T.; Sugimoto, Y.; Tsutsumi, K.; Kagawa, N.; Kakiuchi, K. Highly Linear-Selective Hydroformylation of 1-Alkenes using Formaldehyde as a Syngas Substitute. *Adv. Synth. Catal.* **2010**, *352* (2-3), 299–304. https://doi.org/10.1002/adsc.200900713
(144) Fuentes, J. A.; Pittaway, R.; Clarke, M. L. Rapid Asymmetric Transfer Hydroformylation (ATHF) of Disubstituted Alkenes Using Paraformaldehyde as a Syngas Surrogate. *Chem. Eur. J.* **2015**, *21* (30), 10645–10649. https://doi.org/10.1002/chem.201502049

APPENDIX 1: NMR SPECTRA

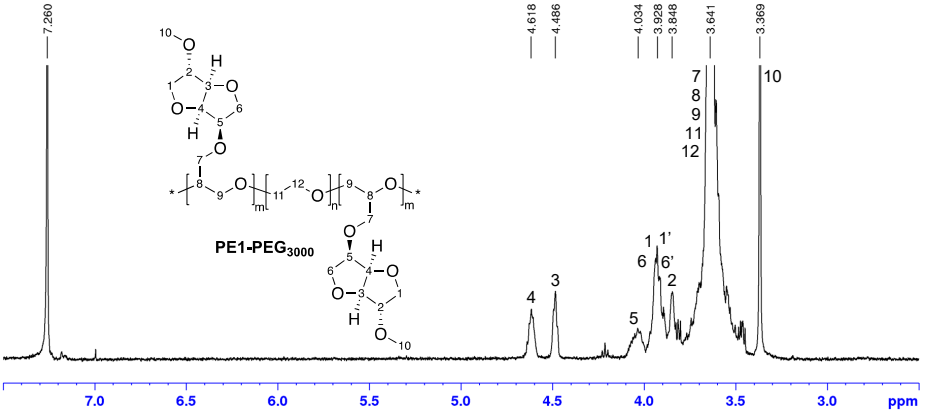

Figure A1. ^{1}H NMR spectrum of **PE1-PEG$_{3000}$**.

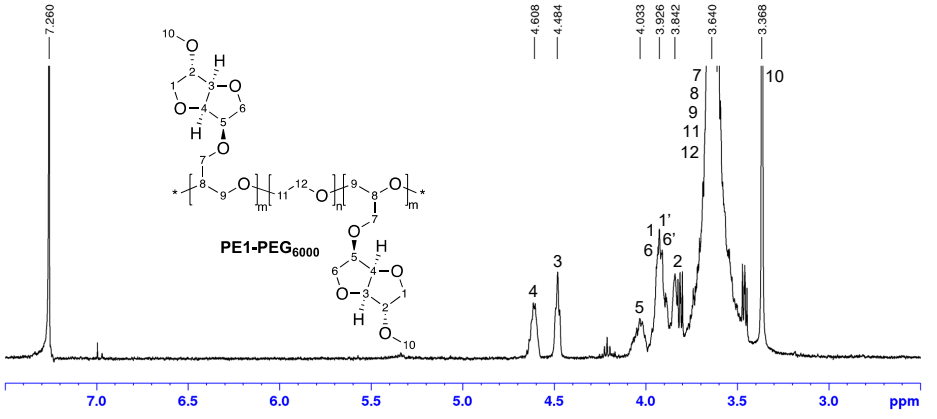

Figure A2. ^{1}H NMR spectrum of **PE1-PEG$_{6000}$**.

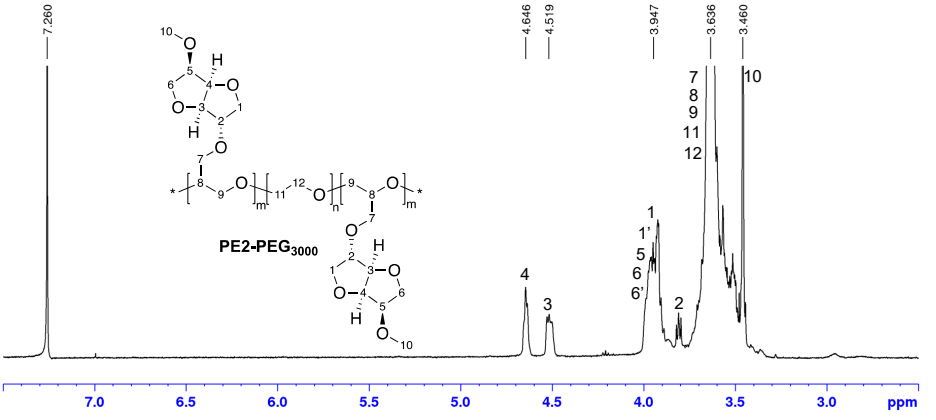

Figure A3. ^{1}H NMR spectrum of **PE2-PEG$_{3000}$**.

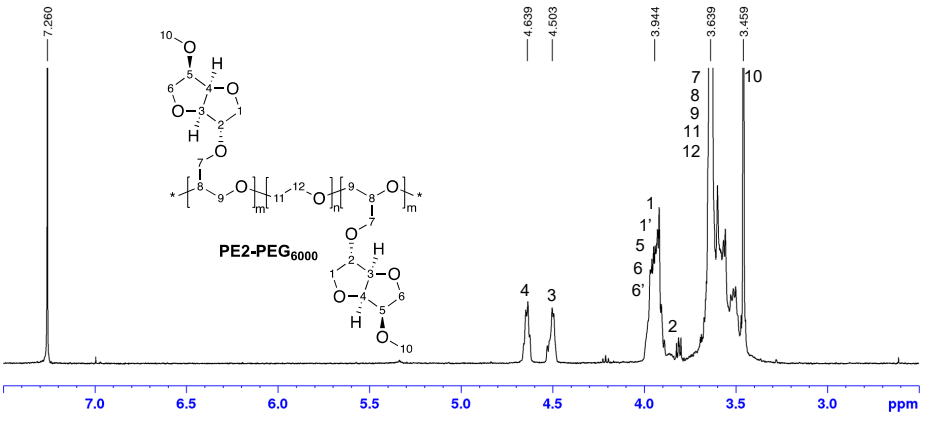

Figure A4. ^{1}H NMR spectrum of **PE2-PEG$_{6000}$**.

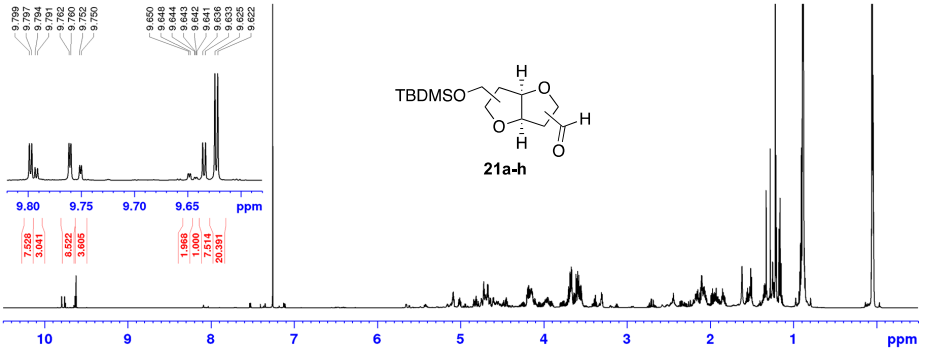

Figure A5. ^{1}H NMR spectrum of aldehyde **21a–h**.

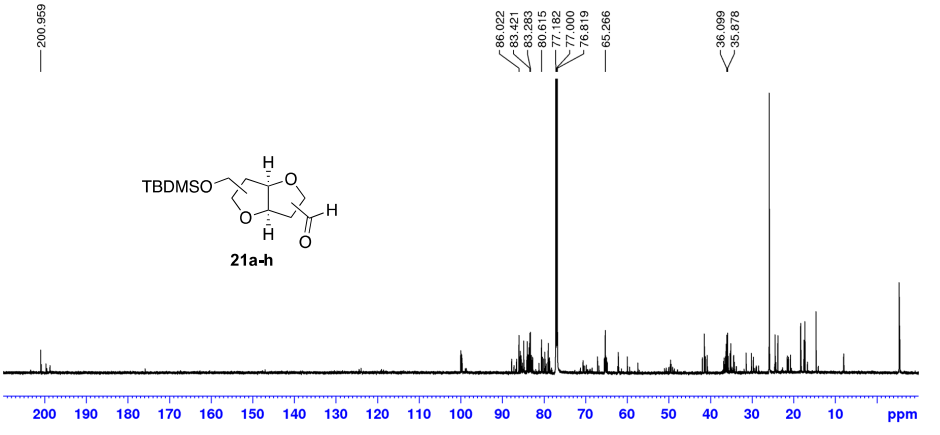

Figure A6. ^{13}C NMR spectrum of **21a–h**.

ACKNOWLEDGEMENT

I would like to express my greatest appreciation to my two supervisors Prof. Patric Jannasch and Assoc. Prof. Lauri Vares for their support and guidance over the years. They have been encouraging, helpful, and always available when advice was needed. Also, I would like to acknowledge all of our group members in the Institute of Technology, notably Ilme Liblikas, who helped me with the synthesis of epoxides, and Piret Villo, who eagerly taught me the essential skills that are needed in organic synthesis research lab.

Furthermore, I would like to thank the co-authors of the articles and all the colleagues from University of Tartu, who have helped me with expert advice and different instrumental methods. I am grateful to Omar Parve and Jaan Parve for the enzymatic synthesis of methacrylic monomers. I also sincerely appreciate the help by Tõnis Pehk from National Institute of Chemical Physics and Biophysics in Tallinn and Lauri Toom from Institute of Chemistry in Tartu with complicated NMR spectra. Many thanks to Thanh Huong Pham who helped me in Lund University, Sweden during my first attempts in the field of polymer synthesis. Likewise, big thanks to Olivier Bonjour for his help with thermal characterization of the polymers. Also, my gratitude to Assoc. Prof. Gerard Llgadas for welcoming me in Rovira i Virgili University, Spain and to all the lab mates in Suspol group who supported me during my time in Tarragona.

I am very thankful to my dear friends who have kept my spirit up during complicated periods. But my special gratitude for their love and support goes to my family and, of course, Karl, without whose patience and encouragement all of it would not have been possible.

Thank you! Aitäh!

PUBLICATIONS

CURRICULUM VITAE

Name: Livia Matt
Date of birth: December 17, 1992
Citizenship: Estonian
Contact: Institute of Technology, University of Tartu,
Nooruse 1, 50411, Tartu, Estonia
E-mail: livia.matt@ut.ee

Education:

2017– ...	University of Tartu, PhD studies in engineering and technology
2015–2017	University of Tartu, MSc in chemistry, *cum laude*
2012–2015	University of Tartu, BSc in chemistry, *cum laude*
2009–2012	Kuressaare Gymnasium, secondary education

Language skills:

Estonian	native language
English	excellent in speech and writing
German	basic knowledge

Professional employment:

2018–...	University of Tartu, Institute of Technology, Junior Research Fellow
2019 July–Aug.	Estiko-Plastar, Summer Internship, Laboratory Assistant
2015–2017	University of Tartu, Institute of Technology, Chemist
2014–2015	University of Tartu, Institute of Technology, Laboratory Assistant

Scientific publications and patent applications:

1. **Matt, L.**; Liblikas, I.; Bonjour, O.; Jannasch, P.; Vares, L. Synthesis and anionic polymerization of isosorbide mono-epoxides for linear biobased polyethers. *Polym. Chem.* **2021**, *12* (41), 5937–5941.
2. Laanesoo, S.; Bonjour, O.; Parve, J.; Parve, O.; **Matt, L.**; Vares, L.; Jannasch, P. Poly(alkanoyl isosorbide methacrylate)s: From Amorphous to Semicrystalline and Liquid Crystalline Biobased Materials. *Biomacromolecules* **2021**, *22*, 640–648.
3. **Matt, L.**; Parve, J.; Parve, O.; Pehk, T.; Pham, T. H.; Liblikas, I.; Vares, L.; Jannasch, P. Enzymatic Synthesis and Polymerization of Isosorbide-Based Monomethacrylates for High-T_g Plastics. *ACS Sus. Chem. Eng.* **2018**, *6* (12), 17382–17390.
4. Jannasch, P.; **Matt, L.**; Vares, L.; Parve, J.; Parve, O.; Gathergood, N.; Pehk, T. Synthesis and Polymerization of Isosorbide-Based Monomethacrylates. Patent application GB1807794.1, **2018**.

5. Villo, P.; **Matt, L.**; Toom, L.; Liblikas, I.; Pehk, T., Vares, L. Hydroformylation of Olefinic Derivatives of Isosorbide and Isomannide. *J. Org. Chem.* **2016**, *81* (17), 7510–7517.

Research grants and scholarships:

2017 2nd prize at *Estonian National Contest for University Students* organized by Estonian Research Council

2016 Kristjan Jaak mobility scholarship by Archimedes (for laboratory internship in Lund University)

Additional scientific activities:

2020 Oct.–Dec. Visiting PhD student at *Suspol* group (supervisor assoc. prof. Gerard Lligadas), University of Rovira i Virgili, Tarragona, Catalonia, Spain

2017 Jan.–Mar. Visiting MSc student at *Polymer Science and Technology* group (supervisor prof. Patric Jannasch), Lund University, Lund, Sweden

ELULOOKIRJELDUS

Nimi: Livia Matt
Sünniaeg: 17. detsember 1992
Kodakondsus: Eesti
Kontakt: Tehnoloogiainstituut, Tartu Ülikool,
Nooruse 1, 50411, Tartu, Eesti
E-mail: livia.matt@ut.ee

Haridus:

2017– ...	Tartu Ülikool, doktorantuur (tehnika ja tehnoloogia)
2015–2017	Tartu Ülikool, magistriõpe (keemia), *cum laude*
2012–2015	Tartu Ülikool, bakalaureuseõpe (keemia), *cum laude*
2009–2012	Kuressaare Gümnaasium, keskharidus

Keeleoskus:

eesti keel	emakeel
inglise keel	väga hea nii kõnes kui ka kirjas
saksa keel	kõnes hea, kirjas rahuldav

Teenistuskäik:

2018–...	Tartu Ülikool, Tehnoloogiainstituut, nooremteadur
2019 juuli–aug	Estiko-Plastar, suvepraktika, laborant
2015–2017	Tartu Ülikool, Tehnoloogiainstituut, keemik
2014–2015	Tartu Ülikool, Tehnoloogiainstituut, laborant

Teaduspublikatsioonid ja patendiavaldused:

1. **Matt, L.**; Liblikas, I.; Bonjour, O.; Jannasch, P.; Vares, L. Synthesis and anionic polymerization of isosorbide mono-epoxides for linear biobased polyethers. *Polym. Chem.* **2021**, *12* (41), 5937–5941.
2. Laanesoo, S.; Bonjour, O.; Parve, J.; Parve, O.; **Matt, L.**; Vares, L.; Jannasch, P. Poly(alkanoyl isosorbide methacrylate)s: From Amorphous to Semicrystalline and Liquid Crystalline Biobased Materials. *Biomacromolecules* **2021**, *22*, 640–648.
3. **Matt, L.**; Parve, J.; Parve, O.; Pehk, T.; Pham, T. H.; Liblikas, I.; Vares, L.; Jannasch, P. Enzymatic Synthesis and Polymerization of Isosorbide-Based Monomethacrylates for High-T_g Plastics. *ACS Sus. Chem. Eng.* **2018**, *6* (12), 17382–17390.
4. Jannasch, P.; **Matt, L.**; Vares, L.; Parve, J.; Parve, O.; Gathergood, N.; Pehk, T. Synthesis and Polymerization of Isosorbide-Based Monomethacrylates. Patent application GB1807794.1, **2018**.
5. Villo, P.; **Matt, L.**; Toom, L.; Liblikas, I.; Pehk, T., Vares, L. Hydroformylation of Olefinic Derivatives of Isosorbide and Isomannide. *J. Org. Chem.* **2016**, *81* (17), 7510–7517.

Tunnustused ja stipendiumid:

2017	II preemia Üliõpilaste teadustööde riiklikul konkursil, korraldaja Eesti Teadusagentuur
2016	Kristjan Jaagu välisõpingute stipendium (laboripraktikaks Lundi Ülikoolis), väljaandja SA Archimedes

Muu teadustegevus:

2020 okt–dets	Külalisdoktorant uurimisgrupis *Suspol* (juhendajaks kaasprofessor Gerard Lligadas), Rovira i Virgili Ülikool, Tarragona, Kataloonia, Hispaania
2017 jaan–märts	Külalistudeng uurimisgrupis *Polymer Science and Technology* (juhendajaks professor Patric Jannasch), Lundi Ülikool, Lund, Rootsi

DISSERTATIONES TECHNOLOGIAE UNIVERSITATIS TARTUENSIS

1. **Imre Mäger**. Characterization of cell-penetrating peptides: Assessment of cellular internalization kinetics, mechanisms and bioactivity. Tartu 2011, 132 p.
2. **Taavi Lehto**. Delivery of nucleic acids by cell-penetrating peptides: application in modulation of gene expression. Tartu 2011, 155 p.
3. **Hannes Luidalepp**. Studies on the antibiotic susceptibility of *Escherichia coli*. Tartu 2012, 111 p.
4. **Vahur Zadin**. Modelling the 3D-microbattery. Tartu 2012, 149 p.
5. **Janno Torop**. Carbide-derived carbon-based electromechanical actuators. Tartu 2012, 113 p.
6. **Julia Suhorutšenko**. Cell-penetrating peptides: cytotoxicity, immunogenicity and application for tumor targeting. Tartu 2012, 139 p.
7. **Viktoryia Shyp**. G nucleotide regulation of translational GTPases and the stringent response factor RelA. Tartu 2012, 105 p.
8. **Mardo Kõivomägi**. Studies on the substrate specificity and multisite phosphorylation mechanisms of cyclin-dependent kinase Cdk1 in *Saccharomyces cerevisiae*. Tartu, 2013, 157 p.
9. **Liis Karo-Astover**. Studies on the Semliki Forest virus replicase protein nsP1. Tartu, 2013, 113 p.
10. **Piret Arukuusk**. NickFects–novel cell-penetrating peptides. Design and uptake mechanism. Tartu, 2013, 124 p.
11. **Piret Villo**. Synthesis of acetogenin analogues. Asymmetric transfer hydrogenation coupled with dynamic kinetic resolution of α-amido-β-keto esters. Tartu, 2013, 151 p.
12. **Villu Kasari**. Bacterial toxin-antitoxin systems: transcriptional cross-activation and characterization of a novel *mqsRA* system. Tartu, 2013, 108 p.
13. **Margus Varjak**. Functional analysis of viral and host components of alphavirus replicase complexes. Tartu, 2013, 151 p.
14. **Liane Viru**. Development and analysis of novel alphavirus-based multifunctional gene therapy and expression systems. Tartu, 2013, 113 p.
15. **Kent Langel**. Cell-penetrating peptide mechanism studies: from peptides to cargo delivery. Tartu, 2014, 115 p.
16. **Rauno Temmer**. Electrochemistry and novel applications of chemically synthesized conductive polymer electrodes. Tartu, 2014, 206 p.
17. **Indrek Must**. Ionic and capacitive electroactive laminates with carbonaceous electrodes as sensors and energy harvesters. Tartu, 2014, 133 p.
18. **Veiko Voolaid**. Aquatic environment: primary reservoir, link, or sink of antibiotic resistance? Tartu, 2014, 79 p.
19. **Kristiina Laanemets**. The role of SLAC1 anion channel and its upstream regulators in stomatal opening and closure of *Arabidopsis thaliana.* Tartu, 2015, 115 p.

20. **Kalle Pärn**. Studies on inducible alphavirus-based antitumour strategy mediated by site-specific delivery with activatable cell-penetrating peptides. Tartu, 2015, 139 p.
21. **Anastasia Selyutina**. When biologist meets chemist: a search for HIV-1 inhibitors. Tartu, 2015, 172 p.
22. **Sirle Saul**. Towards understanding the neurovirulence of Semliki Forest virus. Tartu, 2015, 136 p.
23. **Marit Orav**. Study of the initial amplification of the human papillomavirus genome. Tartu, 2015, 132 p.
24. **Tormi Reinson**. Studies on the Genome Replication of Human Papillomaviruses. Tartu, 2016, 110 p.
25. **Mart Ustav Jr**. Molecular Studies of HPV-18 Genome Segregation and Stable Replication. Tartu, 2016, 152 p.
26. **Margit Mutso**. Different Approaches to Counteracting Hepatitis C Virus and Chikungunya Virus Infections. Tartu, 2016, 184 p.
27. **Jelizaveta Geimanen**. Study of the Papillomavirus Genome Replication and Segregation. Tartu, 2016, 168 p.
28. **Mart Toots**. Novel Means to Target Human Papillomavirus Infection. Tartu, 2016, 173 p.
29. **Kadi-Liis Veiman**. Development of cell-penetrating peptides for gene delivery: from transfection in cell cultures to induction of gene expression *in vivo*. Tartu, 2016, 136 p.
30. **Ly Pärnaste**. How, why, what and where: Mechanisms behind CPP/cargo nanocomplexes. Tartu, 2016, 147 p.
31. **Age Utt**. Role of alphavirus replicase in viral RNA synthesis, virus-induced cytotoxicity and recognition of viral infections in host cells. Tartu, 2016, 183 p.
32. **Veiko Vunder**. Modeling and characterization of back-relaxation of ionic electroactive polymer actuators. Tartu, 2016, 154 p.
33. **Piia Kivipõld**. Studies on the Role of Papillomavirus E2 Proteins in Virus DNA Replication. Tartu, 2016, 118 p.
34. **Liina Jakobson**. The roles of abscisic acid, CO_2, and the cuticle in the regulation of plant transpiration. Tartu, 2017, 162 p.
35. **Helen Isok-Paas**. Viral-host interactions in the life cycle of human papillomaviruses. Tartu, 2017, 158 p.
36. **Hanna Hõrak**. Identification of key regulators of stomatal CO_2 signalling via O_3-sensitivity. Tartu, 2017, 260 p.
37. **Jekaterina Jevtuševskaja**. Application of isothermal amplification methods for detection of *Chlamydia trachomatis* directly from biological samples. Tartu, 2017, 96 p.
38. **Ülar Allas**. Ribosome-targeting antibiotics and mechanisms of antibiotic resistance. Tartu, 2017, 152 p.
39. **Anton Paier**. Ribosome Degradation in Living Bacteria. Tartu, 2017, 108 p.
40. **Vallo Varik**. Stringent Response in Bacterial Growth and Survival. Tartu, 2017, 101 p.

41. **Pavel Kudrin**. In search for the inhibitors of *Escherichia coli* stringent response factor RelA. Tartu, 2017, 138 p.
42. **Liisi Henno**. Study of the human papillomavirus genome replication and oligomer generation. Tartu, 2017, 144 p.
43. **Katrin Krõlov**. Nucleic acid amplification from crude clinical samples exemplified by *Chlamydia trachomatis* detection in urine. Tartu, 2018, 118 p.
44. **Eve Sankovski**. Studies on papillomavirus transcription and regulatory protein E2. Tartu, 2018, 113 p.
45. **Morteza Daneshmand**. Realistic 3D Virtual Fitting Room. Tartu, 2018, 233 p.
46. **Fatemeh Noroozi**. Multimodal Emotion Recognition Based Human-Robot Interaction Enhancement. Tartu, 2018, 113 p.
47. **Krista Freimann**. Design of peptide-based vector for nucleic acid delivery in vivo. Tartu, 2018, 103 p.
48. **Rainis Venta**. Studies on signal processing by multisite phosphorylation pathways of the *S. cerevisiae* cyclin-dependent kinase inhibitor Sic1. Tartu, 2018, 155 p.
49. **Inga Põldsalu**. Soft actuators with ink-jet printed electrodes. Tartu, 2018, 85 p.
50. **Kadri Künnapuu**. Modification of the cell-penetrating peptide PepFect14 for targeted tumor gene delivery and reduced toxicity. Tartu, 2018, 114 p.
51. **Toomas Mets**. RNA fragmentation by MazF and MqsR toxins of *Escherichia coli*. Tartu, 2019, 119 p.
52. **Kadri Tõldsepp**. The role of mitogen-activated protein kinases MPK4 and MPK12 in CO_2-induced stomatal movements. Tartu, 2019, 259 p.
53. **Pirko Jalakas**. Unravelling signalling pathways contributing to stomatal conductance and responsiveness. Tartu, 2019, 120 p.
54. **S. Sunjai Nakshatharan**. Electromechanical modelling and control of ionic electroactive polymer actuators. Tartu, 2019, 165 p.
55. **Eva-Maria Tombak**. Molecular studies of the initial amplification of the oncogenic human papillomavirus and closely related nonhuman primate papillomavirus genomes. Tartu, 2019, 150 p.
56. **Meeri Visnapuu**. Design and physico-chemical characterization of metal-containing nanoparticles for antimicrobial coatings. Tartu, 2019, 138 p.
57. **Jelena Beljantseva**. Small fine-tuners of the bacterial stringent response – a glimpse into the working principles of Small Alarmone Synthetases. Tartu, 2020, 104 p.
58. **Egon Urgard**. Potential therapeutic approaches for modulation of inflammatory response pathways. Tartu, 2020, 120 p.
59. **Sofia Raquel Alves Oliveira**. HPLC analysis of bacterial alarmone nucleotide (p)ppGpp and its toxic analogue ppApp. Tartu, 2020, 122 p.
60. **Mihkel Örd**. Ordering the phosphorylation of cyclin-dependent kinase Cdk1 substrates in the cell cycle. Tartu, 2021, 228 p.

61. **Fred Elhi.** Biocompatible ionic electromechanically active polymer actuator based on biopolymers and non-toxic ionic liquids. Tartu, 2021, 140 p.
62. **Liisi Talas.** Reconstructing paleo-diversity, dynamics and response of eukaryotes to environmental change over the Late-Glacial and Holocene period in lake Lielais Svētiņu using sedaDNA. Tartu, 2021, 118 p.